



2  
2010



This is to certify that the  
dissertation entitled

SECRETION SIGNALS AND CHAPERONE FUNCTION IN  
*ERWINIA AMYLOVORA*

presented by

LINDSAY R. TRIPLETT

has been accepted towards fulfillment  
of the requirements for the

Doctoral degree in Plant Pathology

Major Professor's Signature

12-7-09

Date



SECRETION SIGNALS AND CHAPERONE FUNCTION IN *ERWINIA AMYLOVORA*

By

Lindsay R. Triplett

A DISSERTATION

Submitted to  
Michigan State University  
in partial fulfillment of the requirements  
for the degree of

DOCTOR OF PHILOSOPHY

Plant Pathology

2009

## ABSTRACT

### SECRETION SIGNALS AND CHAPERONE FUNCTION IN *ERWINIA AMYLOVORA*

By

Lindsay R. Triplett

Like many gram-negative bacterial pathogens, the plant pathogen *Erwinia amylovora* requires a type III secretion system (T3SS) to establish infection in the host. This work investigates the factors required for type III secretion of the *E. amylovora* pathogenicity factor DspE and for its interaction with the specific chaperone DspF. DspE N-terminal fragments fused to the CyaA translocation reporter were used to identify a minimal secretion and translocation signal within the first 51 amino acids, and an optimal translocation signal within 150 N-terminal amino acids. Mutagenesis of portions of the translocation signal revealed that residues 2-10 were required for protein translocation, and that mutagenesis of a segment containing a highly conserved stretch of 5 serines led to diminished translocation levels. Yeast two-hybrid assays, *in-vitro* pull-down assays, and site-directed mutagenesis were used to map the chaperone binding domain of DspE to residues 51-100, with a crucial role for residues 71-85, although the DspE-specific chaperone DspF and the N-terminal chaperone binding domain were not required for translocation of an N-terminal DspE-CyaA fusion.

Type III secretion chaperones have a highly conserved tertiary structure, but few analyses have been completed to determine which residues are critical for which function. One site postulated, but never tested, to be important in chaperone-effector interaction is the helix-binding groove. A homology-based model of DspF was used to identify 11 amino acids with putative localization in the helix-binding groove. Site-

directed mutagenesis of DspF identified four highly-conserved residues required for virulence in DspF, and three of these residues were required for interaction with the N-terminus of DspE. This study supports the significance of polar residues of the helix-binding groove in chaperone-effector interactions.

T3SS chaperones may interact with multiple substrates in the bacterial cell, including regulatory proteins, multiple effectors, and components of the secretion apparatus. A directed yeast two-hybrid screen identified *E. amylovora* secreted proteins Eop1 and Eop3 and homologs to the type III secretion apparatus proteins HrcU and HrcQ as candidate interactors of DspF. Annotation of the unpublished *Erwinia* genome confirmed or revealed the presence of putative chaperone genes next to *eop1* and *eop3*, but not other effectors such as *eop4*. Deletion of *dspF* positively affected cAMP accumulation mediated by translocation of Eop1- and Eop3-CyaA, but not Eop4-CyaA. Deletion of the putative Eop1 chaperone, *esc1*, negatively affected translocation of Eop1-CyaA but not of DspE-CyaA, indicating that Esc1 chaperone action is highly specific. Deletion of Eop1, Eop3, and the corresponding putative chaperone genes had no significant effect on virulence, although Ea1189 $\Delta$ *dspF* $\Delta$ *esc1* showed slightly increased levels of early growth on pear compared with Ea1189 $\Delta$ *dspF*.

## **ACKNOWLEDGEMENTS**

I would like to thank my advisor, Dr. George Sundin, for giving me the opportunity to study in this field, for his continual support and positive attitude, and for being an all-around great mentor. I would also like to thank the members of my committee, Drs. Frances Trail, Cindy Arvidson, and Sheng Yang He, for their helpful advice and comments.

Many thanks to my many former and current co-workers in the Sundin lab, for giving advice and always making the job a little more fun; to my parents, for always believing in me, and to my wonderful husband Preston, whose love and friendship helped me all the way.

## TABLE OF CONTENTS

|   |      |
|---|------|
| <b>List of Tables</b> .....   | vii  |
| <b>List of Figures</b> .....  | viii |
| <b>Chapter 1: Literature Review</b> .....   | 1    |
| I. Signals targeting proteins for bacterial secretion   |      |
| A. Type I, II, IV, and V secretion signals and chaperones.....  | 1    |
| B. Type III secretion system.....   | 2    |
| C. Type III secretion signals   |      |
| i. The N-terminus .....   | 3    |
| ii. Downstream signals that influence secretion and translocation..   | 4    |
| iii. Characteristics of the chaperone binding domain.....   | 5    |
| II. Class I type III secretion chaperones   |      |
| A. Definition and overview .....  | 7    |
| B. General structural features of the chaperone-effector interaction.....   | 7    |
| C. Substrate specificity of T3SS chaperones.....  | 8    |
| D. The roles of T3SS chaperones   |      |
| i. Chaperones dock effector proteins to the secretion apparatus.....  | 9    |
| ii. Chaperones confer secretion specificity.....  | 10   |
| iii. Chaperones stabilize or prevent aggregation of cognate effectors   | 12   |
| iv. Chaperones may regulate the expression of cognate effectors.....  | 13   |
| v. Chaperones may impose a temporal hierarchy of secretion.....   | 14   |
| III. Chaperone-effector interaction in <i>Erwinia amylovora</i>   |      |
| A. <i>Erwinia amylovora</i> biology and economic significance.....  | 16   |
| B. The secreted effector DspE .....   | 17   |
| C. The T3SS chaperone DspF.....   | 18   |
| IV. Rationale and project goals.....  | 19   |
| Works Cited.....  | 24   |
| <br>  |      |
| <b>Chapter 2: Functional analysis of the N-terminus of the <i>Erwinia amylovora</i> secreted effector DspA/E reveals features required for secretion, translocation, and interaction with the chaperone DspB/F.</b> |      |
| Abstract.....   | 33   |
| Introduction.....   | 34   |
| Materials and Methods.....  | 37   |
| Results.....  | 41   |
| Discussion.....   | 58   |
| Tables.....   | 63   |
| Works Cited.....  | 67   |

|  |            |
|--|------------|
| <b>Chapter 3: Homology-based modeling of the <i>Erwinia amylovora</i> type III secretion chaperone DspF used to identify amino acids required for virulence and interaction with the effector DspE</b> |            |
| Abstract.....  | 72         |
| Introduction.....  | 73         |
| Materials and Methods.....   | 75         |
| Results.....   | 78         |
| Discussion.....  | 90         |
| Tables.....  | 97         |
| Works Cited.....   | 100        |
| <br>   |            |
| <b>Chapter 4: A Study of the Roles of DspF and other Class I Secretion Chaperones in <i>Erwinia amylovora</i> in Effector Translocation and Virulence</b>  |            |
| Abstract.....  | 104        |
| Introduction.....  | 105        |
| Materials and Methods.....   | 108        |
| Results.....   | 110        |
| Discussion.....  | 128        |
| Tables.....  | 133        |
| Works Cited.....   | 136        |
| <br>   |            |
| <b>Chapter 5: Conclusions and Future Directions</b>  |            |
| Summary of Work.....   | 140        |
| Questions for the Future .....   | 145        |
| <br>   |            |
| <b>Appendix 1: Genetic Differences Among Blight-Causing <i>Erwinia</i> Species with Differing Host Specificities Identified by Suppression Subtractive Hybridization.....</b>                          | <b>147</b> |

## List of Tables

|  |     |
|--|-----|
| <b>Table 2-1.</b> Strains and plasmids used in Chapter 2 .....   | 43  |
| <b>Table 2-2.</b> Oligonucleotides used in Chapter 2.....  | 45  |
| <b>Table 3-1.</b> Bacterial strains and plasmids used in Chapter 3.....  | 97  |
| <b>Table 3-2.</b> Oligonucleotide primers used for mutagenesis of <i>dspF</i> .....                              | 99  |
| <b>Table 4-1.</b> Bacterial strains and plasmids used in Chapter 4.....  | 133 |
| <b>Table 4-2.</b> Primers for cloning and mutagenesis used in Chapter 4.....                                     | 134 |
| <b>Table 4-3.</b> Yeast two-hybrid identification of putative DspF-interacting proteins.....                     | 135 |
| <b>Table A-1.</b> <i>Erwinia</i> spp. strains and their indigenous plasmid content.....                          | 165 |
| <b>Table A-2.</b> Libraries generated by suppressive subtractive hybridization.....                              | 166 |
| <b>Table A-3.</b> Sequence analysis of SSH inserts specific to <i>E. amylovora</i> Ea110.....                    | 167 |
| <b>Table A-4.</b> Sequence analysis of SSH inserts specific to Ejp556 and <i>E. pyrifoliae</i> ....              | 169 |
| <b>Table A-5.</b> Analysis of the distribution of gene sequence among blight-causing <i>Erwinia</i> strains..... | 170 |

## List of Figures

Figures in this dissertation are presented in color.

|   |     |
|---|-----|
| <b>Figure 1-1.</b> Variations in the binding pattern and roles of T3SS chaperones.....  | 23  |
| <b>Figure 2-1.</b> Pathogenicity and cell death phenotypes of <i>Erwinia amylovora</i> Ea1189, Ea1189 $\Delta$ <i>dspF</i> , and Ea1189 $\Delta$ <i>dspF</i> (pLRT198)..... | 43  |
| <b>Figure 2-2.</b> Kinetics of cAMP accumulation after infiltration into tobacco leaves of Ea1189 $\Delta$ <i>dspE</i> + DspE (1-203)-CyaA.....                             | 45  |
| <b>Figure 2-3.</b> Mapping of the secretion and translocation domain of DspE.....   | 47  |
| <b>Figure 2-4.</b> Analysis of alanine replacement mutants of amino acids 2-40 of DspE.   | 50  |
| <b>Figure 2-5.</b> Mapping of the DspF-interacting regions in the N-terminal half of DspE.....  | 53  |
| <b>Figure 2-6.</b> Alanine-replacement mutagenesis of the N-terminal chaperone-binding domain of DspE.....  | 55  |
| <b>Figure 2-7.</b> Functional analysis of amino acids 51-100 of DspE.....   | 57  |
| <b>Figure 3-1.</b> Structural modeling and site-directed mutagenesis of <i>dspF</i> .....   | 81  |
| <b>Figure 3-2.</b> Virulence phenotype of site-directed mutants.....  | 84  |
| <b>Figure 3-3.</b> Alanine replacement of predicted helix-binding groove residues of DspF disrupts the interaction with the N-terminus of DspE in yeast.....                | 86  |
| <b>Figure 3-4.</b> Site-directed mutants cause moderate reductions in virulence and DspE (1-737)-CyaA translocation when expressed in wild-type <i>E. amylovora</i> .....   | 90  |
| <b>Figure 4-1.</b> DspE-6xHis is detected in Ea1189 $\Delta$ <i>dspF</i> and partially complements the <i>dspF</i> pathogenicity phenotype.....                             | 114 |
| <b>Figure 4-2.</b> Gene organization and interactions of putative chaperone-effector pairs in <i>E. amylovora</i> .....   | 120 |
| <b>Figure 4-3.</b> cAMP accumulation in tobacco leaves mediated by <i>E. amylovora</i> expressing CyaA fusion proteins.....   | 124 |
| <b>Figure 4-4.</b> cAMP accumulation in tobacco leaves mediated by <i>E. amylovora</i> deletion mutants expressing Eop1 and DspE-CyaA fusion proteins.....                  | 125 |
| <b>Figure 4-5.</b> Bacterial population counts on immature pear fruit inoculated with Ea1189 and mutant derivatives.....  | 127 |

**Figure A-1. Symptom expression and bacterial growth in immature pear fruit following inoculation with *Erwinia amylovora* strains..... 150**

## Chapter 1: Literature Review

Bacteria secrete proteins and peptides in order to break down substrates, acquire nutrients, antagonize competitors, or to modify the physiology of hosts or symbionts. Protein transport across two cell membranes and a peptidoglycan layer presents a special challenge, and gram-negative bacteria have evolved at least eight unique protein export systems. At least three of these systems, including the type III secretion system (T3SS), transfer proteins directly into eukaryotic cells. This chapter discusses the nature of the type III secretion signal, the role of chaperones in type III secretion, and the T3SS in *Erwinia amylovora*.

### I. Signals targeting proteins for bacterial secretion.

**IA. Type I, II, IV, and V secretion signals and chaperones.** Signals targeting bacterial proteins for export vary greatly in their nature and complexity. For example, ABC transporter (Type I) secreted proteins are targeted for secretion by non-cleaved, highly variable C-terminal secretion signals rich in  $\alpha$ -helices (25). For secretion through the Sec-dependent pathway known as type II secretion (as well as the type IV pilus system), a protein is first targeted to the general secretory pathway by an N-terminal signal peptide which is cleaved upon entry into the periplasm, then targeted for extracellular secretion. Attempts to define the protein elements required for T2SS targeting have been met with very limited success, and have suggested that the secretion signal is highly complex and may be bipartite or dependent on folding (72). Proteinaceous substrates of the type IV secretion system generally have no conserved signal sequence, although the C-terminus is required for type IV secretion in several secreted substrates of *A. tumefaciens* (27). Specific chaperones are required for secretion of at least some type IV secretion

substrates, and these bind close to the signal sequence (66). Proteins secreted through the autotransporter (Type V) secretion pathway require an N-terminal signal peptide for Sec-dependent secretion into the periplasm before exiting the cell via the  $\beta$ -barrel membrane pore in the C-terminus (86).

**IB. The Type III Secretion System.** The T3SS is a conserved syringe-like apparatus spanning the inner and outer membrane. Roughly 25 proteins are required to build the T3SS, including nine core apparatus proteins universally conserved among plant pathogens (22). Three general components of the apparatus are required for protein translocation into host cells: 1). The base, which spans the inner and outer membrane, is composed of a set of inner membrane rings facing the cytosol, a central rod traversing the periplasm, and a set of outer membrane rings. A number of peripheral inner membrane proteins associate with the inner membrane ring. 2). The needle or pilus is a filamentous macromolecular structure of secreted proteins extending from the bacterial outer membrane rings to the eukaryotic host cell. 3). The translocation apparatus, or translocon, is a structure that may bridge the tip of the pilus to the host cell membrane and create a pore allowing the entry of bacterial proteins. Substrates are most likely unfolded by the inner membrane ATPase as they enter the secretion system before traversing the pilus and refolding in the host cytoplasm (37).

The T3SS is critical for pathogenesis in a wide variety of animal and plant pathogenic bacterial species (22). Phylogenetic analyses have divided the secretion systems into seven families. Plant pathogens in the genera *Erwinia* and *Pseudomonas* encode secretion systems of the *hrp1* family; the regulatory mechanisms controlling *hrp1* systems differ substantially from the *hrp2* family secretion systems found in

*Xanthomonas* and *Ralstonia* (80). Although many components of the core secretion system and secretion mechanism are conserved among all T3SS, the apparatus in plant pathogens share a few key adaptations for expression and infection within the plant system. For example, *hrp1* systems feature a needle of extended relative length, presumably required to traverse the thick plant cell wall. Plant pathogen systems also lack orthologs to many known translocon proteins in *Salmonella* and *Yersinia*, suggesting a divergent method of cell entry (19). Despite major advances in the past 15 years, relatively little is known about how proteins are targeted, loaded, and injected from the T3SS into the host cytosol, especially when the host is a plant. While many exciting recent findings have been made regarding the regulation, assembly, and mechanism of the bacterial T3SS, the discussion here will focus on substrate targeting and the role of effector-specific chaperones in secretion.

### **IC. Type III secretion signals.**

**i. The N-terminus.** There is no conserved signal sequence targeting proteins for type III secretion. The N-terminal secretion domain of type III-secreted proteins do share some common features, such as a hydrophobic third amino acid and an amphipathic, serine rich N-terminus (8, 43). However, these characteristics are not definite indicators that an expressed protein will be secreted by the T3SS (36). The N-terminal 15 amino acids are usually sufficient for secretion of an effector protein into culture media (6, 46), and that the first seven amino acids are especially important in this process (69, 73). While some authors have recorded a very small amount of secretion in the absence of the N-terminal signal (21), most reports concur that the N-terminal secretion domain is absolutely required (17, 49).

Extensive mutational analyses of the N-termini of secreted proteins in *Yersinia* have failed to identify a single sequence feature absolutely required for secretion (52, 69). The DNA and protein sequences of the N-terminal 15 amino acids are highly tolerant of synonymous mutations and frameshift mutations (6, 46, 68), and even a series of synthetic sequences encoding amphipathic N-termini were sufficient to confer secretion to a reporter fusion (53). The ability of the N-terminus to tolerate frameshift mutations caused some debate about whether the N-terminal secretion signal is an RNA signal or proteinaceous (52, 53, 68), but biochemical and microscopic studies on secretion signal-reporter gene fusions have confirmed the secretion-competence of pre-synthesized effector proteins (29, 52, 91). It is possible that an amphipathic, serine-rich, disordered N-terminus is sufficient for the type III secretion of any protein, although it is not intuitive that such a general signal would be sufficient for selection of a few proteins among thousands. Whatever the nature of the secretion signal, it appears to be universal, as the *Erwinia chrysanthemi* and *Xanthomonas campestris* T3SSs can secrete *Yersinia* effectors, and the *Yersinia* secretion apparatus secretes *P. syringae* effectors AvrB and AvrPto (7, 70).

## **ii. Downstream signals that influence secretion and translocation.**

The studies of the N-terminal secretion signal discussed above relied heavily on analyses of the supernatants of bacterial cultures, but the observations gained from these studies were not always consistent with the requirements for translocation of the native effector protein into host cells. For example, while the first 15 amino acids of YopE can be secreted into the culture medium, 50 amino acids were required for translocation into host cells, but only in the presence of a YopE binding chaperone protein, SycE (17, 77).

This and similar observations led to the proposal of a bipartite translocation signal- an N-terminal signal necessary for secretion, followed by a downstream sequence necessary for translocation (48).

Why would a secretion signal be sufficient for secretion into the medium, but not into host cells? How can the two processes be separated? One possible explanation is that the secretion conferred by the N-terminal signal sequence is mediated by an alternate secretion system. In other words, the N-terminal sequence could be an ancient secretion signal sufficient for secretion by the flagellar secretion system, but not by the more recently evolved T3SS (48). A second possibility is that requirements for secretion are different in the artificial medium environment than in the host. Although Cheng and coworkers reported that the N-terminal 15 amino acids of YopE was secreted from a *Yersinia enterocolitica* strain (21), another study found no trace of YopE in the culture media during HeLa cell infections (49). It is also possible that some unknown signal is transmitted upon contact with host cells, changing the requirements for entering the T3SS and preventing translocation. In summary, a secretion signal longer than the N-terminal minimal secretion signal is often required for effector translocation into host cells. Although the reason for this is not yet clear, the longer translocation signal often coincides with the domain which interacts with a type III secretion chaperone (48, 77).

### **iii. Characteristics of the chaperone binding domain.**

Chaperone-binding T3SS-secreted effectors characterized thus far all have a single chaperone-binding domain (CBD), although at least one effector binds two chaperone dimers in this region (2). The CBD is almost always found close to the N-terminus of the effector between amino acid residues 50-200 (51). Notable exceptions are

members of the *Pseudomonas syringae* effector HopO1-1 family, which has a CBD in the middle third of the protein, and HpaB, which binds to the secreted effector HpaA at its C-terminus (42, 56).

The CBD is typically required for protein translocation into host cells (28, 32, 50, 92). However, the chaperone binding domain can exert an inhibitory effect on secretion in the absence of the chaperone. *Yersinia* YopE and SicP from *Salmonella* were both secreted without the chaperone present, but only after fragments of the chaperone binding domain had been deleted (17, 48). The CBD was not required for some functions of YopE. The CBD may confer instability to the effector protein when not stabilized by a chaperone; in fact, several secreted substrates were found to aggregate and destabilize in the absence of the chaperone (17, 32). The CBD of the *Yersinia enterocolitica* effector YopO doubles as a membrane localization signal, providing further evidence that chaperones may bind here to prevent aggregation (50). However, in a study of three *P. syringae* effectors, the domain conferring chaperone-dependent stability was found to be separate from the chaperone binding domain itself, suggesting that the function of the CBD is varied among effectors (58). A second proposed explanation for the apparent secretion-inhibitory role of the chaperone-binding domain is that the chaperone binding domain may form an inhibitory structure, or bind to an unknown inhibitor. This theory is based on the observation that the deletion of the chaperone binding domain of YopE led to translocation in the absence of the chaperone (73). Although the chaperone –effector interaction may have evolved as a means to promote effector stability, stability is not the only functional role of the CBD. The other diverse functions of the CBD are synonymous with those of the chaperone itself, which will be discussed below.

## **II. Class I T3SS Chaperones**

### **IIA. Chaperones are small, dimerized proteins that bind to one or more secreted effector protein.**

Effector-specific (Class 1) type III secretion chaperones were discovered in *Yersinia* as small, acidic proteins required for the accumulation of their cognate effectors and for bacterial virulence (34). Early studies in *Yersinia* confirmed that the Syc chaperones bound directly to Yop effector proteins (35, 88), and this direct binding relationship has been consistently confirmed with other chaperone-effector pairs. Although T3SS chaperones are generally required for secretion of partner effector proteins, several studies have shown evidence of residual levels of chaperone-independent secretion in the absence of the CBD or the chaperone (82, 87, 88). Chaperones also bind to regulatory or secretion system proteins (discussed below). It has been generally observed that chaperones are not themselves secreted; however, evidence for Spa15 secretion into media and host cells was recently reported (31). T3SS chaperones were first discovered in plant pathogens in 1998 (38, 84) and have been characterized or predicted in a wide range of gram-negative phytopathogenic bacteria.

### **IIB. General Structural features of the chaperone-effector interaction.**

Several crystallization studies have revealed that despite a complete lack of sequence conservation among the chaperones, they have a highly conserved structure consisting of three  $\alpha$ -helices and a five-stranded  $\beta$ -sheet (54, 59, 67, 85). Crystal structures of chaperones bound to effectors show that the unfolded chaperone-binding domain of the effector protein wraps around the exterior chaperone dimer (12, 51, 76). Cross-complementation studies have suggested that the T3SS targeting mechanism is universal

and conserved between animal and plant pathogens (7, 70); Birtalan *et al.* proposed that the conserved three-dimensional structure of the effector-chaperone complex might be part of this universal signal (13).

### **IIC. Chaperone-effector specificity.**

Most characterized chaperones bind to a single partner effector with a high degree of specificity. Some exceptions are known; Page *et al.* (2002) reported that the *Shigella dysenteriae* chaperone Spa15 binds multiple effectors, leading the authors to propose that Spa15 belongs to a subclass of chaperones (class IIB) with broad specificity. Although it has been speculated that a novel structural variant of Spa15 might be a feature associated with broad specificity (85), the molecular basis of chaperone-effector specificity has not been determined. CesT and InvB are other examples of chaperones that interact with and facilitate secretion of multiple effectors (28).

Although specific chaperone-effector pairs have been characterized, T3SS chaperones in at least two well-characterized plant pathogen systems interact with multiple secreted effectors. The *P. syringae* chaperones ShcO, ShcS1, and ShcS2 can each bind, stabilize, and facilitate secretion of three cognate effectors with sequence similarity (42), and the *X. campestris* chaperone HpaB is a “global chaperone” required for secretion of five different effectors and for pathogenicity (18). It is possible that, because *P. syringae* and *X. campestris* express a large number of effectors, it would be beneficial for T3SS chaperones in these species to bind more than one effector protein. Chaperone-effector binding range in plant pathogens with fewer effectors, such as *Dickeya chrysanthemi* and *Erwinia amylovora*, has not been reported, but it could

provide clues as to whether broad effector-binding specificity is an effect of high effector number.

### **IID. The roles of T3SS chaperones.**

#### **i. Chaperones dock effector proteins to the secretion apparatus.**

The requirement of chaperones for secretion of some effectors has long led to speculation that chaperones may serve as a docking device for effector interaction with the T3SS. Indeed, since 2003, *in-vivo* co-immunoprecipitation and co-localization studies have confirmed that several class I chaperones interact directly with the ATPase component of the T3SS. Akeda and Galan (2005) found that the *Salmonella enterica* sv. Typhimurium ATPase InvC not only binds to the T3SS chaperone SicP, but also catalyzes the dissociation of the chaperone from its cognate effector in an ATP-dependent manner. The chaperone-effector complex of CesT and Tir from enteropathogenic *Escherichia coli* also interacts with the ATPase in a chaperone-dependent manner (40, 82). However, membrane localization of CesT is not ATPase-dependent.

Recently, evidence has emerged that some T3SS chaperones interact with secretion system components other than the ATPase. For example, HpaB in *Xanthomonas campestris* pv. *vesicatoria* interacts with the conserved inner membrane proteins HrcU and HrcV *in vitro* (57). HrcU and its homologs (i.e., FlhB and YscU) interact with T3SS substrate specificity switches and may be involved in T3SS substrate recognition (5, 33, 55). Another potential interactor with a T3SS chaperone is CdsQ in *Chlamydia trachomatis*, orthologous to the putative C-ring component of T3SS and flagellar secretion apparatuses (75). Members of the YscU and HrpQ families are known interactors with the HrcN central ATPase (57). The recently-discovered interactions

between chaperones and multiple components of the apparatus base suggest a more complex T3SS-targeting role for secretion chaperones than previously assumed.

The structural basis of the interaction between T3SS chaperones and secretion apparatus components is not known. Evidence suggests that the C-terminal end of the ATPase is required for interacting with chaperones (2, 94). The recent solution of the first crystal structure of a T3SS ATPase, InvC, led to the identification of a putative chaperone docking interface on the ATPase (94). Mutation of a conserved hydrophobic residue at this site (V394) abolished the ability of the ATPase to bind a T3SS chaperone. Since this structure is not present on ATPases of the flagellar secretion system, it was proposed that pathogenicity-associated T3SS ATPases are specially adapted to bind class I chaperones (94). Less is known about what chaperone factors may be required for interaction with the ATPase. Hydrostatic amino acids of two chaperones, SigE from *S. enterica* and CesT from *E. coli*, have been identified that are required for effector secretion but not for effector binding (47, 82). The authors speculated that these residues may be involved in interaction with the T3SS ATPase, but no specific amino acids have been confirmed to be involved in the chaperone-T3SS interaction.

#### **ii. Chaperones confer secretion system specificity to effectors.**

Consistent with the effector-ATPase docking model, several T3SS chaperones are thought to confer secretion system specificity upon various effectors. Lee and Galan reported that although *S. enterica* effectors SopE and SptP are secreted through the SPI-1 T3SS in the presence of the chaperone binding domain (CBD), a mutant SptP or SopE that does not bind the chaperone is *only* secreted through a second T3SS normally dedicated to secretion of flagellar components (48). Another group reported that SopE

chaperone binding-negative mutants are secreted through *both* the flagellar T3SS and the SPI-1 system, but are not translocated into host cells (28). It was unclear what led to the difference in their findings, and why the SopE mutants were able to be secreted but not translocated by the same secretion system. However, the collected findings of these studies point to the conclusion that the chaperone and CBD are important in trafficking *Salmonella* effectors to the correct secretion system. The authors speculated that the N-terminal 15-20 amino acids could represent an “ancestral” secretion signal recognized by the flagellar T3SS, and this recognition may be somehow overcome by chaperone binding downstream (28).

Because chaperones bind directly to the T3SS apparatus and play a role in secretion system specificity, the chaperone-T3SS interaction is one possible point at which effector-T3SS specificity might be conferred. This role would be especially important in the presence of two pathogenicity-associated T3SS, as is the case in *Salmonella*. Whether chaperones can interact with a broad or narrow spectrum of T3SS components has not been determined, although both chaperones and the secretion apparatus are highly structurally conserved. It has been reported that the *Y. pestis* effector YopE can be secreted by *Salmonella enterica* and the plant pathogen *Xanthomonas campestris*, but only in the presence of its cognate chaperone SycE (70). This might suggest that SycE could interact with a wide variety of T3SS ATPases, but it also could be possible that the stabilization of YopE by SycE is sufficient to allow low levels of secretion by multiple T3SSs. Interestingly, another study demonstrated that YopE can be secreted by the *Erwinia chrysanthemi* T3SS without the SycE chaperone present (7), but this study was conducted in an *E. coli* expression system that resulted in extremely low

levels of secretion. In any case, it is clear that the activity of chaperones is conserved in multiple systems. Whether this includes direct binding to T3SS components is a question yet to be addressed in the literature.

### **iii. Chaperones stabilize or prevent aggregation of cognate effectors.**

The observation that the chaperone binding domain may inhibit secretion in the absence of a chaperone led some to question whether the chaperone may function in masking a structure inhibitory to secretion. Ehrbar *et al.* proposed that the chaperone could competitively prevent the CBD from binding to an unknown secretion inhibitor (28), but other studies have demonstrated that the chaperone binding domain is itself secretion-inhibitory, conferring destabilization to the effector protein (50). Effectors in several different systems have reduced half-lives in the absence of the chaperone (39, 58). It was originally proposed, based on the crystal structures of several secreted effectors, that effectors tend to have a disordered, proteolysis-labile N-terminus. The chaperone might mask this disorder and prevent proteolysis (13, 76). However, not all chaperone-aided effectors have a disordered N-terminus (67). Letzelter *et al.* (2006) found that the chaperone binding domains of several effectors in *Y. pestis* are prone to autoaggregation, conferring insolubility to the protein in the absence of the chaperone (50). In one of these effectors, YopO, the CBD coincided with a membrane localization domain responsible for targeting the effector to the host cell membrane. So, in some cases the chaperone directly binds to destabilizing domain necessary for function in the host cell.

In other cases, there is evidence that the chaperone may confer stability by a slightly different mechanism. In the plant pathogen *Pseudomonas syringae*, stability assays showed that the chaperones ShcB1, ShcM, and ShcV1 protect effector proteins

from degradation by the Lon protease, but that the target for proteolysis lies outside the chaperone binding domain (58). The stabilization function of chaperones is not universal, as some effectors are not destabilized in the absence of their cognate chaperone (18, 84, 88). It should be noted however, that the possibility of stabilization by other undiscovered chaperones was not ruled out.

#### **iv. Chaperones may regulate the expression of cognate effectors.**

Some of the earliest reports of chaperones proposed a function as regulators of effector gene expression (34). Although this initial characterization was due to effector destabilization in the absence of the chaperone, it was later discovered that some T3SS chaperones also regulate transcription or translation of specific effector proteins. In *Salmonella typhimurium*, the chaperone SicA binds directly to the transcription factor InvF to cause it to activate transcription from effector gene promoters (23). The chaperone-like protein ExsC in *P. aeruginosa* binds to and inhibits the anti-activator ExsD, relieving ExsD-mediated transcriptional repression (24). Among plant pathogens, a protein similar in structure to classic T3SS chaperones, HrpG, is an indirect transcriptional de-repressor of the *P. syringae* T3SS (89).

The *Yersinia pestis* YopH chaperone SycH works at the posttranscriptional level to activate expression of *yop* genes; by binding to translational repressors YscM1 and YscM2, SycH relieves the repression to initiate Yop synthesis (20). Recently, it was shown that the chaperone SycO also binds to YscM1 (Dittman *et al.* 2007), suggesting that posttranscriptional regulation by chaperones could be more widespread than originally suspected.

#### **v. Chaperones may impose a temporal hierarchy of secretion.**

Upon contact with the host cell, the T3SS of *S. enterica* begins translocating a pre-synthesized pool of effectors into the host cell within seconds (74). While the phenomenon of substrate-specificity switching between the secretion apparatus and effectors has long been recognized, microscopic and biochemical translocation assays have only recently demonstrated a hierarchical order of translocation among the effectors themselves (93). This fine-tuning of effector secretion could be important to deliver proteins critical early in the interaction first (for example, cell invasion and immune response avoidance factors), or to temporally separate effectors with opposing functions (for example, actin polymerization and depolymerization factors).

The observation that some effectors have chaperones while others do not led to the proposal that chaperones may function in the preferential secretion of “early burst” effectors (13). There is now evidence that chaperones are involved in imposing this hierarchy of secretion in both *Yersinia* and *Salmonella*. For example, the N-terminus of the *Y. pestis* effector YopE is translocated in the absence of its chaperone if all other effector genes are deleted from the cell. Addition of the other effectors reduces YopE translocation levels unless the chaperone SycE binds, suggesting that SycE may confer a competitive advantage to YopE (17), which in turn may limit the translocation levels of other effectors (1). In *Salmonella enterica*, the effector SipA is translocated earlier than the effector SptP, even when both effectors are pre-formed in the bacterial cytosol (91). Computer modeling experiments demonstrated that this hierarchy of secretion might result from the SipA and SptP cognate chaperones binding to limited T3SS sites at slightly different affinities. In enterohemorrhagic *E. coli*, a system in which the

chaperone CesT binds many effectors, differential effector-chaperone binding affinity was proposed to impose the secretion hierarchy (62). Although it is logical to assume that differential chaperone-T3SS or chaperone-effector binding affinity could confer a competitive advantage to some effectors over others, this theory has not been tested biochemically.

While SycE and SptP may help YopE compete with other effectors for access to the secretion system, the *Yersinia* chaperone SycH works to impose a hierarchy using a more advanced mechanism. SycH binds to the negative regulator LcrQ to form what may be an inhibitory complex at the secretion apparatus (93). This complex decreases the secretion levels of all Yops except YopH, allowing YopH to be secreted earlier than the other Yops.

It is not known whether a temporal hierarchy of effector secretion is common in plant pathogens, and even substrate specificity switching mechanisms of the T3SS in plant pathogens are poorly understood. *Pseudomonas* and *Erwinia* effector secretion into culture media can occur during active growth of the Hrp needle (45), which could suggest that substrate specificity switching is not regulated in the same manner as in *Yersinia*. However, a Hrp needle is required for secretion of effectors into the media, even during full levels of effector expression (90). It is possible that secretion could be differently regulated in the plant environment than *in vitro*, and some plant pathogens are known to secrete T3SS substrates in a specific order. *Ralstonia solanacearum* T3SS secretion is host cell contact-dependent, for example (4), and substrate specificity of the *Xanthomonas campestris* T3SS is controlled by the regulatory protein HpaC and the T3SS chaperone HpaB (55). HpaB is sequestered by the secretion control protein HpaA,

preventing other secreted effectors from premature Hpa-dependent secretion (56). The secretion of HpaA prior to other effectors is the first known example of a temporal secretion hierarchy among effectors in plant pathogenic bacteria. Of the many complex roles of chaperones discussed here, mediation of secretion dynamics among effectors is perhaps the least-understood.

### **III. *Erwinia amylovora* as a system for studying chaperone-effector interaction**

#### **IIIA. *Erwinia amylovora* biology and economic significance**

*Erwinia amylovora*, a gram-negative bacterium of the family *Enterobacteriaceae*, causes a devastating fire blight disease of apple trees and other plants in the family Rosaceae. The bacterium enters the tree through blossoms or through wounds in actively growing shoots, replicating rapidly and causing tissue necrosis (83). Infected shoots have a crooked shape and burnt appearance characteristic of fire blight. *E. amylovora* spreads throughout the tree via the xylem, and produces copious amounts of a saccharide-rich exopolysaccharide (EPS) which aids the bacteria in movement throughout the plant and in dispersal by wind and insects (83). *E. amylovora* causes significant yield losses every year in apple and pear growing regions, and can lead to the death of young and highly susceptible trees. Unfortunately, options for chemical control of fire blight are very limited; the few commercially available antibiotic sprays are becoming reduced in efficacy due to bacterial antibiotic resistance (60). Research into the molecular mechanisms of *E. amylovora* pathogenesis will be important in revealing new targets for control.

### **IIIB. The *E. amylovora* effector DspE**

Biochemical analysis of culture supernatants has indicated that *E. amylovora* secretes at least four putative effector proteins into media via the T3SS: Eop1, Eop3, AvrRpt2Ea/Eop4, and DspE (63). *eop1* and *avrRpt2Ea* deletion mutants have been characterized and were shown to affect host range and virulence, respectively, in the laboratory (9, 95). In contrast, the effector DspE is required for *E. amylovora* pathogenicity and population growth *in planta*. The *dspE* gene was identified as the result of several transposon mutagenesis screens for mutants that abolished pathogenicity but not the hypersensitive response on tobacco (10, 78). DspE is 1,838 amino acids long, among the largest secreted effectors characterized, with homologs in several important plant pathogens including *Pseudomonas syringae*, *Ralstonia solanacearum*, and *Pantoea stewartii*. Deletion of these DspE homologs typically leads to a reduction in virulence or complete loss of pathogenicity (16). *avrE*, a *dspE* homolog in *Pseudomonas syringae*, can partially complement a *dspE* mutant, suggesting functional conservation within the DspE class of effectors (14). The sequence of *dspE* is highly conserved among strains of *E. amylovora* and *E. pyrifoliae* (41), and *dspE* from *E. pyrifoliae* and from *Rubus*-infecting species of *E. amylovora* complement the virulence of a *dspE* knockout mutant of *E. amylovora* strain Ea1189 (Triplett, unpublished). As the above studies indicate, DspE is an ancient, essential component of many pathogen-host interactions.

Although its specific function is unknown, DspE suppresses salicylic acid-mediated cell wall defenses when transiently expressed in plant cells, and induces necrotic cell death in host and nonhost cells (16, 26). The DspE homolog AvrE is functionally redundant to the *P. syringae* effector HopM1, which mediates the

degradation of vesicle trafficking pathway components (64), so it is possible that AvrE and DspE work through a similar mechanism to suppress host immunity. The functional targets of DspE are unknown, but several leucine rich-repeat (LRR) kinases have been identified in apple which interact with DspE in yeast and *in vitro* (61). RNAi silencing of these DspE-interacting proteins of *Malus*, or DIPMs, led to a slight increase in resistance to *E. amylovora* (15). Although the localization of DspE in the host cell has not been reported, the sequences of DspE and its homologs include a WXXXE motif required for function and another conserved motif similar to an endoplasmic reticulum targeting signal (44). Taken together, these studies suggest that DspE could function in multiple and novel roles in the plant infection process.

### **IIIC. The *E. amylovora* chaperone DspF.**

The first sequence analyses of the *dsp* region of *E. amylovora* showed that *dspE* shared a transcriptional unit with a small orf, named *dspB* or *dspF* (14, 38). For this discussion, the gene will heretofore be referred to as *dspF*. The predicted gene product of the *dspF* orf had the defining characteristics of a class I T3SS chaperone: a size of 16 kDa, an acidic pI, and a helical structure. Disruption of the *dspF* gene caused a drastic reduction in virulence and led to an apparent disappearance of DspE protein from the supernatant, strongly indicating that *dspF* encoded a DspE chaperone (38). Biochemical studies showed that the protein DspF binds directly to DspE *in vitro*, as well as another unknown interactor of about 80 kDa (39). DspF was required for immunodetection of DspE in *E. amylovora* cells, although the chaperone did not significantly affect DspE transcriptional levels, indicating that DspF must affect either stability or translation of DspE. Despite the apparent lack of DspE in the culture supernatants in the *dspF* mutant

background, the fact that the *dspF* mutant retains a reduced degree of T3SS-dependent pathogenicity suggests that DspE is still secreted at some level in the absence of its chaperone (39).

Many of the sequenced bacterial pathogens containing a *dspE* homolog also carry a gene homologous to *dspF*. The role of a *dspF* homolog has only been characterized in *Pantoea stewartii* (44). The *P. stewartii* gene *wtsF* has a positive effect on the stability of the effector WtsE, but is not required for virulence, possibly due to the presence of a redundant chaperone. In fact, among characterized chaperones in plant pathogens, only DspF and HpaB from *Xanthomonas campestris* have a significant effect on virulence. (As mentioned previously, HpaB is the only known T3SS chaperone in *X. campestris*). In other effector systems studied, redundancy of effectors and chaperones precludes a virulence phenotype for mutants of a single chaperone. The requirement of DspF in virulence makes *E. amylovora* a useful system for the study of chaperone function in plant pathogens.

#### **IV. Rationale and project goals.**

There are few studies illustrating the role of type III secretion chaperones in plant pathogen systems. However, these studies have expanded the known diversity of chaperone functional roles and challenged some previous paradigms of secretion signalling. Figure 1-1 compares three variations of chaperone-effector binding between *P. syringae*, *X. campestris*, and enterobacterial pathogens such as *Salmonella enterica* sv. Typhimurium. In the Enterobacteriaceae, chaperones each bind to the N-terminus of a single secreted effector in a highly specific manner. Little or no effector secretion occurs in the absence of each cognate chaperone (Figure 1-1A). However, in *P. syringae*, which

expresses a large number of chaperones and secreted effectors during infection, some chaperones may interchangeably bind to and stabilize several paralogous effector proteins (Figure 1-1B). While *Xanthomonas campestris* pv. *vesicatoria* also harbors numerous putative secreted effectors, HpaB is the only known chaperone. HpaB is required for the translocation, but not the stabilization, of multiple effector proteins, but it also aids in the development of a secretion hierarchy via a novel mechanism (Figure 1-1C). Thus, the roles and binding patterns of chaperone-effector pairs may vary substantially between systems. How great is the diversity of chaperone roles among other plant pathogens and symbionts, and what selective pressures among different organisms contributed to this divergence? Study of chaperone-effector interaction in a wider variety of pathogens and symbionts is needed to understand the spectrum of T3SS regulation and targeting mechanisms.

The purpose of this research is to identify translocation signals of the effector DspE and further characterize DspF chaperone function in *E. amylovora*, a system that is both enterobacterial and plant-associated. As previously mentioned, the strong virulence phenotype of *dspE* and *dspF* deletion strains makes this effector-chaperone pair a conducive system for study. First, the project aims to characterize the general mechanism of interaction between the critical *E. amylovora* effector, DspE, and its chaperone, DspF. Toward this objective, I performed an extensive series of targeted mutagenesis experiments in both DspE and DspF. Secretion assays, adenylate-cyclase reporter-based translocation assays, and protein-protein interaction studies were used to analyze these mutants. In Chapter 2, I demonstrated that between 31 and 51 N-terminal amino acids are required for both DspE secretion and for translocation into tobacco cells, while longer

fragments lead to higher translocation levels. I identified a conserved regions between amino acids 2-10 and 31-40 required for optimal translocation, and showed that an N-terminal chaperone binding domain of DspE lies between amino acids 51-100, although neither this domain nor the presence of DspF was required for translocation. In Chapter 3, I used a computer-generated, homology-based model of DspF to identify amino acid residues required for full virulence of *E. amylovora*. In mutagenesis studies, four highly-conserved residues with predicted localization in a helix-binding groove were identified as required for DspF function; three of these residues were required for interaction with DspE in yeast, supporting the putative role of electronegative residues of the helix-binding groove in chaperone function.

The second aim of this project has been to identify potential new roles of DspF by identifying putative DspF interactors in *E. amylovora*, and assessing the function of some of these predicted interactions (Chapter 4). In a directed yeast two-hybrid screen, four novel putative DspF-interacting proteins were identified, including two putative components of the T3SS machinery (HrcQ and HrcU) and two effector proteins with little previous characterization (Eop1 and Eop3). Eop1 and Eop3 have predicted chaperones, while Eop4, an effector that does not interact with DspF in yeast, has no predicted chaperone. Although DspF interacted with Eop1 and Eop3, translocation assays indicated that deletion of *dspF* did not have a negative impact on effectors other than DspE. Interestingly, translocation levels of Eop1 and Eop3 were increased in the absence of DspF, leading to the hypothesis that DspF could have a direct or indirect negative role on translocation of some effectors by facilitating competition by DspE or through a regulatory mechanism. The phenotype of a *dspF* deletion mutant could be complemented

by ectopic DspE expression, suggesting that DspF has a role in maintaining adequate DspE concentrations within the cell. Thus, this study provides support for formerly hypothesized roles of DspF, and points to new interactors and potential DspF functions. A fourth, unrelated study I completed on genomic differences between *Erwinia amylovora* and close taxonomic relatives is included in the appendix. In combination with the mapping and characterization of the DspE-DspF interaction, the work in this dissertation contributes significantly to the understanding of *Erwinia amylovora* molecular pathogenesis.

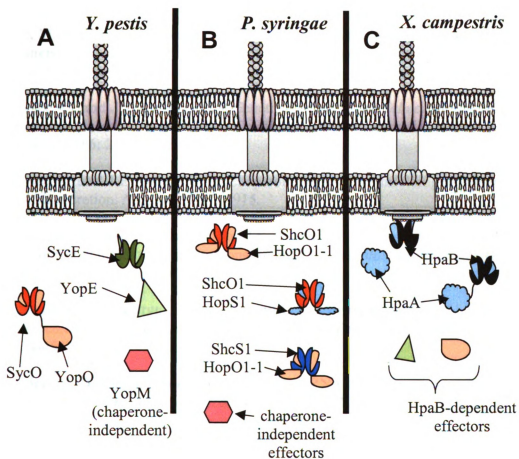


**Figure 1-1.** Variations in the binding pattern and roles of T3SS chaperones. **A.** Specific chaperone-effector interactions in *Yersinia pestis*. The N-terminus of secreted effectors including YopE and YopO each bind a single chaperone, SycE (in green) and SycO (in orange), respectively, which may stabilize and dock the effector to peripheral inner membrane components of the secretion system. A small number of effector proteins, such as the effector YopM, have no known chaperone. **B.** While some chaperone-effector interactions in the plant pathogen *Pseudomonas syringae* are thought to be highly specific, some chaperones interact with multiple related effectors. The chaperones ShcO1 (orange) and ShcS1 (blue) can interchangeably facilitate secretion of HopO1-1 (light orange) and HopS1 (light blue). Chaperone binding sites have been mapped to the N-terminus or to the central portion of various effectors. **C.** The *Xanthomonas campestris* chaperone HpaB (in black) interacts with the C-terminus of the secretion control protein HpaA (light blue). Upon HpaA translocation into host cells, HpaB binds the N-terminus of multiple other HpaB-dependent effectors and renders them competent for secretion.

## WORKS CITED

1. **Aili, M., E.L. Isaksson, S.E. Carlsson, H. Wolf-Watz, R. Rosqvist and M.S. Francis.** 2008. Regulation of *Yersinia* Yop-effector delivery by translocated YopE. *Int. J. Med. Microbiol.* **298**: 183-192.
2. **Akeda, Y., and J.E. Galan.** 2004. Genetic analysis of the *Salmonella enterica* type III secretion-associated ATPase InvC defines discrete functional domains. *J. Bacteriol.* **186**: 2402-2412.
3. **Akeda, Y. and J.E. Galan.** 2005. Chaperone release and unfolding of substrates in type III secretion. *Nature* **437**: 911-915.
4. **Aldon, D., B. Brito, C. Boucher, and S. Genin.** 2000. A bacterial sensor of plant cell contact controls the transcriptional induction of *Ralstonia solanacearum* pathogenicity genes. *EMBO J* **19**: 2304-2314.
5. **Allaoui, A., S. Woestyn, C. Sluiter, and G.R. Cornelis.** 1994. YscU, a *Yersinia enterocolitica* inner membrane protein involved in Yop secretion. *J. Bacteriol.* **176**: 4534-4542.
6. **Anderson, D.M., O. Schneewind.** 1997. An mRNA signal for the secretion of Yop proteins by *Yersinia enterocolitica*. *Science* **278**: 1140-1143.
7. **Anderson, D.M., D.E. Fouts, A. Collmer and O. Schneewind.** 1999. Reciprocal secretion of proteins by the bacterial type III machines of plant and animal pathogens suggests universal recognition of mRNA targeting signals. *Proc. Natl. Acad. Sci. USA* **96**: 12839-12843.
8. **Arnold, R., S. Brandmaier, F. Kleine, P. Tischler, E. Heinz, S. Behrens, A. Niinikoski, H.W. Mewes, M. Horn, T. Rattei.** 2009. Sequence-based prediction of type III secreted proteins. *PLoS Pathog* **5**: e1000376.
9. **Asselin, J.E., K.N. Yip, and S.V. Beer.** 2008. Eop1 differs in strains of *Erwinia amylovora* that differ in host specificity. Proceedings of the XI International Workshop on Fire Blight. Ed. K.B. Johnston and V.O. Stockwell. *Acta Hort* **793**: 213-214.
10. **Barny, M.A., M.H. Guoinebretiere, B. Marcais, E. Coissac, J.P. Paulin and J. Laurent.** 1990. Cloning of a large gene cluster involved in *Erwinia amylovora* CFBP 1430 virulence. *Mol. Microbiol.* **4**: 777-786.
11. **Belleman, P., and K. Geider.** 1992. Localization of transposon insertions in pathogenicity mutants of *Erwinia amylovora* and their biochemical characterization. *J. Gen. Microbiol.* **138**: 931-940.

12. **Birtalan, S., and P. Ghosh.** 2001. Structure of the *Yersinia* type III secretory system chaperone SycE. *Nat Struct Biol.* **8**: 974-8.
13. **Birtalan, S.C., R.M. Phillips, and P. Ghosh.** 2002. Three-dimensional secretion signals in chaperone-effector complexes of bacterial pathogens. *Mol. Cell* **9**: 971-980.
14. **Bogdanove, A.J., J.F. Kim, Z. Wei, P. Kolchinsky, A.O. Charkowski, A.K. Conlin, A. Collmer, and S.V. Beer.** 1998. Homology and functional similarity of an hrp-linked pathogenicity locus, *dspEF*, of *Erwinia amylovora* and the avirulence locus *avrE* of *Pseudomonas syringae* pathovar tomato. *Proc. Natl. Acad. Sci. USA* **95**: 1325-1330.
15. **Borejsza-Wysocka, E.E., M. Malnoy, X. Ment, J.M. Bonasera, R.M. Nissinen, J.F. Kim, S.V. Beer, and H.S. Aldwinckle.** 2006. The fire blight resistance of apple clones in which DspE-interacting proteins are silenced. *Acta Hort.* **704**: 509-513.
16. **Boureau, T., H. El Maarouf-Boteau, A. Garnier, M.-N. Brisset, C. Perino, I. Pucheu, and M.-A. Barny.** 2005. DspA/E, a type III effector essential for *Erwinia amylovora* pathogenicity and growth in planta, induces cell death in host apple and nonhost tobacco plants. *Mol. Plant Microbe Interact.* **19**: 16-24.
17. **Boyd, A.P., I. Lambermont, and G.R. Cornelis.** 2000. Competition between the Yops of *Yersinia enterocolitica* for delivery into eukaryotic cells: role of the SycE chaperone binding domain of YopE. *J. Bacteriol.* **182**: 4811-4821.
18. **Büttner, D., D. Gurlebeck, L.D. Noel, and U. Bonas.** 2004. HpaB from *Xanthomonas campestris* pv. *vesicatoria* acts as an exit control protein in type III-dependent protein secretion. *Mol Microbiol* **54**: 755-768.
19. **Büttner, D. and S.-Y. He.** 2009. Type III protein secretion in plant pathogenic bacteria. *Plant Physiol.* **150**: 1656-1664.
20. **Cambronne, E.D., J.A. Sorg and O. Schneewind.** 2004. Binding of SycH chaperone to YscM1 and YscM2 Activates effector yop expression in *Yersinia enterocolitica*. *J. Bacteriol.* **186**: 829-841.
21. **Cheng, L.W., D.M. Anderson and O. Schneewind.** 1997. Two independent type III secretion mechanisms for YopE in *Yersinia enterocolitica*. *Mol. Microbiol.* **24**: 757-765.
22. **Cornelis, G.** 2006. The Type III secretion injectosome. *Nature Rev. Microbiol.* **4**: 811-825.
23. **Darwin, K.H. and V.L. Miller.** 2001. Type III secretion chaperone-dependent regulation: activation of virulence genes by SicA and InvF in *Salmonella typhimurium*. *EMBO J.* **20**: 1850-1862.

24. **Dasgupta, N., G.L. Lykken, M.C. Wolfgang, and T.L. Yahr.** A novel anti-anti-activator mechanism regulates expression of the *Pseudomonas aeruginosa* type III secretion system. *Mol. Microbiol.* **53**: 297-308.
25. **P. Delepelaire.** 2004. Type I secretion in gram-negative bacteria. *Biochim. Biophys. Acta* **1694**: 149-161.
26. **Debroy, S., R. Thilmony, Y.-B. Kwack, K. Nomura, and S.-Y. He.** 2004. A family of conserved bacterial effectors inhibits salicylic acid-mediated basal immunity and promotes disease necrosis in plants. *Proc. Natl. Acad. Sci. USA* **101**: 9927-9932.
27. **Ding, Z., K. Atmakuri and P. J. Christie.** 2003. The outs and ins of bacterial type IV secretion substrates. *Trends in Microbiol.* **11**: 527-535.
28. **Ehrbar, K., B. Winnen and W. Hardt.** 2005. The chaperone binding domain of SopE inhibits transport via flagellar and SPI-1 TTSS in the absence of InvB. *Mol. Microbiol.* **59**: 248-264.
29. **Enninga, J., J. Mounier, P. Sansonetti and G.T. Nhieu.** 2005. Secretion of type III effectors into host cells in real time. *Nat Methods* **2**: 959-965.
30. **Evans, L.D.B., G.P. Stafford, S. Ahmed, G.M. Fraser and C. Hughes.** 2006. An escort mechanism for cycling of export chaperones during flagellum assembly. *Proc. Natl. Acad. Sci. USA* **103**: 17474-17479.
31. **Faherty, C.S., and A.T. Morelli.** 2009. Spa15 of *Shigella flexneri* is secreted through the type-III secretion system and prevents staurosporine-induced apoptosis. *Infection and Immunity* online ahead of print. doi:10.1128/IAI.00800-09.
32. **Feldman, M.A., Muller, S., Wuest, E., and Cornelis, G.R.** 2002. SycE allows secretion of YopE-DHFR hybrids by the *Yersinia enterocolitica* type III Ysc system. *Mol. Microbiol* **46**: 1183-1197.
33. **Ferris, H.U., Y. Furukawa, T. Minamino, M.B. Kroetz, M. Kihara, K. Namba, and R.M. McNab.** 2005. FlhB regulates ordered export of flagellar components via autocleavage mechanism. *J. Biol. Chem.* **280**: 41236- 41242.
34. **Forsberg, A. and H. Wolf-Watz.** 1990. Genetic analysis of the YopE region of *Yersinia* spp.: Identification of a novel conserved locus, yerA, regulating Yop gene expression. *J. Bacteriol.* **172**: 1547-1555.
35. **Frithz-Lindsten, E., R. Rosqvist, L. Johansson and A. Forsberg.** 1995. The chaperone-like protein YerA of *Yersinia pseudotuberculosis* stabilizes YopE in the cytoplasm but is dispensable for targeting to the secretion loci. *Mol. Microbiol.* **16**: 635-647.

36. **Furutani, A., M. Takaoka, H. Sanada, Y. Noguchi, T. Oku, K. Tsuno, H. Ochiai, and S. Tsuge.** 2009. Identification of novel type III secretion effectors in *Xanthomonas oryzae* pv. *oryzae*. *Mol. Plant Microbe Interact.* **22**: 96-106.
37. **Galan, J., and H. Wolf-Watz.** 2006. Protein delivery into eukaryotic cells by Type III secretion machines. *Nature* **444**: 567-573.
38. **Gaudriault, S., L. Malandrin, J.-P. Paulin and M.-A. Barny.** 1997. DspA, an essential pathogenicity factor of *Erwinia amylovora* showing homology with AvrE of *Pseudomonas syringae*, is secreted via the Hrp secretion pathway in a DspB-dependent way. *Mol. Microbiol.* **26**: 1057-1069.
39. **Gaudriault, S., J.-P. Paulin and M.A. Barny.** 2002. The DspB/F protein of *Erwinia amylovora* is a type III secretion chaperone ensuring efficient intrabacterial production of the Hrp-secreted DspA/E pathogenicity factor. *Mol. Plant Pathology* **3**: 313-320.
40. **Gauthier, A. and B.B. Finlay.** 2003. Translocated intimin receptor and its chaperone interact with ATPase of the type III secretion apparatus of enteropathogenic *Escherichia coli*. *J. Bacteriol.* **185**: 6747-6755.
41. **Giorgi, S. and M. Scortichini.** 2005. Molecular characterization of *Erwinia amylovora* strains from different host plants through RFLP analysis and sequencing of *hrpN* and *dspA/E* genes. *Plant Pathology* **254**: 789-798.
42. **Guo, M., S.T. Chancey, F. Tian, Z. Ge, Y. Jamir, and J.R. Alfano.** 2005. *Pseudomonas syringae* type III chaperones ShcO1, ShcS1, and ShcS2 facilitate translocation of their cognate effectors and can substitute for each other in the secretion of HopO1-1. *J. Bacteriol.* **187**: 4257-4269.
43. **Guttman DS, Vinatzer BA, Sarkar SF, Ranall MV, Kettler G, Greenberg JT.** 2002. A functional screen for the type III (Hrp) secretome of the plant pathogen *Pseudomonas syringae*. *Science* **295**: 1722-1726.
44. **Ham, J.H., D.R. Majerczak, A.S. Arroyo-Rodriguez, D.M. Mackey and D.L. Coplin.** 2006. WtsE, an AvrE-family effector protein from *Pantoea stewartii* subsp. *stewartii*, causes disease-associated cell death in corn and requires a chaperone protein for stability. *Mol. Plant Microbe Interact.* **19**: 1092-1102.
45. **Jin, Q., W. Hu, I. Brown, G. McGhee, P. Hart, A. Jones and S.-Y. He.** 2001. Visualization of secreted Hrp and Avr proteins along the Hrp pilus during type III secretion in *Erwinia amylovora* and *Pseudomonas syringae*. *Mol. Microbiol.* **40**: 1129-1139.

46. **Karavolos, M.H., M. Wilson, J. Henderson, J.J. Lee and C.M.A. Khan.** 2004. Type III secretion of the secreted effector SopE is mediated by an N-terminal amino acid signal and not an mRNA sequence. *J. Bacteriol.* **187**: 1559-1567.
47. **Knodler, L.A., M. Bertero, C. Yip, N.C.J. Strynadka and O. Steele-Mortimer.** 2006. Structure-based mutagenesis of SigE verifies the importance of hydrophobic and electrostatic residues in type III chaperone function. *Mol. Microbiol.* **62**: 928-940.
48. **Lee, S.H. and J.E. Galan.** 2004. Salmonella type III secretion-associated chaperones confer secretion pathway specificity. *Mol. Microbiol.* **51**: 483-495.
49. **Lee, V.T., D.M. Anderson and O. Schneewind.** 1998. Targeting of *Yersinia* Yop proteins into the cytosol of HeLa cells: one-step translocation of YopE across bacterial and eukaryotic membranes is dependent on SycE chaperone. *Mol. Microbiol.* **28**: 593-601.
50. **Letzelter, M. I. Sorg, L. J. Mota, S. Meyer, J. Stalder, M. Feldman, M. Kuhn, I. Callebaut and G.R. Cornelis.** 2006. The discovery of SycO highlights a new function for type III secretion effector chaperones. *EMBO J.* **25**: 3223-3233.
51. **Lilic, M., M. Vujanac and E. Stebbins.** 2006. A common structural motif in the binding of virulence factors to bacterial secretion chaperones. *Mol. Cell* **21**: 653-664.
52. **Lloyd, S.A., M. Norman, R. Rosqvist and H. Wolf-Watz.** 2001. *Yersinia* YopE is targeted for type III secretion by N-terminal, not mRNA, signals. *Mol. Microbiol.* **39**: 520-532.
53. **Lloyd, S.A., M. Sjostrom, S. Andersson and H. Wolf-Watz.** 2002. Molecular characterization of type III secretion signals via analysis of synthetic N-terminal amino acid sequences. *Mol. Microbiol.* **43**: 51-59.
54. **Locher, M., B. Lehnert, K. Krauss, J. Heesemann, M. Groll, and G. Wilharm.** 2005. Crystal structure of the *Yersinia enterocolitica* type III chaperone SycT. *J. Biol. Chem.* **280**: 31149-55.
55. **Lorenz, C., S. Schulz, T. Wolsch, O. Rossier, U. Bonas, and D. Buttner.** 2008. HpaC controls substrate specificity of the *Xanthomonas* type III secretion system. *Plos Pathogens* **4**: doi e1000094.
56. **Lorenz, C., O. Kirchner, M. Egler, J. Stuttmann, U. Bonas, and D. Buttner.** 2008. HpaA from *Xanthomonas* is a regulator of type III secretion. *Mol. Microbiol.* **69**: 344-360.
57. **Lorenz, C. and D. Buttner.** 2009. Functional characterization of the type III secretion ATPase HrcN from the plant pathogen *Xanthomonas campestris* pv. *vesicatoria*. *J. Bacteriol.* **191**: 1414-1428.

58. **Losada, L.C. and S.W. Hutcheson.** 2005. Type III secretion chaperones of *Pseudomonas syringae* protect effectors from Lon-associated degradation. *Mol. Microbiol.* **55**: 941-953.
59. **Luo, Y., M.G. Bertero, E.A. Frey, R.A. Pfuetzner, M.R. Wenk, L. Creagh, S.L. Marcus, D. Lim, F. Sicheri, C. Kay, C. Haynes, B.B. Finlay, and N.C.J. Strynadka.** 2001. Structural and biochemical characterization of the type III secretion chaperones CesT and SigE. *Nature Struct. Biol.* **8**: 1031-1036.
60. **McManus, P.S., V.O. Stockwell, G.W. Sundin, and A.L. Jones.** Antibiotic use in plant agriculture. *Annu. Rev. Phytopathol.* **40**: 443-465.
61. **Meng, X, J.M. Bonasera, J.F. Kimm R. M. Nissinen and S.V. Beer.** 2006. Apple proteins that interact with DspA/E, a pathogenicity factor of *Erwinia amylovora*, the fire blight pathogen. *Mol. Plant Microbe Interactions* **19**:53-61.
62. **Mills, E., K. Baruch, X. Charpentier, S. Kobi, and I. Rosenshine.** 2008. Real-time analysis of effector translocation by the type III secretion system of enteropathogenic *Escherichia coli*. *Cell Host and Microbe* **3**: 104-113.
63. **Nissinen, R.M., A.J. Ytterburg, A.J. Bogdanove, K.J. Van Wijk and S.V. Beer.** 2006. Analyses of the secretomes of *Erwinia amylovora* and selected hrp mutants reveal novel type III secreted proteins and an effect of HrpJ on extracellular harpin levels. *Mol. Plant Pathol.* **8**: 55-67.
64. **Nomura, K., S. Debroy, Y. H. Lee, N. Pumplun, J. Jones, and S.-Y. He.** 2006. A bacterial virulence protein suppresses host innate immunity to cause plant disease. *Science* **313**: 220-223.
65. **Page, A.L., P. Sansonetti, and C. Parsot.** 2002. Spa15 of *Shigella flexneri*, a third type of chaperone in the type III secretion pathway. *Mol. Microbiol.* **43**: 1533-1542.
66. **Pattis, I., E. Weiss, R. Laugks, R. Haas and W. Fischer.** 2007. The *Helicobacter pylori* CagF protein is a type IV secretion chaperone-like molecule that binds close to the C-terminal secretion signal of the CagA effector protein. *Microbiology* **153**: 2896-2909.
67. **Phan, J., J.E. Tropea, and D.S. Waugh.** 2004. Structure of the *Yersinia pestis* type III secretion chaperone SycH in complex with a stable fragment of YscM2. *Acta Crystallographica* **60**: 1591-1599.
68. **Ramamurthi, K.S., and O. Schneewind.** 2002. *Yersinia enterocolitica* type III secretion: mutational analysis of the *yopQ* secretion signal. *J. Bacteriol.* **184**: 3321-3328.

69. **Ramamurthi, K., and O. Schneewind.** 2005. A synonymous mutation in *Yersinia enterocolitica yopE* affects the function of the YopE type III secretion signal. *J. Bacteriol.* **187**: 707-715.
70. **Rossier, O., K. Wengelnik, K. Hahn, and U. Bonas.** 1999. The *Xanthomonas hrp* type III system secretes proteins from plant and mammalian bacterial pathogens. *Proc. Natl. Acad. Sci. USA* **96**: 9368-73.
71. **Rosqvist, R., S. Hakansson, A. Forsberg and H. Wolf-Watz.** 1995. Functional conservation of the secretion and translocation machinery for virulence proteins of *Yersiniae*, *Salmonellae*, and *Shigellae*. *EMBO J.* **14**: 4187-4195.
72. **Sandkvist, M.** 2004. The biology of type II secretion. *Mol. Microbiol.* **40**: 271-283.
73. **Schesser, K., E. Frithz-Lindsten and H. Wolf-Watz.** 1996. Delineation and mutational analysis of the *Yersinia pseudotuberculosis* YopE domains which mediate translocation across bacterial and eukaryotic cellular membranes. *J. Bacteriol.* **178**: 7227-7233.
74. **Schlumberger, M.C., A.J. Muller, K. Ehrbar, B. Winnen, I. Duss, B. Stecher, and W.D. Hardt.** 2005. Real-time imaging of type III secretion: *Salmonella* SipA injection into host cells. *Proc. Natl. Acad. Sci. USA* **102**: 12548–12553.
75. **Spaeth, K.E., Y.-S. Chen, and R.H. Valdivia.** 2009. The *Chlamydia* type III secretion C-ring engages a chaperone-effector protein complex. *PloS Pathog.*: e1000579.
76. **Stebbins, C.E. and J.E. Galan.** 2001. Maintenance of an unfolded peptide by a cognate chaperone in type III secretion. *Nature* **414**: 77-81.
77. **Sory, M.P., A. Boland, I. Lambermont, and G.R. Cornelis.** 1995. Identification of the YopE and YopH domains required for secretion and internalization into the cytosol of macrophages, using the *cyaA* gene fusion approach. *Proc. Natl. Acad. Sci. USA* **92**: 11998-12002.
78. **Steinberger, E.M. and S.V. Beer.** 1988. Creation and complementation of pathogenicity mutants of *Erwinia amylovora*. *Mol. Plant Microbe Interactions* **1**: 135-144.
79. **Tamano, K., Katayama, E., Toyotome, T. & Sasakawa, C.** 2002. *Shigella* Spa32 is an essential secretory protein for functional type III secretion machinery and uniformity of its needle length. *J. Bacteriol.* **184**: 1244–1252.
80. **Tang, X., Y. Xiao, and J.M. Zhao.** 2006. Regulation of the type III secretion system in phytopathogenic bacteria. *Mol. Plant Microbe Interact.* **19**: 1159-1166.

81. **Thomas, J., G.P. Stafford and C. Hughes.** 2004. Docking of cytosolic chaperone-substrate complexes at the membrane ATPase during flagellar type III protein export. *Proc. Natl. Acad. Sci. USA* **101**: 3945-3950.
82. **Thomas, N., W. Deng, J. Puente, E.A. Frey, C.K. Yip, N.C.J. Strynadka and B.B. Finlay.** 2005. CesT is a multi-effector chaperone and recruitment factor required for the efficient type III secretion of both LEE and non-LEE-encoded effectors of enteropathogenic *Escherichia coli*. *Mol. Microbiol.* **57**: 1762-1779.
83. **Vanneste, J.L.** 2000. Fire Blight: The disease and its causative agent, *E. amylovora*. Oxfordshire, UK: CABI publishing.
84. **van Dijk, K., V.C. Tam, A.R. Records, T. Petnicki-Ocwieja, and J.R. Alfano.** 2002. The ShcA protein is a molecular chaperone that assists in the secretion of the HopPsyA effector from the type III (Hrp) protein secretion system of *Pseudomonas syringae*. *Mol. Microbiol.* **44**: 1469-1481.
85. **Van Eerde, A., C. Hamiaux, J. Perez, C. Parsot, B.W. Dijkstra.** 2004. Structure of Spa15, a type III secretion chaperone from *Shigella flexneri* with broad specificity. *EMBO Rep.* **5**: 477-483.
86. **Veiga, E., Sugawara, E., Nikaido, H., de Lorenzo, V., and Fernandez, L. A.** 2002. *EMBO J.* **21**: 2122-2131.
87. **Wattiau, P., and G.R. Cornelis.** 1993. SycE, a chaperone-like protein of *Yersinia enterocolitica* involved in the secretion of YopE. *Mol. Microbiol.* **8**: 123-131.
88. **Wattiau, P., Bernier, B., P. Deslee, T. Michiels, and G.R. Cornelis.** 1994. Individual chaperones required for Yop secretion by *Yersinia*. *Proc. Natl. Acad. Sci. USA* **91**:10493-10497.
89. **Wei, C.-F., W.-L. Deng and H.-C. Huang.** 2005. A chaperone-like HrpG protein acts as a suppressor of HrpV in regulation of the *Pseudomonas syringae* pv. *syringae* type III secretion system. *Mol. Microbiol.* **57**: 520-536.
90. **Wei, W., Plovanich-Jones, A., W.-L. Deng, Q.-L. Jin, A. Collmer, H.-C. Huang and S.-Y. He.** 2000. The gene coding for the Hrp pilus structural protein is required for type III secretion of Hrp and Avr proteins in *Pseudomonas syringae* pv. *tomato*. *Proc. Natl. Acad. Sci.* **97**: 2247-2252.
91. **Winnen, B., M.C. Schlumberger, A. Sturm, K. Schupbach, S. Siebenmann, P. Jenny and W. Hardt.** 2008. Hierarchical effector protein transport by the *Salmonella typhimurium* SPI-1 type III secretion system. *PLOS One* **3**: e2178 1-8.

92. **Woestyn, S., M.-P. Sory, A. Boland, O. Lequenne, and G.R. Cornelis.** 1996. The cytosolic SycE and SycH chaperones of *Yersinia* protect the region of YopE and YopH involved in translocation across eukaryotic cell membranes. *Mol. Microbiol.* **20**:1261-1271.
93. **Wulff-Strobel, C.R., A.W. Williams and S.C. Straley.** 2002. LcrQ and SycH function together at the Ysc type III secretion system in *Yersinia pestis* to impose a hierarchy of secretion. *Mol. Microbiol.* **43**: 411-423.
94. **Zarivach, R., Vuckovic, M., Deng, W., Finlay, B.B., and Strynadka, N.C.J.** 2007. Structural analysis of a prototypical ATPase from the type III secretion system. *Nature Struct. and Mol. Biol.* **14**: 131-137.
95. **Zhao, Y., S.-Y. He and G. Sundin.** 2006. The *Erwinia amylovora* avrRpt2EA gene contributes to virulence on pear and AvrRpt2EA is recognized by Arabidopsis RPS2 when expressed in *P. syringae*. *Mol. Plant Microbe Interact.* **19**: 644-654.

**Chapter 2: Functional analysis of the N-terminus of the *Erwinia amylovora* secreted effector DspA/E reveals features required for secretion, translocation, and binding to the chaperone DspB/F.**

This chapter has been modified from a publication of the same title in *Molecular Plant Microbe Interactions* (2009, vol. 22: 1282-1292), co-authored by Maeli Melotto and George Sundin.

**ABSTRACT**

DspA/E is a type III secreted effector protein required for pathogenicity in the apple and pear pathogen *Erwinia amylovora*, and DspB/F is a small chaperone protein involved in DspA/E secretion. While the secretion and translocation signals of many type III secretion effector proteins in human enteric pathogens have been characterized extensively, relatively little is known about the translocation requirements of many effectors in plant pathogens, including large DspE-like proteins. In this study, we report a functional analysis of the N-terminus of DspE. The minimal requirements for secretion, translocation, and chaperone binding were characterized. Translocation assays using an adenylate cyclase (CyaA) reporter indicated that the first 51 amino acids of DspE were sufficient for translocation, and that 150 amino acids were required for optimal translocation levels. The minimal translocation signal corresponded with the requirements for secretion into culture media. Mutations of conserved regions in amino acids 2-10 and 31-40 were found to influence translocation levels of an N-terminal DspE-CyaA fusion. Yeast two-hybrid and *in-vitro* pull-down assays revealed a chaperone binding site within amino acids 51-100 of DspE and binding to DspF in this region was disrupted by specific mutations. However, neither disruption of the chaperone binding domain nor deletion of the *dspF* gene had a significant impact on translocation levels of N-terminal DspE-CyaA fusions.

## INTRODUCTION

Type III secretion systems (T3SS) are syringe-like structures central to the infection strategy of many bacterial pathogens and symbionts. Through these systems, effector proteins are injected into host cells and then function to suppress innate defenses and/or induce infection. Although the N-terminal 15 amino acids is sufficient for the secretion of many effectors into the external medium, this minimal portion is often insufficient to elicit measurable effector translocation into host cells, and a longer downstream translocation signal is required (45, 47). The translocation signal often coincides with a domain within the N-terminal 200 amino acids that binds to a type III secretion chaperone (17, 22, 32, 53).

Type III secretion chaperones are small proteins that facilitate secretion of effector, translocator, and secretion apparatus proteins through the T3SS. These chaperones have been divided into several classes; of these, class I chaperones are small structurally conserved dimers that interact specifically with T3SS effector proteins, while class II and III chaperones interact with the translocon and secretion apparatus, respectively (43). Chaperones typically bind to a single site within residues 30 through 150 of the cognate effector protein (35). Co-crystallization studies have provided a model of the chaperone-effector interaction in which the chaperone binding domain of the effector wraps around the exterior of the chaperone dimer, interacting with a helix-binding groove and hydrophobic surfaces on the chaperone (3, 48). In many cases, the chaperone binding domain coincides with or is adjacent to a destabilizing, aggregation-prone, or otherwise secretion inhibitory domain masked by chaperone binding (6, 19, 34). In addition to stability, chaperone binding can confer secretion system specificity to a

cognate effector or modulate the order in which effectors are translocated into host cells (10, 11, 17). Interaction with a chaperone is necessary for substantial levels of protein translocation of many T3SS effectors (19), although chaperone-independent translocation of some effectors can be detected (13, 18, 49).

In the past decade, it has become increasingly clear that class I T3SS chaperones have an important role in plant pathogenesis. T3SS chaperones in plant pathogenic bacteria, like their counterparts in animal pathogens, exhibit a conserved three-helix architecture and bind directly to cognate effector proteins to confer stability and efficient secretion (11). Despite these similarities, studies focusing on the role of the effector-chaperone interaction in plant pathogenesis have yielded several novel finds. For example, while class I T3SS chaperones were previously thought to universally bind to the N-terminus of their cognate effector, the *Pseudomonas syringae* effector HopO1-1 was reported to have a chaperone binding site in the middle third of the protein (24). Second, while the chaperone binding domain itself is a destabilization domain for several *Yersinia*-secreted effectors, the chaperones of *P. syringae* effectors were shown to prevent proteolytic cleavage targeted to a site outside the chaperone binding domain (36). Third, studies of secretion signalling in plant pathogens have provided several new examples of broad specificity chaperones that facilitate the secretion of multiple partners (10, 24). Thus, additional examinations of chaperone-effector interactions in plant pathogens could greatly further our understanding of chaperone-effector specificity and secretion system targeting.

*Erwinia amylovora*, the causal agent of fire blight disease of apple and pear, secretes at least four effector-like proteins in a T3SS-dependent manner (41). Of these,

only the effector called DspA or DspE (henceforth DspE) is known to be required for pathogenicity (1, 5, 20, 55). At 189 kDa, DspE is an unusually large secreted effector protein that interacts with at least four apple proteins (38). The functional role of DspE in apple pathogenesis is unknown, although it has been shown to suppress salicylic acid-mediated host defenses and cause necrotic cell death in host and nonhost plants (7, 16). DspE binds directly to a Class I T3SS chaperone protein, DspF (20), which is also apparently required for efficient intrabacterial DspE production or stability of DspE, although it is not thought to affect transcription levels (21). Likewise, the related chaperone protein WtsF from *Pantoea stewartii* subsp. *stewartii* is involved in the temperature-dependent stability and secretion of WtsE, a DspE homolog (25). Thus, initial analyses of DspF-like chaperones have been performed; however, to our knowledge, a detailed analysis of the chaperone-effector interaction and of sequences in the effector important to chaperone binding have not been conducted.

We hypothesized that sequence features in the N-terminus of DspE would affect the binding of DspF, with the caveat that additional sequences independent of DspF binding could also affect the translocation of DspE. In this study, we used a combination of secretion and translocation assays, virulence studies, and protein-protein interaction studies to characterize the minimal and optimal requirements for secretion, translocation, and chaperone binding in the N-terminus of DspE. We demonstrate that the N-terminus of DspE interacts with DspF and identify specific sequences that contribute to this interaction. Finally, we show that site-directed and deletion mutations of DspE that abolish DspF binding to the N-terminus do not abolish the translocation of N-terminal DspE reporter fusions into host cells.

## MATERIALS and METHODS

**Genetic manipulations and analyses.** The bacterial strains and plasmids utilized in this study are listed in Table 1. Primers are listed in supplementary table S1. Genetic manipulations were performed using standard techniques and protocols (2). The inserts of all plasmid constructs were sequenced at the Michigan State University genomics facility. Sequence alignments were performed using T-Coffee (42, <http://www.ch.embnet.org/software/TCoffee.html>). Secondary structural prediction was performed by Psipred (29, <http://bioinf.cs.ucl.ac.uk/psipred/>) and supported by other secondary structure prediction programs.

**Deletion mutagenesis of *dspE* and *dspF*.** *E. amylovora* nonpolar chromosomal deletion mutants were constructed according to the Red recombinase method (15). Briefly, the primers DspE\_F1 and DspE\_R1, and DspF\_F1 and DspF\_R1 were used to generate recombination fragments consisting of 50-nucleotide homology arms of the *dspE* or *dspF* genes flanking the neomycin phosphotransferase cassette from the plasmid pKD4. PCR products were purified, concentrated, and electroporated into Ea1189 expressing recombinase genes from the helper plasmid pKD46. Mutants were selected on LB agar media amended with 50  $\mu\text{g mL}^{-1}$  kanamycin. Single gene disruption was confirmed by PCR, sequencing, and functional complementation. Virulence assays were conducted using immature pears as previously described (54).

**Cloning of *dspE* and derivative deletion mutants.** To create pLRT5, a 6.5-kb stretch encompassing the *dspE* and *dspF* orfs was amplified using primers DF1 and DspF-R and the Expand Long Template PCR system (Roche Diagnostics; Indianapolis, IN), according to the manufacturer's instructions. The product was cloned into pGem T-Easy, and

complementation of Ea1189 $\Delta$ *dspE* and  $\Delta$ *dspF* was confirmed. To create site-directed and deletion mutants of the full-length DspE, fragments were amplified from pLRT113, pLRT114, and pLRT116 using primers DF1-Apa and DR7 and cloned into the *ApaI* and *BsmI* sites of pLRT5.

**Site-directed alanine replacement and deletion mutagenesis.** Alanine replacement constructs of DspE (pLRT 113, 114, 116, 149, 150, 151, and 152) and deletions of the DspE N-terminus (pLRT109) were created using the SLIM mutagenesis technique (14). A set of two short primers were designed flanking each mutation site. In addition, two tailed primers were designed consisting of the short primer sequences with a 5' tail encoding a stretch of 10 alanines. Mutagenesis primer sequences are shown in supplementary figure S1; FT and RT denote tailed mutagenesis primers and FS and RS denote short flanking primers for each mutagenesis site. The four primers were combined in a PCR reaction to amplify the entire plasmid pLRT14 with complementary overhang ends. The PCR product was digested with *DpnI* to remove the template, the complementary ends were hybridized together, and the products were transformed into *Escherichia coli* strain DH5 $\alpha$ . Plasmids were extracted from the transformants and screened by digestion to test for the addition of a *SacII* site incorporated into the alanine linker. Inserts were sequenced using the primers DF1 and CyaAR. The sequenced alanine replacement or deletion fragments were amplified, digested, and ligated into pMJH20 to create pLRT113, 114, and 116, into pGilda to create pLRT149, 150, 151, and 152, and into pLRT5 to create pLRT137, 138, and 140.

**The CyaA translocation assay.** N-terminal DspE fragments of increasing length, preceded by the native promoter, were amplified with primers DF1 and DR1 through

DR8 and cloned into the *XbaI* and *SmaI* sites of the plasmid pMJH20 in fusion with residues 2-402 of the adenylate cyclase CyaA. DspE-CyaA constructs were introduced into Ea1189 $\Delta$ *dspE* and Ea1189 $\Delta$ *dspF*. Stable fusion protein expression was confirmed via western blot with anti-CyaA antibody (Santa Cruz Biotechnology; Santa Cruz, CA), and *in-vitro* calmodulin-dependent adenylate cyclase activity of DspE(1-203)-CyaA was confirmed using a published assay (46). Overnight cultures were suspended to  $6 \times 10^8$  cfu/mL in phosphate-buffered saline and infiltrated into the youngest three fully expanded leaves of 8-wk old *Nicotiana tabacum* cv. *Samsun* plants. Each treatment was infiltrated into three replicate leaves on different plants. Two 1-cm leaf disks were collected and flash-frozen at 20 h post-inoculation. cAMP was extracted according to the method of Casper-Lindley *et al.* (12); leaf disks were ground in liquid nitrogen and resuspended in 325  $\mu$ L HClO<sub>4</sub> (1.1 M), and 280  $\mu$ L of the supernatants was neutralized with 37.5  $\mu$ L K<sub>2</sub>CO<sub>3</sub> (6M). cAMP levels in the resulting supernatants were measured using the cyclic AMP EIA kit (Cayman Chemical Co.; Ann Arbor, MI) according to the manufacturer's instructions. Protein levels in leaf pellets were measured using the Bio-Rad protein assay. Statistical analyses were done using a one-way analysis of variance and a mean separation was accomplished using Fisher's protected least significant difference test.

**Yeast two-hybrid assays.** *dspE* fragments were cloned in fusion with the LexA DNA binding domain in the *BamHI* and *XhoI* sites of the bait vector pGilda (Clontech; Mountain View, CA). *dspF* was cloned into the *BamHI* and *EcoRI* sites of the prey vector pB42AD. Bait and prey constructs were co-transformed into the *Saccharomyces cerevisiae* strain EGY48 p80(pLacZ) using the Yeast Transformation Kit (Zymo

Research Corporation; Orange, CA). Transformants were selected on minimal SD agar amended with –Ura/-His/-Trp dropout supplement (Clontech). Reporter expression was visualized on minimal SD-galactose agar amended with –Ura/-His/-Trp/-Leu dropout supplement and 80 µg mL<sup>-1</sup> 5-bromo-4-chloro-3-indolyl-beta-D-galactopyranoside (X-gal). Stable expression of prey constructs was confirmed by Western Blot using anti-LexA antibody (Millipore).

**Secretion assays.** 50 mL overnight cultures of Ea1189Δ*dspE* strains expressing DspE-CyaA fusions were grown overnight in LB broth, pelleted by centrifugation, washed with 40 mL water, and resuspended in 20 mL Hrp-inducing minimal medium, pH 5.7 (27). Cultures were induced for 9 h at room temperature. Induced cultures were pelleted for 20 min at 2600xg. The uppermost 35 mL of supernatant was removed, amended with PMSF to a concentration of 0.5 mM, centrifuged again, and the uppermost 30 mL of supernatant was removed and centrifuged a third time. The resulting supernatant was concentrated to 75 µL (400x) using the Amicon 15 mL centrifugal filter unit (10 kDa MWCO) and the Ultrafree 0.5 mL microcentrifugal filter unit (Millipore; Billerica, MA). Protein concentrations were measured by Bradford assay and adjusted to 200 µg/mL; 3 µg of total supernatant protein was analyzed by western blot using anti-CyaA antibody (Santa Cruz Biotechnology, Santa Cruz, CA). Anti-NPTII antibody (US Biological, Swampscott, MA) was used as a lysis control.

**In-vitro protein interaction assay.** *dspF* was cloned into the *Bam*HI and *Xho*I sites of the vector pGex 4T-1 (GE Healthcare; Piscataway, NJ) in fusion with an N-terminal glutathione S-transferase tag. *E. coli* DH5α cells carrying the fusions were induced in 1 mM isopropyl β-D-1-thiogalactopyranoside for 4 h at 37° C. To induce 15 mL overnight

cultures of *E. amylovora*, Ea1189 $\Delta$ *dspF* cells harboring DspE-CyaA fusion vectors were washed twice with water and resuspended in 30 mL modified Hrp-inducing minimal medium, and incubated at 25° C for 6 h. Induced *E. coli* and *E. amylovora* cells were pelleted and lysed in 1 mL B-Per reagent (Thermo-Fisher; Rockford, IL). Lysates were diluted 1:1 in tris buffered saline (TBS; 20 mM tris, 150 mM NaCl, pH 7.4), cleared by centrifugation, and amended with phenylmethanesulphonylfluoride to a final concentration of 0.5 mM. 0.5 mL bait (DspF-GST) lysate was incubated with 0.5 mL prey (DspE-CyaA) lysate and 50  $\mu$ L TBS-equilibrated glutathione agarose (GE Life Sciences) overnight at 4 °C. The glutathione agarose fraction was washed eight times in ten bed volumes of TBS and boiled for 10 minutes in 100  $\mu$ L SDS loading buffer (2% sodium dodecyl sulfate, 4 mM EDTA, 5% B-mercaptoethanol, 0.02% bromophenol blue, and 10% glycerol). 20  $\mu$ L was resolved on a 12% polyacrylamide gel, transferred to nitrocellulose, and probed with anti-CyaA or anti-GST antibody (Precision Antibody; Columbia, MD).

## RESULTS

### **Creation and assessment of a *dspF* deletion mutant in *E. amylovora* Ea1189.**

Gaudriault *et al.* reported that a *dspF* mutant of *E. amylovora* was weakly pathogenic on pear seedlings (21). To confirm these results and to determine whether a *dspF* mutant also caused symptoms on immature pear fruits, *E. amylovora* knockout strains Ea1189 $\Delta$ *dspE* and Ea1189 $\Delta$ *dspF* were constructed as described in Materials and Methods. Ea1189 $\Delta$ *dspF* was complemented with the plasmid pLRT198, a construct containing the *dspF* gene and its promoter sequence. In a virulence assay on immature pear, Ea1189 $\Delta$ *dspE* caused no symptoms, while Ea1189 $\Delta$ *dspF* caused symptoms that

were dramatically reduced compared with that of the wild type strain (Figure 2-1A). The virulence phenotype of Ea1189 $\Delta$ *dspF* was complemented by pLRT198. When infiltrated into leaves of *Nicotiana tabacum* cv. *Samsun*, wild type Ea1189 caused complete HR-like cell collapse within 24 h. *dspE* and Ea1189 $\Delta$ *dspF* caused little to no necrosis, while Ea1189 $\Delta$ *dspF*(pLRT198) caused near wild-type levels of cell collapse (data not shown). Within 48 h, Ea1189 $\Delta$ *dspE* and Ea1189 $\Delta$ *dspF* caused a cell collapse, but this did not appear as severe as that caused by wild-type Ea1189 (Figure 2-1B). Taken together, these results indicate that while DspE is required for *E. amylovora* pathogenicity on pear, its chaperone DspF is not. However, Ea1189 $\Delta$ *dspF* causes greatly diminished symptoms on pear and elicits a response on tobacco visually identical to that of Ea1189 $\Delta$ *dspE*.

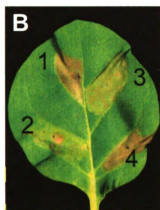
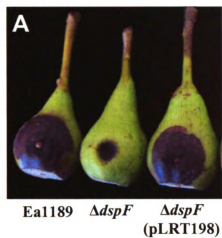


**Figure 2-1.** Pathogenicity and cell death phenotypes of *Erwinia amylovora* Ea1189, Ea1189 $\Delta dspF$ , and Ea1189 $\Delta dspF$  (pLRT198). **A.** Symptom development on immature pears 5 days after inoculation with  $3 \times 10^3$  cfu of three *E. amylovora* strains. **B.** Tobacco leaf cell death 48 hours after infiltration with suspensions of Ea1189 (1), Ea1189 $\Delta dspE$  (2), Ea1189 $\Delta dspF$  (3), and Ea1189 $\Delta dspF$  (pLRT198) (4).

**Kinetics of DspE(1-203) -CyaA translocation into tobacco leaves.** Bocsanczy *et al.* recently demonstrated that the N-terminal 737 amino acids of DspE confer translocation of the reporter CyaA into tobacco leaf cells from wild-type *E. amylovora*, and that translocation levels increase steadily between two and 10 h post-infiltration (4). Adenylate cyclase levels cannot be measured from tobacco infiltrated with wild-type *E. amylovora* after 12 h due to rapid cell collapse. To determine the time required for maximum levels of DspE translocation into tobacco cells, and to determine the kinetics of effector translocation into tobacco over a more extended time period, we examined translocation levels of a DspE-CyaA fusion from Ea1189 $\Delta$ dspE. Ea1189 $\Delta$ dspE causes a delayed and greatly reduced cell collapse, allowing an extended period of time in which translocation assays can be performed. A fusion of DspE residues 1-203 to the CyaA reporter fragment was constructed and introduced into Ea1189 $\Delta$ dspE. The resulting strain was infiltrated into tobacco leaves, and cAMP accumulation in the leaves was measured after various timepoints. To control for the possibility that bacterial infiltration itself causes increase in cAMP levels, we also measured cAMP accumulation elicited by Ea1189 $\Delta$ dspE carrying the parent vector pMJH20. cAMP accumulation of DspE(1-203)-CyaA expressed by Ea1189 $\Delta$ T3SS was measured to confirm that DspE translocation is dependent on the T3SS. Timepoints were optimized by preliminary studies indicating that a significant increase in cAMP levels was first detectable between 2 and 8 h post-infiltration with Ea1189 $\Delta$ dspE expressing DspE(1-203)-CyaA (data not shown). cAMP level increased significantly between 0 and 8 h, increased to a greater degree between 7 and 11 h, and remained steady between 11 and 24 (Figure 2-2). cAMP levels did not

increase in leaves infiltrated with the pMJH20 or type III secretion-deficient controls. These results show that, in the absence of cell collapse, *E. amylovora* requires up to 11 h to reach maximum levels of effector translocation. cAMP levels can fluctuate transiently in plant cells (28, 31), so the persistence of high cAMP levels after 24 h suggests that *E. amylovora* maintains maximum effector expression and translocation levels for at least a day in a non-host system. Based on these results, leaf samples in all subsequent studies were collected at 16 h post-infiltration.

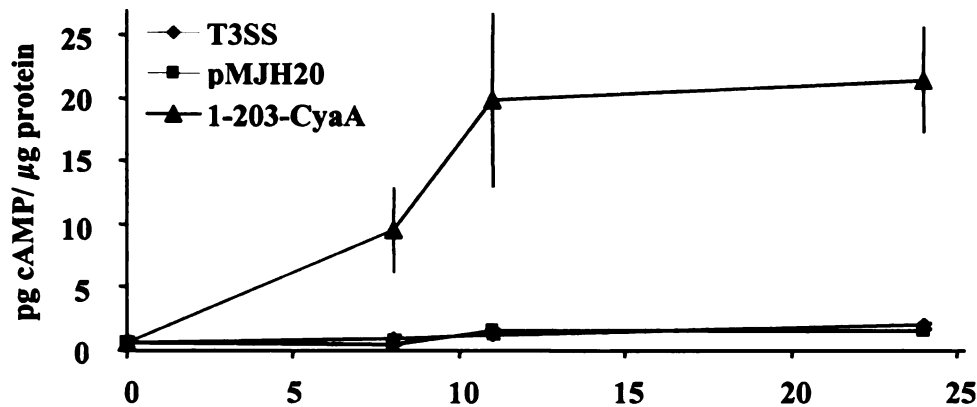


**Figure 2-2.** Kinetics of cAMP accumulation after infiltration into tobacco leaves of *Ea1189ΔdspE* + DspE(1-203)-CyaA (▲), *Ea1189ΔT3SS* + DspE(1-203)-CyaA (◆), and *Ea1189ΔdspE* + pMJH20 (■). Samples were collected at 0, 8, 11, and 24 hours. Data points represent the mean and standard error of three replicate samples.

**Mapping of the secretion and translocation signals of DspE.** The minimal secretion signal of most model type III effector proteins is shorter than the minimal sequence required for translocation into host cells, and this translocation signal often coincides with the chaperone binding domain (13). The N-terminal 15, 33, 51, 77, 101, 150, 203, and 737 amino acids of DspE were fused to the CyaA reporter protein to map the minimal secretion and translocation signal of DspE. Fusion constructs were introduced

into Ea1189 $\Delta$ *dspE*, and stable expression in Hrp-inducing minimal medium was confirmed by western blot (Figure 3A).

To determine the minimal signal for secretion of DspE, secretion of the shortest three fusion proteins from Ea1189 $\Delta$ *dspE* was assayed by western blot of supernatants as described in Materials and Methods. While DspE(1-51)-CyaA was strongly detected in the *E. amylovora* supernatant fraction, secretion of DspE(1-15)-CyaA and DspE(1-33)-CyaA could only be detected very faintly (Figure 3B). These results suggest that while the N-terminal 15 amino acids of DspE are sufficient to allow residual levels of secretion, 51 amino acids are required for substantial levels of secretion into culture medium. Fusions of longer DspE fragments were secreted at levels similar to that of DspE(1-51)-CyaA (data not shown).

Translocation levels of the CyaA fusions were determined by assaying for cAMP accumulation in leaf disks. DspE(1-15)-CyaA and DspE(1-33)-CyaA did not cause an increase in cAMP levels in tobacco compared with the vector control, but fragments of 51 amino acids or longer caused an increase in cAMP levels that were significantly different from the pMJH20 control (Figure 3C). These results indicate that the minimal signal for translocation is within the first 51 amino acids, but not the first 33 amino acids, of DspE. Fragments of 150 and 737 amino acids caused significantly greater levels of cAMP accumulation in plant cells than the first 51 amino acids, indicating that 51 amino acids are not sufficient for optimal translocation. Instead, optimal levels of translocation occurred with fragments of 151 amino acids or greater, even though, for unknown reasons, the DspE(1-101)-CyaA fragment was translocated at lower levels than DspE(1-51)-CyaA. The experiments were repeated three additional times with consistent results.

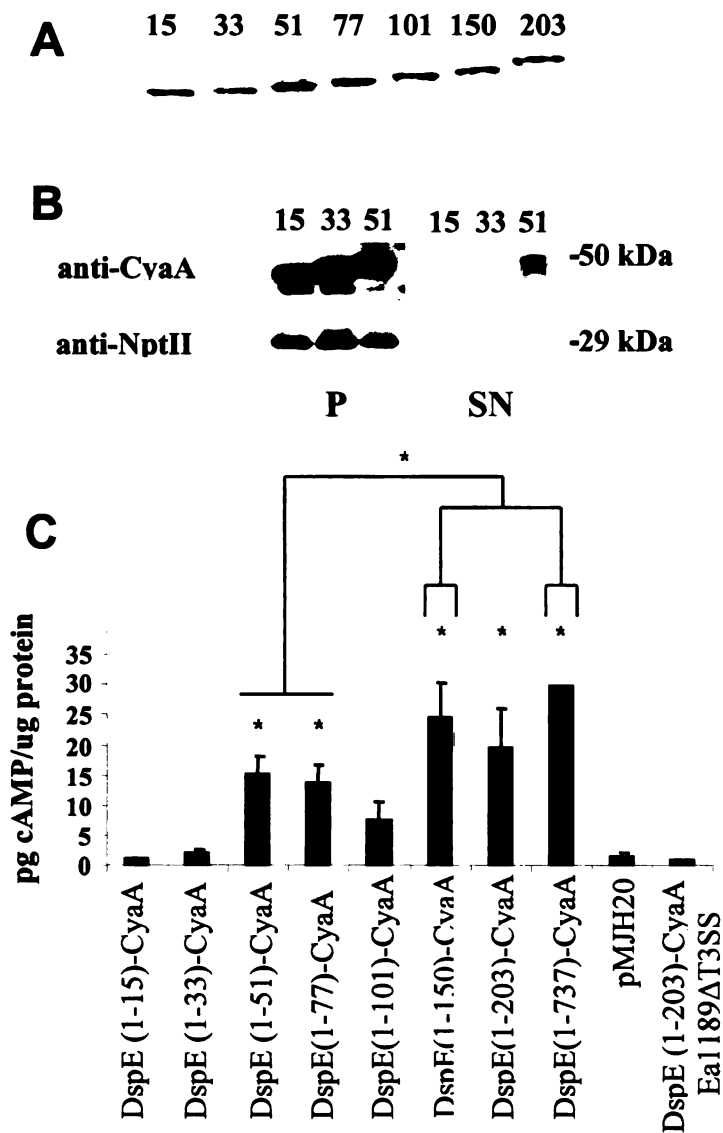


**Figure 2-3.** Mapping of the secretion and translocation domain of DspE. **A.** The first 15, 33, 51, 77, 101, 150, and 203 amino acids of DspE were expressed in fusion with amino acids 2-402 of CyaA, and stable fusion expression in *Ea1189ΔdspE* was confirmed by western blot. **B.** Western blot of CyaA fusion proteins in supernatants (SN) and pellets (P) of *Ea1189ΔdspE* expressing the first 15, 33, and 51 amino acids of DspE fused to CyaA. Samples were probed with anti-NptII antibody as a cell lysis control. **C.** Translocation levels of N-terminal fragments of DspE as measured by cAMP accumulation in tobacco leaves 16 h after infiltration with  $10^8$  cfu/mL *Ea1189ΔdspE* cells expressing DspE-CyaA fusions. Bars represent mean cAMP levels of three leaves on separate plants, plus or minus standard error. Asterisks above bars denote values significantly different from that of the pMJH20 control ( $P < 0.05$ ). Asterisks above brackets denote values significantly different from one another ( $P < 0.05$ ).

**Mutational analysis of conserved segments of the N-terminal 50 amino acids of DspE.** To identify features that might be important for translocation within the first 50 residues of DspE, the N-terminal fragment of DspE was aligned with that of seven homologs from related *Erwinia* species as well as *Pantoea agglomerans* pv. *gypsophila*e, *Pantoea stewartii*, and *Pseudomonas syringae* B728A (Figure 2-4A). While the N-terminal 50 amino acids of these proteins did not share a high degree of conservation, there were two highly conserved stretches within residues 1-11 and 28-40. To determine whether specific residues within the translocation signal of *E. amylovora* might play an important role as part of the translocation signal, we used site-directed ligase independent mutagenesis (SLIM) to replace amino acids 2-10, 11-20, and 31-40 with stretches of consecutive alanine residues on the plasmid pLRT14, yielding plasmids pLRT113, 114, and 116. Alanine stretch replacement is a common strategy to assess the functional role of a sequence without imposing extreme steric constraints (33). Due to the nature of the SLIM technique, the number of amino acids varied by one or two; residues 2-10 and 11-20 were replaced with ten alanines, while 31-40 were replaced with eight alanine residues. Alanine-replacement mutants were subcloned into pLRT5, a full length, high-copy clone of *dspE*, to create plasmids pLRT137, 138, and 140. These constructs were tested for complementation of the virulence phenotype of Ea1189 $\Delta$ *dspE* on immature pear. While *dspE* (2-10A) did not complement Ea1189 $\Delta$ *dspE* on immature pear after four days, *dspE* (11-20A) and *dspE* (31-40A) complemented the mutant to levels similar to that of the parent vector (Figure 2-4B), indicating that only residues 2-10 were required for translocation. To measure translocation levels of the site-directed mutants, DspE (1-203; 2-10=10A)-CyaA, DspE (1-203; 11-20=10A)-CyaA, and DspE (1-203; 31-40=8A)-

CyaA were amplified and re-cloned into the CyaA fusion vector pMJH20. Constructs were introduced into *Ea1189ΔdspE*, expression was confirmed, and levels of translocation into tobacco were assayed. Translocation levels of DspE (1-203; 11-20=10A)-CyaA were not significantly different than those of DspE(1-203)-CyaA, but DspE (1-203; 31-40=8A)-CyaA was consistently translocated at levels significantly lower than the wild-type. DspE (1-203; 2-10= 10A)-CyaA was translocated at greatly reduced levels, although cAMP levels were significantly higher than the vector control (Figure 2-4C). We did not obtain an alanine-replacement mutant of the conserved sequences between residues 41 and 50, but deletion of residues 35-125 from DspE(1-203)-CyaA did not have a significant impact on translocation levels (data not shown), indicating that these residues are not important for protein translocation. Together, these results suggest that the first 10 amino acid residues of DspE are required for translocation into host cells and pathogenicity, and that other portions of the translocation signal, while tolerant to mutagenesis, could have a small but additive effect on translocation levels. The fact that decreases in translocation levels did not correspond to a decrease in virulence suggests that small reductions in DspE translocation do not adversely affect virulence levels.

**A**

```

Ea1189  MEIKSLGTEHRAAAVHTAAHNPVGHGVALQOGSSSSSPQNAAASLAAEEGRN
E. pyr.  MVLKLGQTEHKTAVQIAAHNPVGGVALQOGSSSSSPQNAAASLASEGRN
E. tasm. MVLKLGQTEHRAAIIQTATHGPAGPGAALQOGSSSSSAQTAAVSLAEEGRN
D. dad.  MRINLHATEKKTITVQNVENPNNSTI PPLQOGSSSSAPQASGGTLASEGRN
P. gyp.  MKLIGHLTEQKTTVVQNVERTVYDAGTTLQOGSSSCSAPQAAGLLTSEGRN
Pss.    MGKRLLLKSVGRVVFQKSRAPRQSAARPPSTOPESSSPRRSS...REAGRN

```

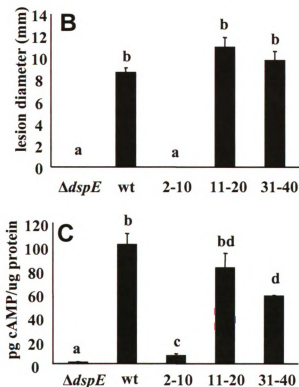
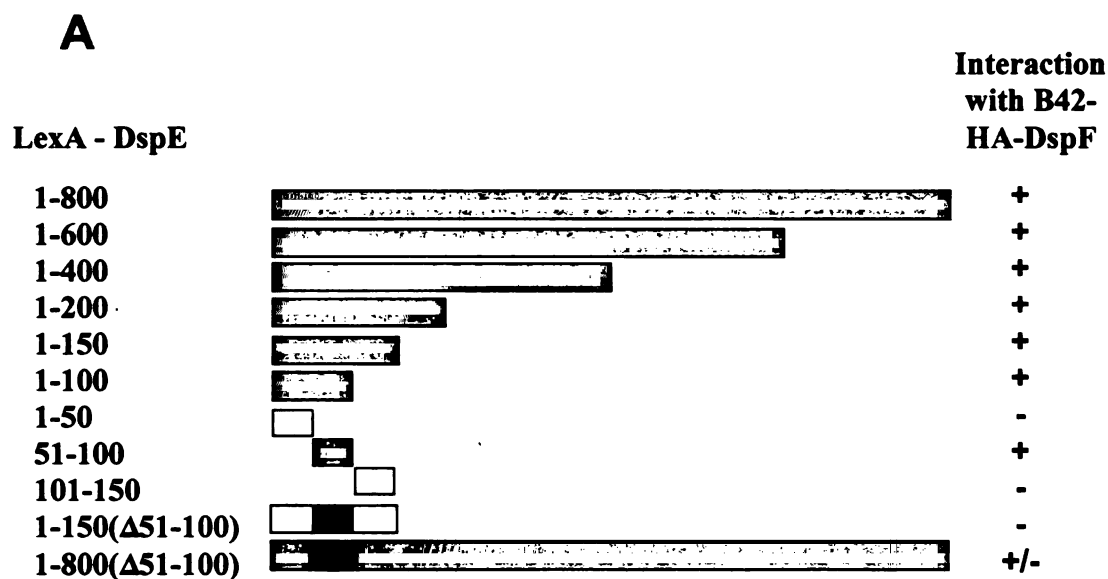


**Figure 2-4.** Analysis of alanine replacement mutants of amino acids 2-40 of DspE. **A.** Sequence alignment of amino acids 1-50 of DspE and homologs from other phytopathogenic bacteria. Bacterial species and Genbank accessions are as follows: *E. amylovora* (AAC04850) *E. pyrifoliae* (AY530755), *E. tasmaniensis* (YP\_001906490), *Pantoea agglomerans* (AAF76343), *P. stewartii* (AAG01467), and *Pseudomonas syringae* B728A (YP\_234280). **B.** Lesion diameters of immature pears infected with Ea1189 $\Delta dspE$  and Ea1189 $\Delta dspE$  carrying pLRT5, a full-length clone expressing DspE, or pLRT137, 138, and 140, pLRT5 variants expressing DspE with amino acids 2-10, 11-20, or 31-40 replaced with stretches of alanine. **C.** cAMP levels of tobacco leaves infiltrated with Ea1189 $\Delta dspE$  carrying the pMJH20 parent vector, pLRT 14 (DspE (1-203)-CyaA) or alanine replacement variants pLRT113, 114, and 116. Bars represent means plus or minus standard error. Letters above bars denote groups with significant differences ( $P < 0.05$ ).

**DspF binds to DspE between amino acids 51-100.** Affinity blot experiments have previously detected a direct interaction between DspE and DspF (21). To date, almost all reported T3SS chaperones have interacted with cognate effector proteins via a single chaperone binding domain near the N-terminus (43). However, recent studies showed that some chaperones of *Pseudomonas* effectors may bind to the middle third of an effector protein (24). Here, a yeast two-hybrid (Y2H) approach was used to identify the portion of the N-terminus of DspE that interacts with the secretion chaperone DspF. N-terminal DspE fragments of varying lengths were fused to the LexA DNA binding domain and tested for interaction with a B42-HA-DspF fusion in yeast as described in Materials and Methods. The N-terminal 800, 600, 400, 200, 150, and 100 amino acids of DspE all interacted strongly with B42-HA-DspF, but the N-terminal 50 amino acids did not (Figure 2-5A). Further analyses showed that residues 51-100 of DspE were sufficient for strong interaction with DspF, while deletion of residues 51-100 from LexA-DspE(1-150) abolished the interaction with DspF (Figure 2-5A). Constructs expressing LexA -DspE(25-75) and LexA -DspE(75-125) interacted very weakly with B42-HA-DspF (data not shown), suggesting that the chaperone binding domain is located squarely within residues 51-100 of DspE. Deletion of residues 51-100 from LexA -DspE(1-800) reduced the strength of the interaction with DspF, but did not abolish the interaction. Further analysis mapped additional DspF yeast two-hybrid interaction sites to residues 151-200, 401-450, 651-700, and 1000-1200 of DspE (data not shown). Because these secondary candidate chaperone binding sites interacted weakly with DspF, and because the N-terminal binding site in residues 51-100 corresponds to the chaperone binding sites of the majority of characterized type III effector proteins, this study is focused on

characterization of DspE residues 51 to 100 as a probable requirement for DspF chaperone function.

To confirm the DspE-DspF interaction *in vitro*, a glutathione S-transferase pull-down assay was performed. A GST-DspF fusion immobilized on glutathione agarose was tested for the ability to pull down DspE(1-150)-CyaA and DspE(1-150 $\Delta$ 51-100)-CyaA. DspE(1-150)-CyaA was pulled down by GST-DspF *in vitro*, but DspE(1-150 $\Delta$ 51-100)-CyaA was not (Figure 2-5B). This supports the yeast two-hybrid evidence that residues 51 to 100 are required for interaction of the DspE N-terminus with DspF.



**B.**

| DspF-GST                  | + | + | - |
|---------------------------|---|---|---|
| DspE 1-150-CyaA           | + | - | + |
| DspE 1-150 (Δ51-100)-CyaA | - | + | - |

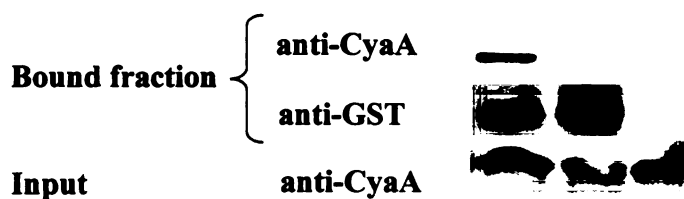


**Figure 2-5.** Mapping of the DspF- interacting regions in the N-terminal half of DspE. **A.** Yeast two-hybrid analysis of the N-terminal 800 amino acids of DspE. LexA-DspE fusions were co-expressed with fusions of DspF with B42-HA. **B.** Pull-down analysis of DspE (1-150)-CyaA and DspE (1-150 Δ51-100)-CyaA with DspF-GST. Lysates of *Ea1189ΔdspE* carrying plasmids pLRT13 (DspE(1-150)-CyaA) or pLRT109 (DspE (1-150Δ51-100)-CyaA) were incubated overnight with lysates of *E. coli* overexpressing GST-DspF and glutathione beads, or with glutathione beads alone.

**DspE residues 51-60 and 71-85 affect the yeast two-hybrid interaction between DspE (1-150) and DspF.** Crystallization studies and analyses of amino acid sequences have identified secondary structures and specific residues thought to be involved in chaperone-effector binding. Lilic and Stebbins showed that deletions of a single 3-residue motif, the  $\beta$ -motif, in the chaperone binding domains of several effector proteins led to a loss of chaperone-effector binding (35). Co-crystallization studies have indicated that hydrophobic grooves in Class I chaperones interact with one or more  $\alpha$ -helices on their cognate effector protein, but few functional analyses have been performed of specific chaperone binding features on the effector (17, 35). To identify DspE sequences within residues 51-100 that were important for DspF binding, and to determine whether single or multiple sequences were involved, an alanine replacement strategy was employed. SLIM mutagenesis was used to replace DspE residues 51-60, 61-70, 71-85, and 86-100 with stretches of 8 to 10 alanines as described in Materials and Methods. Residues 71-85 were mutated at once because they correspond to a putative  $\alpha$ -helix-rich region predicted by the secondary structure prediction program PsiPred. In addition, we identified a potential  $\beta$ -motif consisting of residues L79, L83, and K86 which would be functionally disrupted by the 71-85 mutant (Figure 2-6A). Alanine replacement constructs are described in Table 2-1. DspE residues 1-150 containing site-directed mutants in the 51-100 region were fused to the LexA protein and tested for interaction with B42-HA-DspF in a yeast two-hybrid assay. Replacement of residues 61-70 and 86-100 had no apparent effect on the interaction between LexA-DspE (1-150) and B42-HA-DspF (Figure 2-6B). However, replacement of residues 51-60 appeared to cause a slight decrease in yeast growth and color development, while replacement of residues 71-85 caused a drastic reduction in

growth and color development (Figure 2-6B). Faint color development was still visible when the 71-85 alanine replacement strain was plated in high concentrations on a less-selective medium amended with leucine, although this color development was not seen in a double mutant in which residues 51-60 and 73-82 were replaced with 7 and 10 alanines, respectively (data not shown). These results demonstrate that residues 71-85, which contain a putative  $\alpha$ -helix and chaperone binding motif, contribute strongly to the DspE-DspF interaction, and that residues 51-60 may also contribute to this interaction.

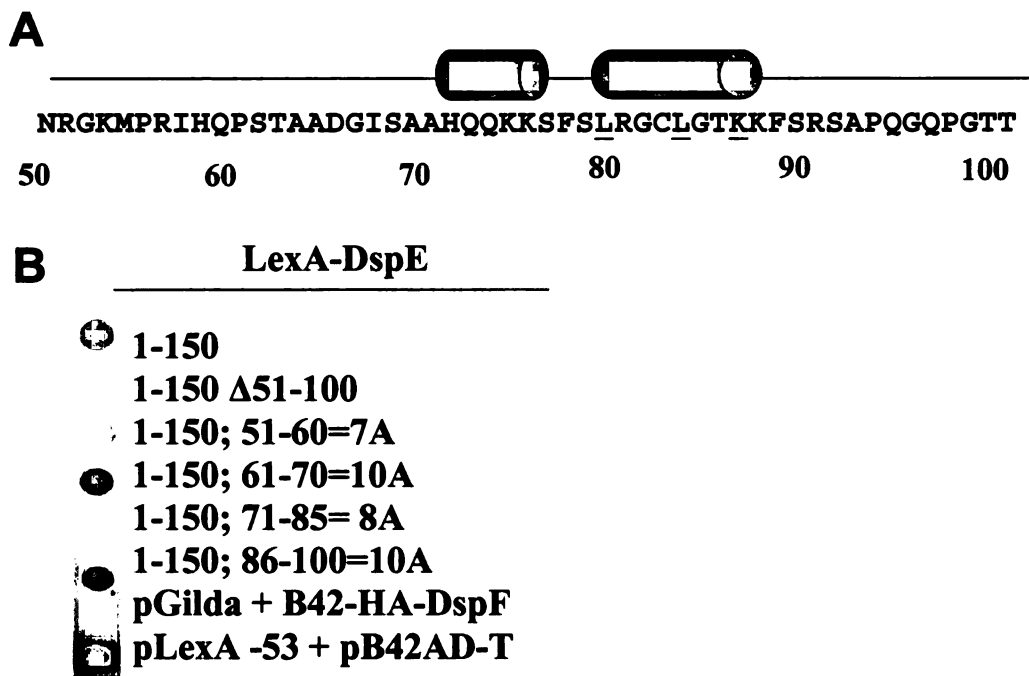


**Figure 2-6.** Alanine-replacement mutagenesis of the N-terminal chaperone-binding domain of DspE. A. Amino acid sequence of residues 51-100. Cylinders represent predicted  $\alpha$ -helices. Underlined residues denote residues of a potential  $\beta$ -motif. B. Yeast two-hybrid interaction between alanine-replacement variants of LexA-DspE (1-150) and B42-HA-DspF. The negative control strain carries the empty pGilda bait vector and B42-HA-DspF; the positive control strain carries pLexA-53 and pB42AD-T.

**The DspF-binding domain is not required for translocation of the N-terminus of DspE.** The N-terminal chaperone binding domain is required for translocation of many type III-secreted effector proteins (26, 32). To determine whether the chaperone binding domain in residues 51-100 of DspE affects protein translocation levels, a plasmid expressing DspE(1-150)-CyaA lacking residues 51-100 was constructed. CyaA expression levels in Ea1189 $\Delta$ *dspE* were confirmed by western blot to be equivalent to Ea1189 $\Delta$ *dspF*, and translocation levels into tobacco cells were tested. Deletion of amino acids 51-100 from residues 1-150 did not cause a change in translocation levels (Figure 2-7A). To control for the possibility that residual chaperone binding sites outside the 51-100 range were not affecting translocation levels, we also tested constructs with residues 35 to 125 deleted, and these were not reduced in translocation (data not shown). We also tested constructs of DspE(1-737)-CyaA with residues 51-100 deleted, and found no effect of residues 51-100 on the longer fragment (data not shown). Although we hypothesized that translocation of the N-terminus of DspE would be DspF-dependent, DspE(1-150)-CyaA was translocated from Ea1189 $\Delta$ *dspE* and Ea1189 $\Delta$ *dspF* at similar levels (Figure 2-7B). PCR and pear virulence assays were used to confirm that the bacterial samples were not contaminated with any DspF-expressing cells. These results suggest that the accumulation and translocation of plasmid-expressed N-terminal fragments of DspE is not dependent on DspF binding, and that the chaperone binding domain itself does not inhibit or destabilize the N-terminus of DspE in the absence of DspF.

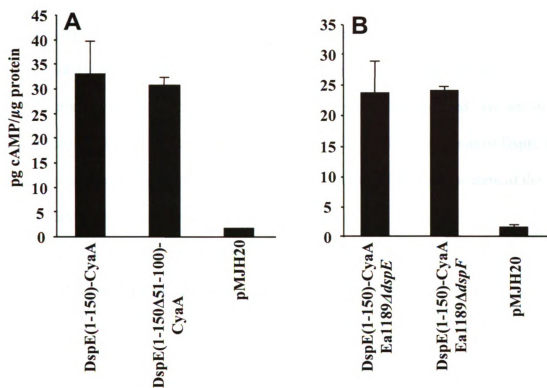


**Figure 2-7.** Functional analysis of amino acids 51-100 of DspE. **A.** cAMP accumulation in tobacco leaves infiltrated with Eal1189ΔdspE expressing DspE(1-150)-CyaA and DspE(1-150Δ 51-100)-CyaA. **B.** cAMP accumulation in leaves infiltrated with Eal1189ΔdspE and Eal1189ΔdspF expressing DspE(1-150)-CyaA. Results are the means and standard errors from three replicate leaves on separate plants.

## DISCUSSION

This work reports a multi-faceted analysis of the N-terminal 200 amino acids of the *E. amylovora* secreted effector protein DspE. Three areas were examined with regards to functionality: requirements for secretion, requirements for translocation, and requirements for binding to the chaperone DspF. Our results demonstrated that, while DspF is required for virulence and binds to a specific site on the N-terminus of DspE, the N-terminal minimal chaperone binding domain is not required for translocation of the DspE N-terminus .

We report a time-course analysis of DspE(1-203)-CyaA translocation into tobacco leaves. cAMP accumulation in tobacco cells was detected at moderate levels after 8 h, but had reached maximum levels within 11 h. This supports the recent finding of Boczanscy *et al.* that, after a short initial lag period, DspE translocation levels increase continuously up to 10 h post-inoculation (4). *hrp* gene promoters require about 6 h for expression during induction in tobacco (52), which could explain the delay between leaf disk infiltration and cAMP accumulation. In repeated studies, DspE-CyaA induced cAMP levels remained at maximum levels until at least 24 h post-inoculation. Work by Schecter *et al.* demonstrated that *Xanthomonas* protein translocation (cAMP accumulation) levels into nonhost tobacco cells drops precipitously after about 8 h post-infiltration (2004), and Wei *et al.* showed a decrease in *hrp* gene transcription in *E. amylovora* during the same timeframe (52). Our findings indicate that in the absence of DspE-induced cell death, maximum translocation levels can be maintained for extended periods of time.

Studies on a variety of Type III- secreted effectors in animal and plant pathogens have led to a model of two functional T3SS signals- a short N-terminal fragment

sufficient for secretion into culture media, and a longer fragment required for translocation into host cells (40, 47). Here, we found that the N-terminal 15 and 33 amino acids of DspE were sufficient to allow very low levels of secretion of the CyaA reporter gene into Hrp-inducing minimal medium, while DspE(1-51)-CyaA was strongly secreted. These results suggest that DspE does have a minimal secretion signal separate from the translocation signal, but that optimal levels of secretion require a functional translocation domain. Previous work in plant pathogens indicated that while the *X. campestris* effector AvrBs2 has separate secretion and translocation signals (12, 40), the secretion and translocation requirements of the *P. syringae* effector AvrPto are not separate (44).

This study found that translocation of the CyaA reporter protein required greater than 33 N-terminal amino acids of DspE, and that translocation levels increased with greater than 51 amino acids. This finding echoes previous work which reported minimal and optimal translocation signals of the secreted effectors AvrPto, AvrBs2, SspH2, and YopE, among others (12, 39, 44, 45). These findings suggest that the translocation signal itself could have multiple components. The basis for increasing secretion competence of longer fragments is not known. In some cases, the structural conformation of effector or effector-reporter hybrids may be more secretion compatible in longer fragments. In some cases, longer gene fragments may allow greater levels of chaperone binding.

Mutational studies on the minimal translocation domain demonstrated that the sequence in residues 2-10 is required for all but the smallest detectable levels of translocation, a finding supported by previous studies on type III secretion signalling (6, 45). Alanine replacement of residues 11-20 caused a minor, but not significant, decrease in translocation levels. Mutation of residues 31-40, a stretch rich in serine, caused a 40%

to 60% reduction in translocation levels of DspE(1-203)-CyaA in multiple studies. Residues 31-40 contain a stretch of five highly conserved serines. A high serine content (>10%) is a defining feature of the N-terminus of T3SS effectors in plant pathogens, although the N-terminus of DspE does not contain any serines outside of residues 31-40. While at least one serine residue in the N-terminus of the *Pseudomonas syringae* effector protein AvrRpt2 was involved in protein stability, a fragment containing the serine-rich motif SSASS increased secretion or translocation efficiency without affecting levels of protein accumulation (51). Mutagenesis of residues 31-40 did not affect accumulation of DspE(1-203)-CyaA in western blot experiments. Further studies are needed to determine whether the serine-rich stretch of DspE itself contributes to translocation efficiency.

Yeast-two hybrid and GST pulldown analyses in this study identified a DspF binding domain within the first 150 residues of DspE, specifically within residues 51 to 100. Fifty amino acid-domain is comparable to the sizes of other characterized chaperone binding domains (3). Disruption of residues 51-60 and 71-86, respectively, strongly interfered with this interaction. Yeast two-hybrid studies also pointed to the possibility of several downstream sites of chaperone interaction, but these interactions have not been confirmed *in vitro*. To our knowledge, there are no previous reports of multiple distinct chaperone binding sites on an effector. Bogdanove *et al.* reported that a deletion in the C-terminal half of DspE is complemented with a cosmid expressing the overlapping C-terminal fragment, suggesting that DspE forms two independently folding domains (5). The mechanism of secretion of the C-terminal fragment is not known, but given the large size of DspE and the possibility of multiple secreted domains, multiple DspF interaction sites could be important for stabilization and secretion targeting of downstream portions

of the protein. Although this study focused on the N-terminus of DspE, it will be interesting in future studies to determine whether DspF binds to multiple downstream sites of DspE in a functionally significant manner.

Deletion of amino acids 51-100 of DspE or deletion of *dspF* did not result in a decrease in translocation levels of DspE(1-150)-CyaA. Furthermore, DspE (1-150)-CyaA showed no signs of destabilization in the absence of the chaperone binding domain or DspF. These results would support a model in which the chaperone binding domain does not have an effect on translocation of a stably expressed N-terminus of DspE. This was surprising, since the N-terminal chaperone binding domain is required for the T3SS-dependent translocation of the N-terminus of many effectors (43). One possibility for this difference is that a primary role of the chaperone binding domain is to protect DspE from destabilization targeted to the C-terminal portions of the protein, as does the chaperone binding domain of HopPtoM (36). If this were the case, deletion of the chaperone binding domain would have little effect on translocation of N-terminal DspE fragments.

Alternatively, expression of the N-terminal CyaA fusion of DspE from the medium-copy vector pMJH20 could overcome the need for the chaperone binding domain, as multiple copies of the gene could potentially saturate proteolytic degradation or help DspE compete against other effectors in a hypothetical secretion hierarchy. However, it would be very unlikely for ectopic expression of the CyaA fusion to abolish the importance of chaperone binding, as effectors such as SspA and YscP require the chaperone for translocation even when expressed as a CyaA fusion from pMJH20-derived vectors (8, 37). This would suggest that the role of the N-terminal chaperone binding domain of DspE differs from that of YscP and SspA, and our current work is directed at determining

whether alternate chaperones or chaperone binding sites contribute to DspE secretion. Together, our results indicate that the N-terminal 150 amino acids of DspE are secretion- and translocation-competent even in the absence of DspF binding, and that the chaperone binding domain within residues 51-100 of DspE is not inhibitory to translocation in the absence of DspF. While chaperone-independent translocation of some effectors has been documented (50), the virulence phenotype and secretion profile of *E. amylovora dspF* mutants demonstrates a strong role for the chaperone in translocation of wild-type DspE (21). Studies involving full-length DspE will be helpful in determining the true functional significance of the N-terminal chaperone binding domain and its interaction with DspF.

In summary, our results provide evidence that the DspE chaperone binding domain and the DspE-DspF interaction have the same basic configuration as other characterized chaperone-effector pairs, including a minimal and optimal translocation signal and an N-terminal chaperone binding domain. However, we have shown that the N-terminus of DspE has some characteristics unlike that of many smaller secreted effectors, in that the N-terminus of DspE required a functional translocation signal for substantial levels of secretion *in vitro*, and did not require interaction with DspF for translocation competence.

**Table 2-1.** Strains and plasmids used in Chapter 2.

| Strain or plasmid                | Characteristics  | Source     |
|----------------------------------|--|------------|
| <i>Escherichia coli</i> strain   |  |            |
| DH5 $\alpha$                     | F- 80 <i>dlacZ</i> $\Delta$ M15 $\Delta$ ( <i>lacZYA-argF</i> )U169 <i>endA1</i><br><i>recA1</i> <i>hsdR1</i> 7(rK-mK+) <i>deoR</i> <i>thi-1</i> <i>supE44</i><br><i>gyrA96</i> <i>relA1</i> $\lambda$ - | Invitrogen |
| <i>Erwinia amylovora</i> strains |  |            |
| Ea1189                           | Wild type  | 9          |
| Ea1189 $\Delta$ <i>dspE</i>      | <i>dspE</i> deletion mutant, KmR   | This study |
| Ea1189 $\Delta$ <i>dspF</i>      | <i>dspF</i> deletion mutant, KmR   | This study |
| Ea1189 $\Delta$ T3SS             | T3SS deletion mutant, KmR  | 56         |
| pBRR1-MCS5                       | broad host-range cloning vector, GmR   | 30         |
| Plasmids                         |  |            |
| pLRT198                          | pBRR1-MCS5 expressing <i>dspF</i>  | This study |
| pMJH20                           | pWSK29 containing codons 2 to 406 of CyaA, AmpR  | 39         |
| pLRT8                            | pMJH20 expressing DspE(1-15)-CyaA  | This study |
| pLRT9                            | pMJH20 expressing DspE(1-33)-CyaA  | This study |
| pLRT10                           | pMJH20 expressing DspE(1-51)-CyaA  | This study |
| pLRT11                           | pMJH20 expressing DspE(1-77)-CyaA  | This study |
| pLRT12                           | pMJH20 expressing DspE(1-101)-CyaA   | This study |
| pLRT13                           | pMJH20 expressing DspE(1-150)-CyaA   | This study |
| pLRT14                           | pMJH20 expressing DspE(1-203)-CyaA   | This study |
| pLRT201                          | pMJH20 expressing DspE(1-737)-CyaA   | This study |
| pLRT109                          | pMJH20 expressing DspE(1-150d. 51-100)-CyaA  | This study |
| pLRT113                          | pMJH20 expressing DspE (1-203; 2-10=10A)-CyaA  | This study |
| pLRT114                          | pMJH20 expressing DspE (1-203; 11-20=10A)-CyaA   | This study |
| pLRT116                          | pMJH20 expressing DspE (1-203 31-40=8A)-CyaA   | This study |
| pGilda                           | <i>HIS3</i> LexA BD bait vector, AmpR  | Clontech   |
| pB42AD                           | <i>TRP1</i> B42 AD prey vector, AmpR   | Clontech   |
| pLexA-53                         | positive control bait vector, AmpR   | Clontech   |
| pB42-HA-T                        | positive control prey vector, AmpR   | Clontech   |
| pLRT192                          | LexA-DspE(1-800)   | This study |
| pLRT216                          | LexA-DspE(1-400)   | This study |
| pLRT217                          | LexA-DspE(1-200)   | This study |
| pLRT31                           | LexA-DspE(1-150)   | This study |
| pLRT30                           | LexA-DspE(1-100)   | This study |
| pLRT29                           | LexA-DspE(1-50)  | This study |
| pLRT32                           | LexA-DspE(51-100)  | This study |
| pLRT35                           | LexA-DspE(101-150)   | This study |
| pLRT37                           | LexA-DspE(151-200)   | This study |
| pLRT155                          | LexA-DspE(1-150 $\Delta$ 51-100)   | This study |
| pLRT149                          | LexA-DspE(1-203; 51-60=7A)   | This study |
| pLRT150                          | LexA-DspE (1-203; 61-70=10A)   | This study |

Table 2-1 (cont'd).

|             |   |               |
|-------------|---|---------------|
| pLRT151     | LexA-DspE (1-203; 71-86= 8A)                        | This study    |
| pLRT152     | LexA-DspE (1-203; 86-100= 10A)                      | This study    |
| pLRT215     | B42-HA-DspF   | This study    |
| pGEM T-Easy | high-copy TA cloning vector                         | Promega       |
| pLRT5       | 5.6 kb <i>dspEF</i> locus in pGem T-Easy            | This study    |
| pLRT137     | pLRT5 derivative expressing DspE (1-203; 2-10=10A)  | This study    |
| pLRT138     | pLRT5 derivative expressing DspE (1-203; 11-20=10A) | This study    |
| pLRT140     | pLRT5 derivative expressing DspE (1-203; 31-40=8A)  | This study    |
| pGEX 4T-1   | Bacterial expression vector expressing a GST tag    | GE Healthcare |
| pLRT184     | pGEX 4T-1 derivative expressing GST-DspF            | This study    |
| pKD4        | AmpR, KmR, mutagenesis cassette template            | 15            |
| pKD46       | AmpR, expresses $\lambda$ red recombinase           | 15            |

**TABLE 2-2. Oligonucleotides used in Chapter 2.**

| Name     | sequence   |
|----------|--|
| DF1      | gttctagacctggtgggaaccggttgcag  |
| DR1-15   | gtccataatattgtgtactgccgccttgtgtt                                       |
| DR2-33   | tggtttaatattctgctgtaaggcaacacat  |
| DR3-51   | agtccaatattacgattttgccttctgccg   |
| DR4-77   | catggaatattgaaggatttctttgctggtgag                                      |
| DR5-101  | tagccaatattttgctgtgggtgtacctg  |
| DR6-150  | gatctcaatattttcaccattggccgcccg   |
| DR7-203  | gactgaatattcgggatgtcggcggtgtaa   |
| DR8-737  | catgaatattgaaggagcgaatgtccccttttc                                      |
| DspF-R   | attatgccgcgctactctcgtcta   |
| DF1-Apa  | gtgggccccctggtgggaaccggttgcag  |
| CyaA-R   | tcggcaatcaggctggtggaatg  |
| dspE_F1  | atggaattaaatcactgggaactgaacacaaggcggcagtacacacagcgcgattgtgtaggctggagct |
| dspE_R1  | ttagctcttcattccagcccttcttctcaaatcagtaagcgcagatgattccgggatccgtcgacc     |
| dspF_F1  | atgacatcgtcacagcagcgggtgaaaggttttacagtatttctccgcgcgattgtgtaggctggagct  |
| dspF_R1  | ttatgccgcgctactctcgtctaattgcgctatatactacgcacttctgattccgggatccgtcgacc   |
| 2-10FT   | gcggcagccgctgcagctgccgcggcagctaaggcggcagtacacacagcgg                   |
| 2-10FS   | aaggcggcagtacacacagcgg   |
| 2-10RT   | agctgccgcggcagctgcagcggctgccgcgacctgtgccccaccctctg                     |
| 2-10RS   | gacctgtgccccaccctctg   |
| 11-20FT  | gcggcagccgctgcagctgccgcggcagctcctgtgggcatggtgttgcct                    |
| 11-20FS  | cctgtgggcatggtgttgcct  |
| 11-20RT  | agctgccgcggcagctgcagcggctgccgcgtgttcagttcccagtgattt                    |
| 11-20RS  | gtgttcagttcccagtgattt  |
| 31-40FT  | gcggcagccgctgcagctgccgcggcagctcattggcggcagaaggcaaaa                    |
| 31-40FS  | tcattggcggcagaaggcaaaa   |
| 31-40 RT | agctgccgcggcagctgcagcggctgccgcctgctgtaaggcaaacacatgc                   |
| 31-40 RS | ctgctgtaaggcaaacacatgc   |
| 51-100FT | tggcggcagaaggcaaaaatcacagcaaaggggcaacattgc                             |
| 51-100FS | cacagcaaaggggcaacattgc   |
| 51-100RT | attttgccttctgccgccaatgatgcagcggcattttgc                                |
| 51-100RS | atgatgcagcggcattttgc   |
| 51-60FT  | gcggcagccgctgcagctgccgcggcagcttctactgcggctgatggtatca                   |
| 51-60FS  | tctactgcggctgatggtatca   |
| 51-60RT  | agctgccgcggcagctgcagcggctgccgcattttgccttctgccgccaat                    |
| 51-60RS  | attttgccttctgccgccaat  |
| 61-70FT  | gcggcagccgctgcagctgccgcggcagctcaccagcaaaagaaatcctcag                   |
| 61-70FS  | caccagcaaaagaaatcctcag   |
| 61-70RT  | agctgccgcggcagctgcagcggctgccgctggctggtgaattctcggcat                    |
| 61-70RS  | tggtggtgaattctcggcat   |
| 71-85FT  | gcggcagccgctgcagctgccgcggcagctaaaaattttccagatcggcaccgcagggc            |
| 71-85FS  | aaaaaattttccagatcggcaccgcagggc   |

Table 2-2 (cont'd).

|          |   |
|----------|---|
| 71-85RT  | agctgccgcggcagctgcagcggctgccgcgctgataccatcagccgtag  |
| 71-85RS  | gctgataccatcagccgtag                                |
| 86-100FT | gcggcagccgctgcagctgccggcagctcacagcaaaggggcaacattgc  |
| 86-100FS | cacagcaaaggggcaacattgc                              |
| 86-100RT | agctgccgcggcagctgcagcggctgccgccgtcccaaacagcccctgaga |
| 86-100RS | cgtcccaaacagcccctgaga                               |

## WORKS CITED

1. **Asselin, J.E., K.N. Yip, and S.V. Beer.** 2008. Eop1 differs in strains of *Erwinia amylovora* that differ in host specificity. *Acta Hort.* **793**: 213-214.
2. **Ausubel, F.M., R. Brent, R.E. Kingston, D.D. Moore, J.G. Seidman, J.A. Smith, and K. Struhl.** eds. 1997. Current Protocols in Molecular Biology. Wiley, New York.
3. **Birtalan, S.C., R.M. Phillips, and P. Ghosh.** 2002. Three-dimensional secretion signals in chaperone-effector complexes of bacterial pathogens. *Mol. Cell* **9**: 971-980.
4. **Bocsanczy, A.M., R.M. Nissinen, C.-S. Oh, and S.V. Beer.** 2008. HrpN of *E. amylovora* functions in the translocation of DspA/E into plant cells. *Mol. Plant Pathol.* **9**: 425-434.
5. **Bogdanove, A.J., J.F. Kim, Z. Wei, P. Kolchinsky, A.O. Charkowski, A.K. Conlin, A. Collmer, and S.V. Beer.** 1998. Homology and functional similarity of an *hrp*-linked pathogenicity locus, *dspEF* of *Erwinia amylovora* and the avirulence locus *avrE* of *Pseudomonas syringae* pathovar tomato. *Proc. Natl. Acad. Sci. USA* **95**: 1325-1330.
6. **Boyd, A.P., I. Lambermont, and G.R. Cornelis.** 2000. Competition between the Yops of *Yersinia enterocolitica* for delivery into eukaryotic cells : role of the SycE chaperone binding domain of YopE. *J. Bacteriol.* **182**: 4811-4821.
7. **Boureau, T., H. El Maarouf-Boteau, A. Garnier, M.-N. Brisset, C. Perino, I. Pucheu, and M.A. Barny.** 2005. DspA/E, a type III effector essential for *Erwinia amylovora* pathogenicity and growth in planta, induces cell death in host apple and nonhost tobacco plants. *Mol. Plant-Microbe Interact.* **19**: 16-24.
8. **Bronstein, P.A., E.A. Miao, and S.I. Miller.** 2000. InvB is a type III secretion chaperone specific for SspA. *J. Bacteriol.* **182**: 6638-6644.
9. **A. Burse, H. Weingart, and M.S. Ullrich.** 2004. The phytoalexin-inducible multidrug efflux pump AcrAB contributes to virulence in the fire blight pathogen, *Erwinia amylovora*. *Mol. Plant-Microbe Interact.* **17**: 43-54.
10. **Buttner, D., D. Gurlebeck, L.D. Noel, and U. Bonas.** 2004. HpaB from *Xanthomonas campestris* pv. *vesicatoria* acts as an exit control protein in type III-dependent protein secretion. *Mol. Microbiol.* **54**: 755-768.
11. **Buttner, D. and U. Bonas.** 2006. Who comes first? How plant pathogenic bacteria orchestrate type III secretion. *Curr. Opin. Microbiol.* **9**: 193-200.
12. **Casper-Lindley, C., D. Dahlbeck, E.T. Clark, and B.J. Staskawicz.** 2002. Direct biochemical evidence for type III-dependent translocation of the AvrBs2 effector into plant cells. *Proc. Natl. Acad. Sci. USA* **99**: 8336-8341.

13. **Cheng, L.W., D.M. Anderson, and O. Schneewind.** 1997. Two independent type III secretion mechanisms for YopE in *Yersinia enterocolitica*. *Mol Microbiol* **24**: 757–765.
14. **Chiu, J., P.E. March, R. Lee and D. Tillett.** 2004. Site-directed, ligase-independent mutagenesis (SLIM): a single-tube methodology approaching 100% efficiency in 4 h. *Nucleic Acids Res.* **32**: e174.
15. **Datsenko, K.A. and Wanner, B.L.** 2000. One-step inactivation of chromosomal genes in *Escherichia coli* using PCR products. *Proc. Natl. Acad. Sci. USA* **97**: 6640-6645.
16. **Debroy, S., R. Thilmony, Y.-B. Kwack, K. Nomura, and S.-Y. He.** 2004. A family of conserved bacterial effectors inhibits salicylic acid-mediated basal immunity and promotes disease necrosis in plants. *Proc. Natl. Acad. Sci. USA* **101**: 9927-9932.
17. **Ehrbar, K., B. Winnen, and W. Hardt.** 2005. The chaperone binding domain of SopE inhibits transport via flagellar and SPI-1 TTSS in the absence of InvB. *Mol. Microbiol.* **59**: 248-264.
18. **Elliott, S.J., S.W. Hutcheson, M.S. Dubois, J.L. Mellies, L.A. Wainwright, M. Batchelor, G. Frankel, S. Knutton, and J.B. Kaper.** 1999. Identification of CesT, a chaperone for the type III secretion of Tir in enteropathogenic *Escherichia coli*. *Mol Microbiol* **33**: 1176–1189.
19. **Feldman, M.A., S. Muller, E. Wuest, and G.R. Cornelis.** SycE allows secretion of YopE-DHFR hybrids by the *Yersinia enterocolitica* type III Ysc system. *Mol. Microbiol* **46**: 1183-1197.
20. **Gaudriault, S., L. Malandrin, J.-P. Paulin, and M.-A. Barny.** 1997. DspA, an essential pathogenicity factor of *Erwinia amylovora* showing homology with AvrE of *Pseudomonas syringae*, is secreted via the Hrp secretion pathway in a DspB-dependent way. *Mol. Microbiol.* **26**: 1057-1069.
21. **Gaudriault, S., J.-P. Paulin, and M.-A. Barny.** 2002. The DspB/F protein of *Erwinia amylovora* is a type III secretion chaperone ensuring efficient intrabacterial production of the Hrp-secreted DspA/E pathogenicity factor. *Mol. Plant Pathol.* **3**: 313-320.
22. **Ghosh, P.** 2004. Process of protein transport by the type III secretion system. *Microbiol. Mol. Biol. Rev.* **68**: 771-795.
23. **Gouet, P., E. Courcelle, D.I. Stuart, and F. Metoz.** 1999. ESPript: multiple sequence alignments in PostScript. *Bioinformatics* **15**: 305-308.
24. **Guo, M., S.T. Chancey, F. Tian, Z. Ge, Y. Jamir, and J.R. Alfano.** 2005. *Pseudomonas syringae* type III chaperones ShcO1, ShcS1, and ShcS2 facilitate

translocation of their cognate effectors and can substitute for each other in the secretion of HopO1-1. *J. Bacteriol.* **187**: 4257-4269.

25. **Ham, J.H., D.R. Majerczak, A.S. Arroyo-Rodriguez, D.M. Mackey, and D.L. Coplin.** 2006. WtsE, an AvrE-family effector protein from *Pantoea stewartii* subsp. *stewartii*, caused disease-associated cell death in corn and requires a chaperone protein for stability. *Mol. Plant-Microbe Interact.* **19**: 1092-1102.
26. **Higashide, W. and D. Zhou.** 2006. The first 45 amino acids of SopA are necessary for InvB binding and SPI-I secretion. *J. Bacteriol.* **188**: 2411-2420.
27. **Huynh, T.V., D. Dahlbeck, and B.J. Staskawicz.** 1989. Bacterial blight of soybean: regulation of a pathogen gene determining host cultivar specificity. *Science* **245**: 1374-1377.
28. **Jiang, J., L.W. Fan, and W.H. Wu.** 2005. Evidences for the involvement of endogenous cAMP in *Arabidopsis* defense responses to verticillium toxins. *Cell Res.* **15**: 585-592.
29. **Jones, D.T.** 1999. Protein secondary structure prediction based on position-specific scoring matrices. *J. Mol. Biol.* **292**: 195-202.
30. **Kovach, M.E., P.H. Elzer, D.S. Hill, G.T. Robertson, M.A. Farris, R.M. Roop, and K.M. Peterson.** 1995. Four new derivatives of the broad-host-range cloning vector pBBR1MCS, carrying different antibiotic-resistance cassettes. *Gene* **166**: 175-176.
31. **Kurosaki, F., and A. Nishi.** 1993. Stimulation of calcium influx and calcium cascade by cyclic AMP in cultured carrot cells. *Archiv. Biochem. Biophys.* **302**: 144-51.
32. **Lee, S.H. and J.E. Galan.** 2004. *Salmonella* type III secretion-associated chaperones confer secretion-pathway specificity. *Mol. Microbiol.* **51**: 483-495.
33. **Lefevre, F., M.H. Remy, and J.M. Masson.** 1997. Alanine-stretch scanning mutagenesis: a simple and efficient method to probe protein structure and function. *Nucleic Acids Res.* **25**: 447-448.
34. **Letzelter, M., I. Sorg, L.J. Mota, S. Meyer, J. Stalder, M. Feldman, M. Kuhn, I. Callebaut, and G.R. Cornelis.** 2006. The discovery of SycO highlights a new function for type III secretion effector chaperones. *EMBO J.* **25**: 3223-3233.
35. **Lilic, M., M. Vujanac, and C.E. Stebbins.** 2006. A common structural motif in the binding of virulence effectors to bacterial secretion chaperones. *Mol. Cell* **21**: 653-664.
36. **Losada, L.C. and S.W. Hutcheson.** 2005. Type III secretion chaperones of *Pseudomonas syringae* protect effectors from Lon-associated degradation. *Mol. Microbiol.* **55**: 941-953.

37. **Matsumoto, H., and G.M. Young.** 2009. Essential role of the SycP chaperone in Type III secretion of the YspP effector. *J. Bacteriol.* **191**: 1703-1715.
38. **Meng, X., J.M. Bonasera, J.F. Kim, R.M. Nissinen, and S.V. Beer.** 2006. Apple proteins that interact with DspA/E, a pathogenicity factor of *Erwinia amylovora*, the fire blight pathogen. *Mol. Plant-Microbe Interact.* **19**: 53-61.
39. **Miao, E.A., and S.I. Miller.** 2000. A conserved amino acid sequence directing intracellular type III secretion by *Salmonella typhimurium*. *Proc. Natl. Acad. Sci. USA* **97**: 7539-7544.
40. **Mudgett, M.B., O. Chesnokova, D. Dahlbeck, E.T. Clark, O. Rossier, U. Bonas, and B.J. Staskawicz.** 2000. Molecular signals required for type III secretion and translocation of the *Xanthomonas campestris* AvrBs2 protein to pepper plants. *Proc. Natl. Acad. Sci. USA* **97**: 13324-13329.
41. **Nissinen, R. M., A.J. Ytterberg, A.J., Bogdanove, K. van Wijk, and S.V. Beer.** 2007. Analyses of the secretomes of *Erwinia amylovora* and selected *hrp* mutants reveal novel type III secreted proteins and an effect of HrpJ on extracellular harpin levels. *Mol. Plant Pathol.* **8**:55-67.
42. **Notredame, C., D. Higgins, and J. Heringa.** 2000. T-Coffee: a novel method for multiple sequence alignments. *J. Mol. Biol.* **302**: 205-207.
43. **Parsot, C., C. Hamiaux, and A.-L. Page.** 2003. The various and varying roles of specific chaperones in type III secretion systems. *Curr. Opin. Microbiol.* **6**: 7-14.
44. **Schechter, L.M., K.A. Roberts, Y. Jamir, J.R. Alfano, and A. Collmer.** 2004. *Pseudomonas syringae* type III secretion system targeting signals and novel effectors studied with a *CyaA* translocation reporter. *J. Bacteriol.* **186**: 543-555.
45. **Schesser, K., E. Frithz-Lindsten, and H. Wolf-Watz.** 1996. Delineation and mutational analysis of the *Yersinia pseudotuberculosis* YopE domains which mediate translocation across bacterial and eukaryotic cellular membranes. *J. Bacteriol* **178**: 7227-7233.
46. **Sory, M.-P., and G.R. Cornelis.** 1994. Translocation of a hybrid YopE-adenylate cyclase from *Yersinia enterocolitica* into HeLa cells. *Mol. Microbiol.* **14**: 583-594.
47. **Sory, M.-P., A. Boland, I. Lambermont, and G.R. Cornelis.** 1995. Identification of the YopE and YopH domains required for secretion and internalization into the cytosol of macrophages, using the *cyaA* gene fusion approach. *Proc. Natl. Acad. Sci. USA* **92**: 11998-12002.
48. **Stebbins, C.E. and J.E. Galan.** 2001. Maintenance of an unfolded peptide by a cognate chaperone in type III secretion. *Nature* **414**: 77-81.

49. **Thomas, N.A., W. Deng, J.L. Puente, E.A. Frey, C.K. Yip, N.C.J. Strynadka, and B.B. Finlay.** 2005. CesT is a multi-effector chaperone and recruitment factor required for the efficient type III secretion of both LEE and non-LEE encoded effectors of enteropathogenic *Escherichia coli*. *Mol. Microbiol.* **57**: 1762-1779.
50. **Trulzsch, K., A. Roggenkamp, M. Aepfelbacher, G. Wilharm, K. Ruckdeschel, and J. Heesemann.** 2003. Analysis of chaperone-dependent Yop secretion/translocation and effector function using a mini-virulence plasmid of *Yersinia enterocolitica*. *Intern. J. Med. Microbiol.* **293**: 167-177.
51. **Vinatzer, B., Jelenska, J., and Greenberg, J.T.** 2005. Bioinformatics correctly identifies many type III secretion substrates in the plant pathogen *Pseudomonas syringae* and the biocontrol isolate *P. fluorescens* SBW25. *Mol. Plant Pathol.* **18**: 877-888.
52. **Wei, Z. M., B.J. Sneath, and S.V. Beer.** 1992. Expression of *Erwinia amylovora* *hrp* genes in response to environmental stimuli. *J. Bacteriol.* **174**: 1875-1882.
53. **Woestyn, S., M.-P. Sory, A. Boland, O. Lequenne, and G.R. Cornelis.** 1996. The cytosolic SycE and SycH chaperones of *Yersinia* protect the region of YopE and YopH involved in translocation across eukaryotic cell membranes. *Mol. Microbiol.* **20**:1261-71.
54. **Zhao, Y., S.E. Blumer, and Sundin, G.W.** 2005. Identification of *Erwinia amylovora* genes induced during infection of immature pear tissue. *J. Bacteriol.* **187**: 8088-8103.
55. **Zhao, Y., S.-Y. He, and G. Sundin.** 2006. The *Erwinia amylovora* *avrRpt2Ea* gene contributes to virulence on pear and AvrRpt2EA is recognized by *Arabidopsis* RPS2 when expressed in *Pseudomonas syringae*. *Mol. Plant-Microbe Interact.* **19**: 644-654.
56. **Zhao, Y., G.W. Sundin, and D. Wang.** 2009. Construction and analysis of pathogenicity island deletion mutants of *Erwinia amylovora*. *Can. J. Microbiol.* **55**: 457-464.

**Chapter 3: Homology-based modeling of the *Erwinia amylovora* type III secretion chaperone DspF used to identify amino acids required for virulence and interaction with the effector DspE.**

**ABSTRACT**

Chaperones involved in bacterial type III secretion are critical to effector translocation into host cells and to virulence of many pathogens. In the past decade, crystallization studies have elucidated the highly conserved structure of numerous type III secretion chaperones and identified a general pattern of surface sites predicted to be essential to interaction with the effector. However, few mutational analyses have been performed to determine the relevance of these sites. Here, the structure of DspF, a T3SS chaperone required for virulence of the fruit tree pathogen *Erwinia amylovora*, was modeled based on predicted structural homology to characterized T3SS chaperones. This model, along with observed sequence conservation, was used to hypothesize which residues could be important for interaction with the secreted effector DspE. Eleven site-directed alanine replacement mutants were constructed and assessed for effect on virulence complementation, dimerization, and interaction with the N-terminal chaperone-binding site of DspE. Four amino-acid residues were identified that did not complement the virulence defect of a *dspF* knockout mutant, and three of these residues were required for interaction with the N-terminus of DspE. In addition, these four site-directed mutants of DspF caused a moderate reduction in virulence when introduced into wild-type Ea1189, and two significantly lowered translocation levels of a DspE-CyaA fusion protein. This study supports the significance of the predicted  $\beta$ -sheet helix-binding groove in DspF chaperone function, and suggests that structural homology modeling may be a useful tool in the functional characterization of many T3SS chaperones.

## INTRODUCTION

A wide variety of bacterial pathogens and symbionts require a type III secretion system (T3SS) to inject host cells with effector proteins important for suppressing host defenses and establishing infection. Many of these effector proteins interact with specific type III secretion chaperones prior to secretion. T3SS effector chaperones may perform numerous functions; some chaperones have been shown to bind directly to a specific T3SS apparatus or to hold the N-terminus of the effector in an unfolded position, suggesting a direct loading function (1, 12, 24, 33). T3SS chaperones may also cover an inhibitory or destabilizing domain on the effector, organize a temporal secretion hierarchy among effectors of varying importance, or regulate the transcription of cognate effectors (6, 10, 25, 38).

Despite a lack of sequence conservation, T3SS effector-specific chaperones (heretofore T3SS chaperones) are highly structurally conserved; they are small, acidic dimers with a characteristic shape of three  $\alpha$ -helices and five  $\beta$ -sheets (28). The publication of at least 10 T3SS chaperone crystal structures in the last decade has revealed that most chaperones possess two surface-exposed hydrophobic patches, one of which lies in a twisted  $\beta$ -sheet groove often referred to as the “helix-binding groove” (3, 8, 11, 26, 32, 33, 37). Co-crystal structures of effector-bound chaperones have indicated that the N-terminus of the effector protein wraps around the exterior of the chaperone, burying the helix-binding groove on each monomer as well as a second hydrophobic site (4, 26, 30, 33). Mutagenesis studies of the *Salmonella enterica* sv. *Typhimurium* chaperone gene *sigE* and the *Escherichia coli* gene *cesT* determined that selected external hydrophobic residues play an important role in the chaperone-effector interaction (20,

27). However, there are many additional residues in each chaperone structure predicted to interface with secreted effectors, including hydrophobic and electrostatic residues exposed in the  $\beta$ -sheet helix-binding groove. Very few mutational analyses of chaperones have been performed, and the relative contribution of structural features to different chaperone functions is still poorly understood.

*Erwinia amylovora* is a gram-negative bacterium that causes a devastating blight disease of apple and pear trees. Unlike the model bacterial phytopathogen *Pseudomonas syringae*, members of the genus *Erwinia* are enterobacterial plant pathogens, with strong taxonomic and genomic similarity to *Salmonellae* and *Escherichiae* (35). Pathogenesis of *E. amylovora* is dependent on the secretion of DspE, a large T3SS-secreted effector of unknown function (14). DspF, the specific chaperone of DspE, is a chaperone involved in DspE stability and secretion into the medium (14, 15). DspF is a member of a large family of T3SS chaperones in plant pathogens, with putative or confirmed sequence homologs in *Pseudomonas syringae*, *Pantoea agglomerans*, *Pantoea stewartii*, and *Dickeya dadantii* (5, 13, 18, 31). Deletion of *dspF* from *E. amylovora* causes a strong reduction in virulence (36), making *E. amylovora* a useful system for genetic studies of chaperone function.

Recently, we used site-directed mutation and protein-protein interaction studies to identify N-terminal features of DspE required for secretion and for binding DspF (36). Here, a mutagenesis approach was used to characterize sequence and structural requirements of DspF chaperone function. The tertiary structure of DspF was modeled based on sequence and secondary structural similarities between DspF and structurally characterized type III secretion chaperones from human pathogens. The model guided an

alanine-scanning mutagenesis study of the conserved residues of the predicted helix-binding groove of DspF. We identified multiple amino acid residues required for *E. amylovora* virulence and/or interaction with DspE, suggesting that electronegative groove residues are important to the chaperone-effector interaction.

## **MATERIALS and METHODS**

**Bacterial strains and plasmids and genetic techniques.** The bacterial strains and plasmids used in this study are listed in Table 1. PCR, sequencing, and cloning was performed using standard techniques and protocols (2). All sequencing reactions were conducted at the Michigan State University Research Technology Support Facility.

**Site-directed alanine replacement mutagenesis.** Alanine-replacement mutants were constructed using the Quikchange mutagenesis system following the manufacturer's recommendations (Agilent Technologies, Stratagene Division; La Jolla, CA). The entire plasmid pLRT7, including the *dspF* gene and its native promoter, was amplified using complementary mutagenic primers and the following PCR reaction conditions: 94°C for 30s, 57°C for 30s, and 68°C for 7 m. Primers for mutagenesis of *dspF* are shown in Table 2. One microliter of *DpnI* was added to 50  $\mu$ L reaction mixture and incubated at 37°C for 1 h. PCR products were then transformed into *E. coli* DH5 $\alpha$ . Plasmid inserts were sequenced to ensure that a single-site nucleotide alteration was the only difference between mutant and wild-type vector inserts. pLRT7 and derivatives were introduced into *E. amylovora* Ea1189 $\Delta$ *dspF* by electroporation. The presence of the *dspF* plasmids in each complemented strain was confirmed by PCR.

**Structural prediction methods.** 3D-Jury, a consensus fold-recognition server combining nine structural prediction programs on Metaserver (16;

[http://meta.bioinfo.pl/submit\\_wizard.pl](http://meta.bioinfo.pl/submit_wizard.pl)), was used to search for structural homologs of DspF. Although 3D-Jury hits included most known T3SS chaperone structures, the structure of the chaperone SicP (1jyo\_A) from *Salmonella enterica* sv. *Typhimurium* was ranked the most similar to DspF by the prediction servers. A Phyre analysis also identified SicP as the best match to DspF, with an equivalent overall alignment (19; <http://www.sbg.bio.ic.ac.uk/phyre/>). Using the sequence alignment ranked most highly by 3D-Jury, a backbone homology model of DspF was constructed from the SicP structure using in-house software. Side chain atom positions were also taken from 1jyo for the homology model, but only if the aligned residues in DspF and SicP were identical. The remaining side chain conformations were then constructed using SCWRL (22; <http://dunbrack.fccc.edu/scwrl4/SCWRL4.php>). The DspF structural model is available upon request from the authors. The predicted molecular surface of the structure was visualized using Deepview/swiss PDB viewer (17). To identify conserved residues of DspF, an alignment of DspF, WtsF, and AvrF protein sequences was constructed using T-Coffee (28).

**Yeast two-hybrid assays.** Site-directed mutant sequences of *dspF* were amplified using the primers DspFEcF (5'- catgaattcatgacatcgtcacagcagcgg-3') and DspFXhR (5'- gatcCTCGAGttatgccgctactctcgtc-3'), digested with *EcoRI* and *XhoI*, and ligated into the bait vector pB42AD. To construct the prey vectors pLRT93 and pLRT219, *dspF* was amplified with primers DspFBam1F (gatcggatcctcatgacatcgtcacagcagcgg) and DspFXhR, and nucleotides 1-1800 of *dspE* were amplified with primers DspEBamF (5'- gcggatcctcatggaattaaatcactggg-3') and DspEXhoR800 (5'- cgctcgaggttagaaggagcgaatgtcccc-3'). PCR products were digested with *BamHI* and *XhoI*

and ligated in fusion with the LexA DNA binding domain in the prey vector pGilda (Clontech; Mountain View, CA). Bait and prey constructs were co-transformed into the *Saccharomyces cerevisiae* strain EGY48 p80(*lacZ*) using the Yeast Transformation Kit (Zymo; Orange, CA). Transformation reaction mixtures were plated on SD medium supplemented with -ura-his-trp dropout solution (Clontech). Transformants were re-plated on SD-gal medium (Clontech) supplemented with 5-bromo-4-chloro-3-indolyl-beta-D-galactopyranoside (X-gal; 80 µg/mL), and color development was observed after incubation at 30° C for three days. Expression of DspF-B42-HA was confirmed by western blot of lysed yeast cells using anti-HA-Hrp antibody (Roche; Indianapolis, IN, USA)

**Virulence assays.** Bacterial virulence was assayed using an immature pear fruit assay as previously described (39). Briefly, surface-sterilized immature pears were wounded, and bacterial strains ( $1.5 \times 10^6$  cfu/mL) were pipetted on the wound. Pears were incubated in a humid chamber at 28° C for 9 d. After three days, pears developed a single, circular black lesion spreading out from the inoculation site. Lesion diameters were measured in two perpendicular directions using digital calipers, and the average of these two measurements was recorded as the average lesion diameter for each pear. If the lesions spread to the sides or back of the pears, a piece of twine was used to measure the lateral length of the lesion around the circumference of the pear.

**Translocation assays.** Alanine-replacement mutants of *dspF* and the native *dspF* sequence were amplified with primers FHF (5' gcataagcttcgcatctgcgcttactgattga 3') and FxbR (5' gatcctagattatgccgctactctcgtcta 3'), digested with *HindIII* and *XbaI*, and ligated into the broad host-range vector pBRR1-MCS2 to create plasmids pLRT98 and

pLRT 158-161. pLRT201, expressing DspE(1-737)-CyaA, was introduced into wild-type *E. amylovora* Ea1189. CyaA fusion expression was confirmed via western blot with anti-CyaA antibodies (Santa Cruz Biotechnology; Santa Cruz, CA). pBRR1-MCS2 derivatives were introduced into Ea1189/pLRT201 by electroporation. CyaA-expressing overnight cultures were adjusted to  $4.5 \times 10^8$  cfu/mL (O.D. = 0.3) and infiltrated into the leaves of 8-wk old *Nicotiana tabacum* cv. *Samsun* plants. Leaf disks were collected after 11 h. cAMP was extracted and quantified as previously described (36).

## RESULTS

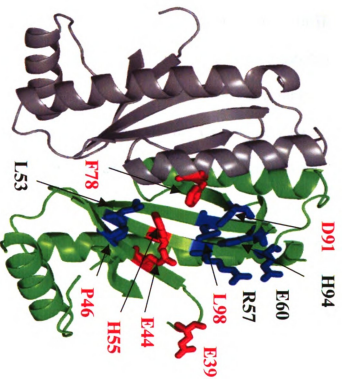
**Structural modeling of DspF.** A combination of secondary structural alignment and computational modeling was used to identify candidate residues of importance for DspF chaperone function. The tertiary structure of DspF was modeled based on predicted structural homology to *S. enterica* subsp. *Typhimurium* SicP and other type III secretion chaperones as described in Materials and Methods. The predicted tertiary structure of DspF is shown in Figure 3-1A; structural alignment with SicP and more closely-related chaperones from other plant pathogens is shown in Figure 3-1B. Although DspF and SicP share only 15% sequence identity, residues 31-98 of DspF, which are predicted to form a dimerization domain and helix-binding groove, share a much higher degree of similarity with SicP. The amino acids predicted to form the  $\beta$ -sheets of the helix-binding groove were roughly 30% identical and 60% similar between SicP and DspF (Figure 3-1B). In addition, the secondary structure of SicP was the most closely aligned to DspF using multiple secondary alignment algorithms in the 3D-Jury suite. Thus, the sequence and secondary structure of the central portion of DspF could be closely aligned to that of SicP. Based on these similarities, the DspF structure is predicted to include the

characteristic features common to class I type III secretion chaperones, including the conserved 3  $\alpha$ -helical structure and an external groove similar to that implicated in helix-binding.

**Identification of candidate DspF residues involved in virulence and effector**

**interaction.** Sequence conservation and surface-exposed side chains are potential indicators that an amino acid could be involved in protein-protein interactions. To identify the most highly conserved amino acids of DspF, psiBLAST search was used to identify unique sequence homologs of DspF including DspF sequences from the related enterobacterial plant pathogens *Erwinia pyrifoliae*, *Pantoea agglomerans* pv. *gypsophila*, *Pantoea stewartii*, and *Pectobacterium carotovora* subsp. *atrosepticum*. The sequence of the related type III secretion chaperone AvrF from *Pseudomonas syringae* was also included. When these protein sequences were aligned, 29 fully conserved residues were identified in DspF (Figure 3-1B). The DspF structural homology model was used to screen conserved residues for putative substrate-exposed side chains. We identified seven amino acids with predicted surface exposure and absolute conservation among the closest homologs of DspF: E39, E44, P46, H55, F78, D91, and L98 (Figure 3-1A). These conserved residues had a predicted localization in a groove similar to the helix-binding groove identified in crystallization studies of type III chaperones (3, 27, 32, 37). To allow for a complete analysis of the predicted helix-binding groove of DspF, we identified four additional amino acids, L53, R57, E60, and H94, predicted to face the helix-binding groove, although these were not completely conserved (Figure 3-1A and 3-1B).

**Figure 3-1.** Structural modeling and site-directed mutagenesis of DspF. **A.** Homology-based model of DspF. Two monomers are depicted in green and grey. Residues selected for alanine-replacement mutagenesis are labeled; residues completely conserved among DspF homologs are labeled in a red font. Alanine replacement of side chains depicted in red prevented complementation of virulence in *E. amylovora*, while replacement of residues colored blue did not affect complementation. Structure was rendered using MolMol (21). **B.** Alignment of the amino acid sequence of DspF with that of 5 closely-related chaperones from plant pathogenic bacteria and with *Salmonella typhimurium* SicP. Residues completely conserved among DspF family chaperones are indicated in black; conservatively replaced residues are indicated in grey. Red asterisks specify highly-conserved DspF residues targeted for site-directed mutagenesis. Blue asterisks indicate the SicP residues buried by interaction with the effector SptP, previously calculated by Singer *et al.* (32) based on the work of Stebbins and Galan (33). Genbank accessions for aligned sequences are: *E. amylovora*, AAC04851; *E. pyrifoliae*, AAS45451; *Pantoea stewartii*, AAG01468, *Pantoea agglomerans*, AAS20350; *Pseudomonas syringae* pv. *phaseolicola*, YP273526; *Pectobacterium carotovorum*, ZP\_03833469; and *S. typhimurium*, AAC38655.



```

Eamy 31 CALYNEQDEEAAVLEVPQHSDSLILHCRITL EADPQTSITLYSMILQNFEMAAMRGCVLADDELHNVRIGF
Epyr 31 CALYNEQNEEAAVLEIPEHSDSLILHCRIT IENPQTSITLYSMILQNFEMAAMRGCVLADDELHNVRIGF
Estw 31 CALYNEQNEEAAVLEIPEHSQCLLFHQCQI IANRHHQAGNFYALLIQNFESAMRGCVLADDELHNVRIGF
Ecar 31 CALREPDGKEAAVLEVEPSAGSALVHSDVRFQGDVGT EYVQILMNFEMAAMRGCVLADDELHNVRIGF
Pagd 31 GPMYTDQGEAAVLEVEPSHSCLLHCELASTAPHSALNFY ALLIQNFEMAAMRGCVLADDELHNVRIGF
Peyr 31 CALYDQNN EAAIIEIPEHSEMVIHCRIRGC- PERAPDILR- ILSNPFVARLHGCVLAVDQ- GDVRIQA
Slcp 31 CILLDSDIPT---SIEAKDIIWILNGMTIIPLSVPCGDS IWRQIMVINGELAAANNRGTIATTDAAETIETI
*****

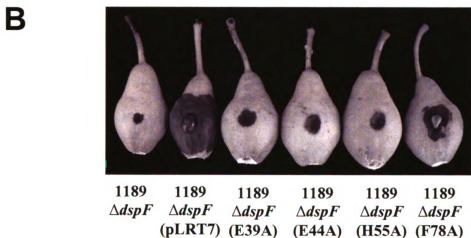
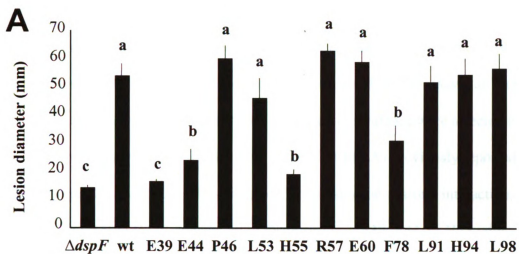
```

Figure 3-1.

To determine whether these residues aligned with helix-binding groove residues in other chaperones, the SicP-based structural model of DspF was compared to three other closely related structures: *P. syringae* AvrPphF Orf1 (PDB accession 1s28), *Yersinia pestis* YscB (PDB accession 1xkp), and the T110839 chaperone protein from *Synechococcus elongatus* (PDB accession 2plg). Despite little sequence conservation, a majority of the 11 amino acids predicted to face the helix-binding groove of DspF aligned with residues previously determined to be exposed in the corresponding groove of AvrPphF orf1 (11 aligned /11 groove residues), YscB (9/11) and T110838 (8/11) in 3D-Jury secondary structure alignments (data not shown). In addition, the 11 candidate helix-binding residues of DspF aligned closely in both sequence and secondary structural alignments with previously identified effector-buried residues of SicP (Figure 3-1A). Thus, the conserved residues in DspF predicted to face the helix-binding groove are strong candidates for interaction with DspE.

**Identification of four conserved residues of DspF required for virulence function.** To determine the functional significance of residues in the putative helix-binding groove, 11 site-directed alanine-replacement mutants of *dspF* were constructed from the parent vector pLRT7, carrying the *dspF* orf and its immediate upstream promoter. Alanine replacement is a common strategy for determining the role of single amino acid surface residues without altering the structural integrity of the protein (9). The alanine-replacement pLRT7 derivatives were introduced into Ea1189 $\Delta$ *dspF*, yielding 11 complemented strains. In a virulence assay, immature pear fruits were inoculated with each complemented strain as described in Materials and Methods. Lesion diameters were measured at eight days post-inoculation. Four site-directed mutants, E39A, E44A, H55A,

and F78A, did not complement the virulence phenotype of *Ea1189ΔdspF*. Strains carrying these plasmids caused lesions that were significantly smaller than the strain complemented with wild-type *dspF* (Figure 3-2). These four amino acids were considered to be required for virulence. The remaining seven of the plasmids expressing *dspF* site-directed mutants fully complemented the virulence phenotype of the *dspF* deletion mutant, with no significant difference in virulence between strains complemented with the wild-type and mutant derivative vectors (Figure 3-2). While *Ea1189ΔdspF* complemented with *dspF*(E39A) caused lesions not significantly larger than that complemented with wild-type DspF, *Ea1189ΔdspF* complemented with *dspF*(E44A), *dspF*(H55A), or *dspF*(F78A) caused levels of virulence intermediate between *Ea1189ΔdspF* and *Ea1189ΔdspF/pLRT7* (Figure 3-2).



**Figure 3-2.** Virulence phenotype of site-directed mutants. **A.** Average lesion diameters on pears inoculated with Eal189 $\Delta dspF$  carrying a plasmid with wild-type *dspF*, an empty vector, or one of 11 site-directed *dspF* mutants. Error bars depict lesion diameters  $\pm$ SE. Letters a, b, and c denote treatments equivalent to wild-type, significantly different from both the wild-type and the vector control ( $p < 0.05$ ), and significantly different from the wild-type only ( $p < 0.001$ ), respectively. **B.** Immature pears after infection with selected strains as described in **A.** Photographs and measurements were taken 8 days post-inoculation.

**Three DspF residues required for virulence are also required for interaction with the N-terminus of DspE.** Previously, we mapped a DspF-binding site to within amino acids 1-150 of DspE (36). Here, a LexA-based yeast two-hybrid (Y2H) assay was used to determine whether site-directed mutants of DspF affected in virulence were affected in their interaction with the N-terminal 150 amino acids of DspE. As previously reported, a fusion of wild type DspF with the B42 activation domain showed a strong interaction with LexA-DspE(1-150) (36). Replacement of DspF residues E39, E44, or H55 with alanine abolished this interaction (Figure 3-3A). Only one virulence-deficient mutant, B42AD-DspF (F78A), showed a strong interaction with the DspE fusion protein. As a control, B42AD-DspF constructs with alanine replacements in residues E60, D91, or H94, residues not required for virulence, interacted strongly with DspE (1-150) in the Y2H assay (Figure 3-3A), suggesting a correlation between effector-binding ability and complementation of virulence phenotype. In a western blot analysis of yeast lysates, B42-HA-DspF and variants were all similarly expressed and migrated at the same size, indicating that a lack of binding was not due to loss of expression (data not shown). All site-directed mutants showed a positive interaction with a longer fragment of DspE, LexA-DspE(1-600), although color development appeared weaker in the interaction between LexA-DspE (1-600) and B42-HA-DspF (E39A), B42-HA-DspF (E44A), and B42-HA-DspF (H55A) (Figure 3-3B). All B42-HA-DspF fusions interacted with a LexA-DspF fusion in yeast (Figure 3-3C), indicating that the site-directed mutations did not affect DspF homodimerization.

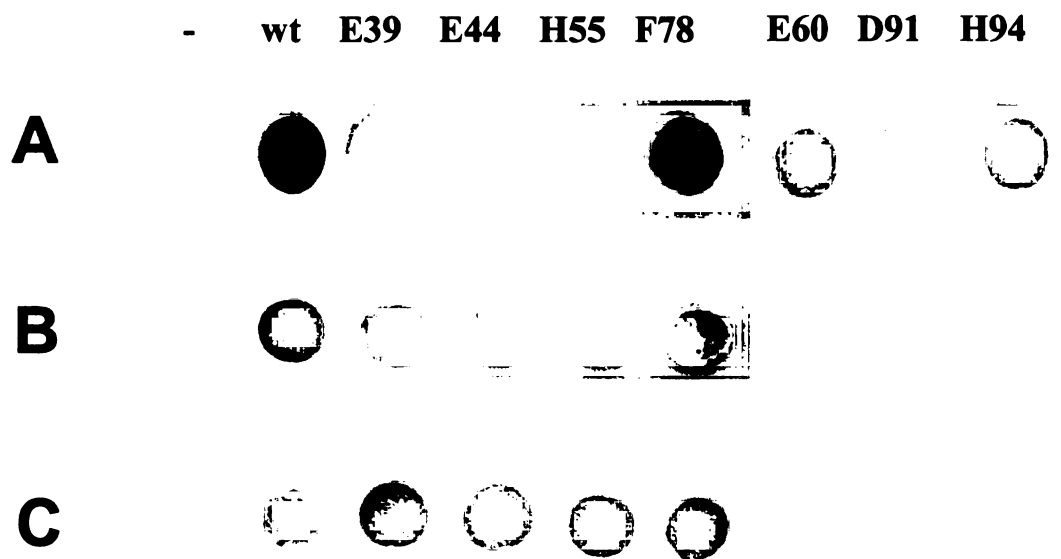


**Figure 3-3.** Alanine replacement of predicted helix-binding groove residues of DspF disrupts the interaction with the N-terminus of DspE in yeast. **A.** Yeast two-hybrid interaction of LexA-DspE(1-150) with pB42-HA-T (-), B42-HA-DspF (wt), or site-directed alanine replacement mutants. Dark coloration indicates a positive interaction. **B.** Interaction of LexA-DspE(1-600) with B42-HA-DspF and site-directed alanine replacement derivatives. **C.** Interaction of LexA-DspF with B42-HA-DspF and site-directed alanine replacement derivatives. All yeast strains were incubated on the same plate and photographed after 72 h at 30° C.

**Site-directed mutants reduce virulence of wild-type Ea1189 and moderately reduce translocation levels of the N-terminus of DspE.** Having observed that site-directed mutants of DspF interact with wild-type DspF in yeast, we hypothesized that ectopic expression of DspF site-directed mutants would have a dominant-negative effect on wild-type DspF function; that is, the alanine-replacement mutants would negatively affect secretion of DspE and virulence of *E. amylovora*. Negative dominance would indicate that site-directed DspF mutants were interacting with wild-type DspF and abrogating its function. On the other hand, a lack of negative dominance would suggest that the DspF dimer may be able to function normally with only one copy of the amino acid in question. To maximize levels of *dspF* expression and any potential effect of negative dominance, we cloned *dspF* and *dspF* site-directed mutants into a pGem high-copy cloning vector to create constructs pLRT215-219. pLRT215, expressing wild-type *dspF*, complemented Ea1189 $\Delta$ *dspF* more strongly than pLRT7 did (data not shown). In an immature pear assay, all strains of Ea1189 expressing site-directed *dspF* mutants showed decreased virulence after five days compared with wild-type Ea1189 or Ea1189 carrying wild-type *dspF* (Figure 3-4A, 3-4B). To determine whether this could be the result of reduced translocation levels of DspE, *dspF* derivatives DspF (E44A), DspF (H55A) and DspF (F78A) were subcloned into the broad host-range vector pBBR1-MCS2 and introduced into Ea1189 expressing DspE (1-737)-CyaA. Translocation levels were assessed as described in Materials and Methods. Expression of each site-directed mutant caused a decrease in translocation levels, although this reduction was not significant for co-expression with DspF (H55A) (Figure 3-4C). To determine whether the reduction in DspE fusion translocation was due to a reduction in expression levels, strains co-

expressing DspE(1-737)-CyaA and DspF variants were grown in *hrp*-inducing minimal medium, and levels of DspE(1-737)-CyaA were analyzed by western blot. DspE-CyaA fusion proteins accumulated to similar approximate levels across treatments (data not shown). Together, these results indicate that overexpression of site-directed mutants of DspF has a moderate dominant-negative effect on virulence, and negatively impacts DspE (1-737)-CyaA translocation to varying degrees.

**Figure 3-4.** Site-directed mutants cause moderate reductions in virulence and DspE(1-737)-CyaA translocation when expressed in wild-type *E. amylovora*. **A.** Lesions on immature pears five days after inoculation with wild-type Ea1189 (Wt) and Ea1189 carrying site-directed *dspF* mutants. **B.** Average lesion diameters on pears inoculated with wild-type Ea1189 (wt), Ea1189 carrying wild-type *dspF* on a plasmid (Wt/*dspF*) and Ea1189 carrying site-directed *dspF* mutants. Bars represent the average of ten replicate pears +/- S.E. **C.** Effect of *dspF* and *dspF* variant expression on translocation levels of DspE(1-737)-CyaA. *dspF* and *dspF* variants were co-expressed with DspE (1-737)-CyaA in wild type *E. amylovora*. Bars represent the average of three replicate leaves +/- S.E. Asterisks denote means which are significantly different from the wild-type ( $p < 0.05$ ). **D.** *In-vitro* expression levels of DspE(1-737)-CyaA when co-expressed with *dspF*, *dspF* (E44A), *dspF* (H55A), and *dspF* (F78A), assayed by western blot of strains induced in *hrp* minimal medium..

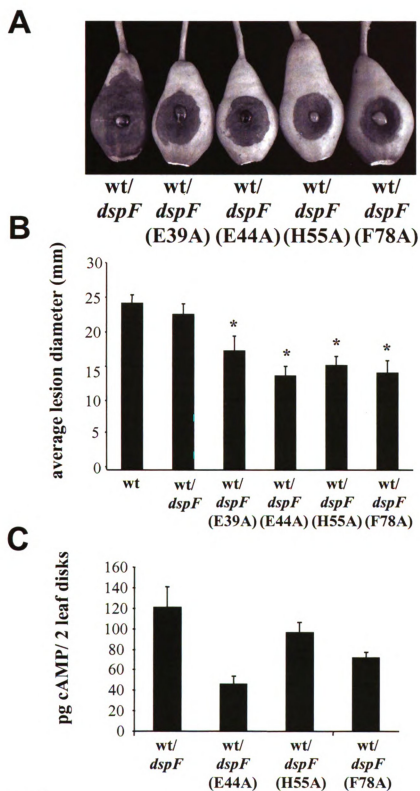


Figure 3-4.

## DISCUSSION

Type III secretion chaperones possess a remarkably conserved structure despite a lack of sequence homology. This conserved shape is suggestive of a divergent co-evolution of chaperones with cognate effector secretion signals, preserving T3SS targeting features while conferring specificity to the chaperone-effector interaction. In this study, we took advantage of structural similarities between T3SS chaperones to predict the residues likely to be exposed in the effector-binding groove of DspF, a member of a conserved family of chaperones important in plant pathogenesis. Of seven highly-conserved amino acid residues with predicted localization in this groove, mutagenesis of four residues led to reduced virulence; none of the four non-conserved residues tested influenced virulence. All but one of the 11 site-directed mutants tested was able to complement the *Ea1189ΔdspF* mutant to some degree, indicating that even the mutants impaired in virulence retained some function. These observations, combined with the high degree of secondary structural similarity among chaperones and the frequency of conserved sequence features between SicP and DspF, support the hypothesis that the residues investigated here face the chaperone-effector interaction site.

Conserved surface hydrophobic patches have been the focus of most discussions regarding the mechanism of T3SS chaperone-effector interactions; the presence and arrangement of these sites have been proposed to contribute to the stability, and perhaps even specificity, of the interaction (3, 26, 27). One of the conserved hydrophobic sites is typically located in the helix-binding groove (3, 8). However, the structure of the AvrPphF chaperone from *Pseudomonas syringae* pv. *phaseolicola* demonstrated a surprising lack of hydrophobic residues exposed in the corresponding groove, contrasting

sharply with the structure of SycE and suggesting a divergent mechanism of chaperone-effector binding (32). The structural model presented here suggests that DspF also lacks an extended hydrophobic surface in the predicted effector binding groove; only four of the 11 side chains predicted to project into the groove are nonpolar. It will be interesting to learn whether a missing or diminished hydrophobic patch at this site is a common feature of chaperones in plant pathogens.

Alanine replacement of three polar amino acids diminished the virulence phenotype of DspF. Electrostatic interactions mediated by external polar residues were proposed to be important contributors to chaperone-effector interactions (4), and we propose that polar DspF residues required for virulence could contribute to electrostatic interactions with the cognate effector DspE. DspF residue H55 aligns with an asparagine at position 49 in SicP, which is predicted to be involved in hydrogen bonding with the effector (33). The other two polar amino acids found to impact virulence are glutamate residues; glutamates have also been identified as predicted contributors to chaperone-effector hydrogen bonding (4, 33). The mechanism by which these three polar residues influence DspE binding and translocation remains unsolved, but the intermediate virulence phenotype of the DspF E44A and H55A mutants suggests that these variants may still interact with DspE at a reduced level. While the possibility of mutation-induced localized structural destabilization was not ruled out experimentally, a previous mutagenesis study of external T3SS chaperone residues identified no alanine replacement which caused chaperone misfolding (20).

The only nonpolar DspF residue found to be required for chaperone function in this study was F78, which is predicted to extend into the groove from the dimerization

helix of the opposite DspF monomer. The alanine-replacement strategy used here does not disrupt a hydrophobic surface and may be limited in determining the significance of many hydrophobic residues; however, alanine replacement is still useful to determine the significance of bulky hydrophobic residues or those with a specialized function. Many crystallized chaperones feature a large hydrophobic or ringed side chain in this relative position; while this feature is absent from SicP, secondary structure alignments suggest that the role of F78A of DspF is likely analogous to that of F69 in SycE, L73 of YscB, F78 of AvrPphF Orf1, W100 in chaperone T110839, and L74 in CesT (PDB accessions 1n5b, 1xkp, 1s28, 2plg, and 1k3e, respectively). In addition, phenylalanine stacking has been identified as a probable mechanism of chaperone-effector binding (33).

Replacement of DspF F78 with alanine caused a significant decrease in virulence and translocation of an N-terminal fusion of DspE, although dimerization and binding to the N-terminus of DspE in yeast were not apparently diminished. It is possible that the interaction of this mutant with the effector is stable enough to yield a positive result in the yeast two-hybrid assay, but destabilized enough to prevent a virulence phenotype. However, if mutation of F78 truly uncouples the virulence of DspF from interaction with DspE, F78 might be involved in some other aspect of type III secretion. To date, at least three other site-directed chaperone mutants have been identified which appear to uncouple chaperone binding from secretion (20, 34), but these were all mutations in surface-exposed electronegative residues. While F78A and similarly-positioned hydrophobic residues in other chaperones are predicted to face the edge of the helix-binding groove, the possibility that conserved external hydrophobic residues could play a role in translocation efficiency cannot be ruled out. Although the mechanism is still

unknown, F78 represents a common conserved feature of DspF family type III chaperones with a role in effector translocation.

Previously, we identified a strong chaperone binding site within residues 51-100 of DspE, although several downstream sites on DspE also interacted with DspF in yeast (36). Here, we show that alanine replacement of certain DspF residues disrupted the yeast two-hybrid interaction between DspF and DspE 1-150, but not between DspF and longer fragments of DspE. This could indicate that DspF could bind to alternate binding sites by slightly different mechanisms, or that the yeast two-hybrid interaction between DspF and downstream segments of DspE is due to weak, nonspecific binding. The requirement of virulence-associated DspF residues for binding the N-terminal 150 amino acids of DspE provides further support for the role of the N-terminus of DspE in chaperone binding and virulence.

This study included analysis of the negative-dominance phenotype of site-directed *dspF* mutants. Although our previous work found no difference in translocation levels of DspE(1-737)-CyaA when compared between Ea1189 $\Delta$ *dspE* and Ea1189 $\Delta$ *dspF* (36), more recent unpublished work indicates that DspE(1-737)-CyaA translocation levels from Ea1189 $\Delta$ *dspF* and  $\Delta$ *dspE* are lower than translocation levels from the wild-type Ea1189. Therefore, although DspF is not required for translocation of the N-terminus of DspE, DspF may be necessary for full levels of N-terminal DspE translocation. Here, we showed that expression of some *dspF* site-directed mutants strongly reduced translocation of DspE(1-737)-CyaA. This finding supports a function of DspF in translocation of the N-terminus of DspE, and shows that co-expression of wild-type DspF with DspF mutants abrogates this function. Introduction of *dspF* (H55A) into 1189 did not significantly

reduce N-terminal DspE translocation levels; it is unknown whether this is because DspF has a weaker requirement for the H55 residue or whether the H55A variant is otherwise limited in function. Site-directed DspF mutants caused a very small reduction in virulence only when expressed from a high-copy vector; this may be because moderate reductions in DspE translocation do not typically lead to a reduction in virulence (36). To our knowledge, this is the first analysis of negative dominance in T3SS chaperones.

As noted in the introduction, the helix-binding groove is not thought to be the sole effector-interaction site of type III secretion chaperones. In addition, several studies have focused on a second hydrophobic binding crevice partially composed of three broadly conserved hydrophobic residues in the  $\beta$ 1 sheet, facing away from the helix-binding groove (26, 32, 33). In SicP, this pocket was predicted to be composed of residues C27, L29, and L31 (26, 33), which align in DspF with C30, L32, and N34. The second hydrophobic patch could play an important role in DspF interaction with DspE, in addition to the relevance of putative helix-binding groove residues investigated here. While these hydrophobic surface patches have been identified as important contributors to chaperone-effector interactions, hydrogen bonds were also proposed to mediate the specificity of the interaction (4), and external electrostatic residues have a demonstrated role in chaperone function (20). Our results also lend further support for the significance of individual hydrophilic residues in the helix-binding groove.

This study presents a homology-based prediction of a conserved DspF helix-binding groove and evidence for the involvement of several residues in this putative groove structure in virulence and chaperone binding. The high degree of conservation of residues required for virulence among chaperones of the DspF family suggests that,

despite significant divergence, DspF-like chaperones bind to cognate effectors using a conserved mechanism. Our results support the importance of exposed polar and hydrophobic residues in T3SS chaperone function, and identify a novel conserved hydrophobic residue required for chaperone function but not for dimerization or effector binding. Through comparative modeling studies and further functional analysis, we submit that known chaperone structures may serve as a rich resource in revealing the mechanisms of T3SS targeting.

**Table 3-1.** Bacterial strains and plasmids used in Chapter 3.

| Strain or plasmid                | Characteristics   | Source                              |
|----------------------------------|---|-------------------------------------|
| <i>Escherichia coli</i> strain   |   |                                     |
| DH5 $\alpha$                     | F-80dlacZ $\Delta$ M15 $\Delta$ (lacZYA-argF)U169 endA1<br>recA1 hsdR17 (rk-mk+)deoR thi-1 supE44 gyrA96<br>relA1 $\lambda$ - | Invitrogen,<br>Carlsbad, CA,<br>USA |
| <i>Erwinia amylovora</i> strains |   |                                     |
| Ea1189                           | Wild type   | 7                                   |
| Ea1189 $\Delta$ dspF             | dspF deletion mutant, KmR   | 36                                  |
| Plasmids                         |   |                                     |
| pAlter-1                         | Cloning vector for mutagenesis, TetR  | Promega                             |
| pLRT7                            | pAlter-1 derivative expressing dspF   | This study                          |
| pLRT8                            | DspE(1-15)-CyaA   | 36                                  |
| pLRT18                           | pLRT7 derivative expressing dspF (E39A)   | This study                          |
| pLRT19                           | pLRT7 derivative expressing dspF(E44A)  | This study                          |
| pLRT20                           | pLRT7 derivative expressing dspF (P46A)   | This study                          |
| pLRT21                           | pLRT7 derivative expressing dspF (L53A)   | This study                          |
| pLRT22                           | pLRT7 derivative expressing dspF (H55A)   | This study                          |
| pLRT23                           | pLRT7 derivative expressing dspF (R57A)   | This study                          |
| pLRT24                           | pLRT7 derivative expressing dspF (E60A)   | This study                          |
| pLRT25                           | pLRT7 derivative expressing dspF (F78A)   | This study                          |
| pLRT26                           | pLRT7 derivative expressing dspF (D91A)   | This study                          |
| pLRT27                           | pLRT7 derivative expressing dspF (H94A)   | This study                          |
| pLRT28                           | pLRT7 derivative expressing dspF (L98A)   | This study                          |
| pGilda                           | HIS3 LexA BD bait vector, AmpR  | Clontech                            |
| pLRT93                           | LexA-DspF   | This study                          |
| pLRT219                          | LexA-DspE(1-600)  | This study                          |
| pB42AD                           | TRP1 B42 AD prey vector, AmpR   | Clontech                            |
| pLRT215                          | B42-HA-DspF   | 36                                  |
| pLRT61                           | B42-HA-DspF E39A  | This study                          |
| pLRT57                           | B42-HA-DspF E44A  | This study                          |
| pLRT58                           | B42-HA-DspF H55A  | This study                          |
| pLRT59                           | B42-HA-DspF F78A  | This study                          |
| pLRT60                           | B42-HA-DspF E60A  | This study                          |
| pLRT62                           | B42-HA-DspF D91A  | This study                          |
| pLRT63                           | B42-HA-DspF H94A  | This study                          |
| pBBR1-MCS2                       | broad host-range cloning vector, KmR  | 21                                  |
| pLRT98                           | pBBR1-MCS2 derivative expressing dspF   | This study                          |
| pLRT158                          | pBBR1-MCS2 derivative expressing dspF (E39A)  | This study                          |
| pLRT159                          | pBBR1-MCS2 derivative expressing dspF (E44A)  | This study                          |
| pLRT160                          | pBBR1-MCS2 derivative expressing dspF (H55A)  | This study                          |
| pLRT161                          | pBBR1-MCS2 derivative expressing dspF (F78A)  | This study                          |

Table 3-1 (cont'd).

|             |   |            |
|-------------|---|------------|
| pGem T-Easy | TA cloning vector, ApR                    | Promega    |
| pLRT201     | DspE(1-737)-CyaA                          | 36         |
| pLRT219     | pGem T-Easy expressing <i>dspF</i>        | This study |
| pLRT220     | pGem T-Easy expressing <i>dspF</i> (E39A) | This study |
| pLRT221     | pGem T-Easy expressing <i>dspF</i> (E44A) | This study |
| pLRT222     | pGem T-Easy expressing <i>dspF</i> (H55A) | This study |
| pLRT223     | pGem T-Easy expressing <i>dspF</i> (F78A) | This study |

**Table 3-2.** Oligonucleotide primers used for mutagenesis of *dspF*

| primer | sequence (5'→ 3')                      |
|--------|--|
| E39F   | taacgaacaagatgaggcggcggcggtgctgga      |
| E39R   | ccagcaccgccgcgcctcatcttgctgta          |
| E44F   | ggcggcggtgctggcagtaccgcaacacag         |
| E44R   | ctgtgtgcggtactgcccagcaccgccgc          |
| P46F   | cggtgctggaagtagcgcaacacagcgaca         |
| P46R   | tgtcgctgtgtgcgctactccagcaccg           |
| L53F   | cacagcgacagcctggcactacactgccg          |
| L53R   | cggcagtgtagtcccaggctgtcgctgtg          |
| H55F   | cagcgacagcctgtactagcctgccgaatcattgagg  |
| H55R   | cctcaatgattcggcaggctagtaacaggctgtcgctg |
| R57F   | ctgttactacactgcgcaatcattgaggctg        |
| R57R   | cagcctcaatgattgcgcagtgtagtaacag        |
| E60F   | cactgcgaatcattgggctgaccacaaac          |
| E60R   | gtttgtgggtcagcccaatgattcggcagtg        |
| F78F   | ctattacagctgaatgctgaaatggcggcc         |
| F78R   | ggccgccatttcagcattcagctgtaatag         |
| D91F   | gttggtggcgtggctgaactgcacaacg           |
| D91R   | cgttgtgcagttcagccagcgccagccaac         |
| H94F   | gctgatgaactggccaacgtgcgttatg           |
| H94R   | cataaacgcacgtggccagttcatccagc          |
| L98F   | ctgcacaacgtgcgtgcatgtttcagcagtc        |
| L98R   | gactgctgaaaacatgcacgcagttgtgcag        |

a. Underlined residues denote the altered codon.

## WORKS CITED

1. **Akeda, Y. and J.E. Galan.** 2005. Chaperone release and unfolding of substrates in type III secretion. *Nature* **437**: 911-915.
2. **Ausubel, F.M., R. Brent, R.E. Kingston, D.D. Moore, J.G. Seidman, J.A. Smith, and K. Struhl,** eds. 1997. *Current Protocols in Molecular Biology*. Wiley, New York.
3. **Birtalan, S., and P. Ghosh.** 2001. Structure of the *Yersinia* type III secretory system chaperone SycE. *Nat. Struct. Biol.* **8**: 974-978.
4. **Birtalan, S.C., R.M. Phillips, and P. Ghosh.** 2002. Three-dimensional secretion signals in chaperone-effector complexes of bacterial pathogens. *Mol. Cell* **9**: 971-980.
5. **Bogdanove, A.J., J.F. Kim, Z. Wei, P. Kolchinsky, A.O. Cahrkowski, A.K. Conlin, A. Collmer, and S.V. Beer.** 1998. Homology and functional similarity of an *hrp*-linked pathogenicity locus, *dspEF*, of *Erwinia amylovora* and the avirulence locus *avrE* of *Pseudomonas syringae* pathovar tomato. *Proc. Natl. Acad. Sci. USA* **95**: 1325-1330.
6. **Boyd, A.P, I. Lambermont, and G.R. Cornelis.** 2000. Competition between Yops of *Yersinia enterocolitica* for delivery into eukaryotic cells: role of the SycE chaperone binding domain of YopE. *J. Bacteriol.* **182**: 4811-4821.
7. **Burse, A., H. Weingart, and M.S. Ullrich.** 2004. NorM, an *Erwinia amylovora* multidrug efflux pump involved in in vitro competition with other epiphytic bacteria. *Appl. Environ. Microbiol.* **70**: 693-703.
8. **Buttner, C.R., G.R. Cornelis, D.W. Heinz, and H.H. Niemann.** 2005. Crystal structure of *Yersinia enterocolitica* type III secretion chaperone SycT. *J. Mol. Biol.* **375**: 997-1012.
9. **Cunningham, B.C., and J.A. Wells.** 1989. High-resolution epitope mapping of hGH-receptor interactions by alanine-scanning mutagenesis. *Science* **244**: 1081-1085.
10. **Darwin, K.H., and V.L. Miller.** 2001. Type III secretion chaperone-dependent regulation: activation of virulence genes by SicA and InvF in *Salmonella typhimurium*. *EMBO J.* **20**: 1850-1862.
11. **Edokimov, A.G., J. Tropea, K. Routzahn, and D.S. Waugh.** 2002. Three-dimensional structure of the type III secretion chaperone SycE from *Yersinia pestis*. *Acta Cryst.* **58**: 398-406.

12. **Ehrbar, K., B. Winnen, and W. Hardt.** 2006. The chaperone binding domain of SopE inhibits transport via flagellar and SPI-1 TTSS in the absence of InvB. *Mol. Microbiol.* **59**: 248-264.
13. **Frederick, R.D., M. Ahmad, D.R. Majerczak, A.S. Arroyo-Rodriguez, S. Manulis, and D.L. Coplin.** 2001. Genetic organization of the *Pantoea stewartii* subsp. *stewartii* *hrp* gene cluster and sequence analysis of the *hrpA*, *hrpC*, *hrpN*, and *wtsE* operons. *Mol Plant Microbe Interact.* **14**: 1213-1222.
14. **Gaudriault, S., Malandrin, L., Paulin, J.-P., and Barny, M.-A.** 1997. DspA, an essential pathogenicity factor of *Erwinia amylovora* showing homology with AvrE of *Pseudomonas syringae*, is secreted via the Hrp secretion pathway in a DspB-dependent way. *Mol. Microbiol.* **26**: 1057-1069.
15. **Gaudriault, S., Paulin, J.-P., and Barny, M.A.** 2002. The DspB/F protein of *Erwinia amylovora* is a type III secretion chaperone ensuring efficient intrabacterial production of the Hrp-secreted DspA/E pathogenicity factor. *Mol. Plant Pathol.* **3**: 313-320.
16. **Ginalski K, A. Elofsson, D. Fischer, and L. Rychlewski.** 2003. 3D-Jury: a simple approach to improve protein structure predictions. *Bioinformatics.* **19**: 1015- 1018.
17. **Guex, N. and M.C. Peitsch.** 1997. Swiss-Model and the Swiss-Pdb viewer: an environment for comparative protein modeling. *Electrophoresis* **18**: 2714-2723.
18. **Ham, J.H., D.R. Majerczak, A.S. Arroyo-Rodriguez, D.M. Mackey, and D.L. Coplin.** 2006. WtsE, an AvrE-family effector protein from *Pantoea stewartii* subsp. *stewartii*, causes disease-associated cell death in corn and requires a chaperone protein for stability. *Mol. Plant Microbe Interact.* **19**: 1092-1102.
19. **Kelley, L.A., and M.J.E. Sternberg.** 2009. Protein structure prediction on the web: a case study using the Phyre server. *Nature Protocols* **4**: 363-371.
20. **Knodler, L.A., M. Bertero, N.C.J. Strynadka, and O. Steele-Mortimer.** 2006. Structure-based mutagenesis of SigE verifies the importance of hydrophobic and electrostatic residues in type III chaperone function. *Mol. Microbiol.* **62**: 928-940.
21. **Koradi, R., M. Billeter, and K. Wuthrich.** 1996. MOLMOL: A program for display and analysis of macromolecular structures. *J. Mol. Graphics* **14**: 51-55.
22. **Kovach, M.E., P.H. Elzer, D. Steven Hill, G.T. Robertson, M.A. Farris, R.M. Roop II, and K.M. Peterson.** 1995. Four new derivatives of the broad-host-range cloning vector pBBR1MCS, carrying different antibiotic-resistance cassettes. *Gene* **166**: 175-176.

23. **G. G. Krivov, M. V. Shapovalov, and R. L. Dunbrack, Jr.** 2009. Improved prediction of protein side-chain conformations with SCWRL4. *Proteins*, early view DOI 10.1002/prot.22488.
24. **Lee, S.H., and J.E. Galan.** 2004. *Salmonella* type III secretion chaperones confer secretion-pathway specificity. *Mol. Microbiol.* **51**:483-495.
25. **Letzelter, M., I. Sorg, L.J. Mota, S. Meyer, J. Stalder, M. Feldman, M. Kuhn, I. Callebaut, and G.R. Cornelis.** 2006. The discovery of SycO highlights a new function for type III secretion effector chaperones. *EMBO J.* **25**: 3223-3233.
26. **Lilic, M., M. Vujanac, and C.E. Stebbins.** 2006. A common structural motif in the binding of virulence factors to bacterial secretion chaperones. *Mol. Cell* **21**: 653-664.
27. **Luo, Y., M.G. Bertero, E.A. Frey, R.A. Pfuetzner, M.R. Wenk, L. Creagh, C. Kay, C. Haynes, B.B. Finlay, and N.C.J. Strydnaka.** 2001. Structural and biochemical characterization of the type III secretion chaperones CesT and SigE. *Nat. Struct. Biol.* **8**: 1031-1036.
28. **Notredame, C., D.G. Higgins, and J. Heringa.** 2000. T-coffee: a novel method for fast and accurate multiple sequence alignment. *J. Mol. Biol.* **302**: 205-217.
29. **Parsot, C., C. Hamiaux, and A.-L. Page.** 2003. The various and varying roles of specific chaperones in type III secretion systems. *Curr. Opin. Microbiol.* **6**: 7-14.
30. **Phan, J., J.E. Tropea, and D.S. Waugh.** 2004. Crystal structure of the *Yersinia pestis* type III secretion chaperone SycH in complex with a stable fragment of YscM2. *Acta Cryst.* **60**: 1591-1599.
31. **Rojas, C.M., J. H. Ham, L.M. Schechter, J.F. Kim, S.V. Beer, and A. Collmer.** 2004. The *Erwinia chrysanthemi* EC16 *hrp/hrc* gene cluster encodes an active Hrp type III secretion system that is flanked by virulence genes functionally unrelated to the Hrp system. *Mol. Plant Microbe Interact.* **17**: 644-653.
32. **Singer, A.U., D. Desveaux, L. Betts, J.H. Chang, Z. Nimchuk, S.R. Grant, J.L. Dangel, and J. Sondek.** 2004. Crystal structures of the type III effector protein AvrPphF and its chaperone reveal residues required for plant pathogenesis. *Structure* **12**: 1669-1681.
33. **Stebbins, C.E., and J.E. Galan.** 2001. Maintenance of an unfolded polypeptide by a cognate chaperone in bacterial type III secretion. *Nature* **414**: 77-81.
34. **Thomas, N.A., W. Deng, J.L. Puente, E.A. Frey, C.K. Yip, N.C.J. Strynadka, and B.B. Finlay.** 2005. CesT is a multi-effector chaperone and recruitment factor required for the efficient type III secretion of both LEE and non-LEE encoded effectors of enteropathogenic *Escherichia coli*. *Mol. Microbiol.* **57**: 1762-1779.

35. **Toth, I.K., L. Pritchard, and P.R.J. Birch. 2006.** Comparative genomics reveals what makes an enterobacterial plant pathogen. *Annu. Rev. Phytopathol.* **44**: 305-336.
36. **Triplett, L.R., M. Melotto, and G.W. Sundin. 2009.** Analysis of the N-terminus of the *Erwinia amylovora* secreted effector DspA/E reveals features required for secretion, translocation, and interaction with the chaperone DspB/F. *Mol. Plant Microbe Interact.* **22**: 1282-1292.
37. **van Eerde, A., C. Hamiaux, J. Perez, C. Parsot, and B.W. Dijkstra. 2004.** Structure of Spa15, a type III secretion chaperone from *Shigella flexneri* with broad specificity. *EMBO Rep.* **5**: 477-483.
38. **Wulff-Strobel, C.R., A.W. Williams, and S.C. Straley. 2002.** LcrQ and SycH function together at the Ysc type III secretion system in *Yersinia pestis* to impose a hierarchy of secretion. *Mol. Microbiol.* **43**: 411-423.
39. **Zhao, Y., S.E. Blumer, and G.W. Sundin. 2005.** Identification of *Erwinia amylovora* genes upregulated during infection of immature pear tissue. *J. Bacteriol.* **187**: 8088-8103.

## Chapter 4: A Study of the Roles of Class I Secretion Chaperones in *Erwinia amylovora* in Effector Translocation and Virulence.

### ABSTRACT

Chaperones specific to type III secreted effector proteins often interact with multiple substrates in the bacterial cell, including regulatory proteins, effectors, and components of the secretion apparatus. A directed yeast two-hybrid screen identified *Erwinia amylovora* secreted proteins Eop1 and Eop3 and the type III secretion apparatus proteins HrcU and HrcQ as putative interactors of the type III secretion system (T3SS) chaperone DspF. Annotation of the unfinished *E. amylovora* genome confirmed or revealed the presence of putative chaperone genes next to *eop1* and *eop3*, but not next to the effector-encoding gene *eop4*, and it was hypothesized that DspF might influence translocation levels of other effectors. Deletion of *dspF* affected translocation levels of DspE, Eop1, and Eop3, but not Eop4, when examined using CyaA translational fusions. Deletion of the putative Eop1 chaperone, *esc1*, negatively affected translocation of Eop1-CyaA but not of DspE-CyaA. Deletion of Eop1, Eop3, and the corresponding putative chaperone genes had no significant effect on virulence, although Ea1189 $\Delta$ *dspF* $\Delta$ *esc1* showed very slightly increased levels of early growth on pear compared with Ea1189 $\Delta$ *dspF*.

## INTRODUCTION

A central theme in the pathogenesis of gram-negative bacteria is the secretion of effector proteins directly into host cells via the type III secretion system (T3SS). Three classes of specific chaperone proteins bind to secreted proteins and components of the T3SS (10); Class I T3SS chaperones (henceforth T3SS chaperones) are chaperones that specifically interact with effector proteins. Despite having little sequence similarity, T3SS chaperones share a highly conserved tertiary structure and similar general mode of substrate binding (28).

Nearly two decades of study of T3SS chaperones in *Escherichia*, *Salmonella*, and *Yersinia* have led to a general understanding of the functional role of chaperones in secretion. Chaperones bind to the N-terminal portion of a cognate effector protein. This interaction holds the N-terminus of the effector in a non-globular state, which may confer secretion competence (16). The direct binding may also stabilize the effector by masking an aggregative or secretion-inhibitory domain (15, 21). T3SS chaperones may interact with multiple proteins other than effectors; for example, direct interaction between a T3SS chaperone and transcriptional or translational regulators mediates the regulatory roles of some T3SS chaperones (11, 12). In addition, T3SS chaperones have been demonstrated to interact directly with the ATPase and other conserved components of the secretion apparatus (1, 9, 30). This interaction could function in docking the effector to the secretion apparatus.

Despite the requirement of a chaperone for secretion of many T3SS effectors, some effectors do not bind or require a corresponding chaperone for secretion into host cells, and secretion of some proteins without a chaperone was observed to be delayed

compared with secretion substrates utilizing a chaperone (7, 22). These results led to the hypothesis that chaperones may establish patterns of intracellular effector dynamics, establishing a temporal order of secretion (27, 34). In *Yersinia enterocolitica*, chaperone-independent secretion of YopE was detected only in the absence of all other effectors, demonstrating a competitive secretion advantage conferred by the YopE chaperone (7, 22). Likewise, the *Salmonella enterica* effector SipA is translocated earlier than the effector SptP despite simultaneous expression; the authors proposed that this hierarchy might result from varying binding affinities between chaperones and the T3SS (34). The chaperone SycH also establishes a secretion hierarchy by forming a secretion-inhibitory complex with the protein LcrQ (33).

Although little work has been done to examine the role of T3SS chaperones in plant pathogenic bacteria, recent studies have demonstrated a similar overall function in these systems, with some novel variations. Like the chaperones previously characterized in animal pathogens, chaperones in plant pathogens have a highly conserved tertiary structure (29), and may function in effector stabilization or direct interaction with the secretion apparatus (24, 25). Although the dynamics of effector secretion has not been studied in depth in plant pathogens, there is recent evidence that a T3SS chaperone is involved in establishing a secretion hierarchy in *X. campestris*. By sequestering the global T3SS chaperone HpaB, the regulatory protein HpaA promotes the secretion of non-effectors prior to effectors (23).

The plant pathogen *Erwinia amylovora* is a member of the Enterobacteriaceae with a close phylogenetic relationship to human enterobacterial pathogens. *E. amylovora* secretes at least four effector proteins under *hrp*-inducing conditions *in vitro*: Eop1,

Eop3, AvrRpt2*Ea*/Eop4, and DspE (28). Deletion mutants of *eop1*, a predicted YopJ family cysteine protease, and *avrRpt2Ea*, a papain-like cysteine protease homolog, have been characterized and were shown to mildly affect host range and virulence, respectively (3, 36). *eop3*, a putative homolog to AvrPphE from *Pseudomonas syringae*, has not been characterized in the literature. Only one effector, DspE, is required for pathogenicity and population growth *in planta* (6, 28). Although its functional targets are unknown, DspE suppresses salicylic acid-mediated cell wall defenses when transiently expressed in plant cells, and induces necrotic cell death in host and nonhost cells (6, 14). DspE is homologous to proteins critical for virulence in several important plant pathogens including *Pseudomonas syringae*, *Ralstonia solanacearum*, and *Pantoea stewartii* (6). DspE binds directly to the T3SS chaperone DspF, which has been implicated in the stable expression and efficient secretion of DspE (18). A *dspF* deletion mutant is pathogenic, but with a greatly reduced level of virulence, and DspE reporter constructs containing the N-terminal 203 amino acids are translocated into plant cells in the absence of DspF (32).

The strong virulence defect of the chaperone DspF has proven useful for studies of chaperone-effector interactions in this organism, and we hypothesized that the relatively small number of effectors produced could facilitate the study of intracellular chaperone-effector dynamics. Because chaperones often interact with a variety of proteins to complete various cellular roles, we decided to examine putative functional interactions between DspE, DspF, and other proteins in the cell. Based on the roles of other T3SS chaperones, we hypothesized that DspF may play a role in modulating translocation levels of multiple effector proteins or in interaction with components of the

T3SS apparatus. In a directed yeast two-hybrid screen, secreted effectors Eop1 and Eop3 were identified as putative interactors of DspF, as were T3SS apparatus components HrpQ and HrcU. The *eop1* and *eop3* genes are localized next to putative chaperone genes, here named *esc1* and *esc3*. To determine whether *dspF*, *esc1*, and *esc3* influence the translocation levels of multiple effector proteins, a series of chaperone and effector mutants were constructed and assessed for virulence and population growth *in planta* and translocation levels of effector-CyaA reporter constructs. Results indicated that deletion of *eop1* and *eop3* and corresponding specific chaperones had no effect on virulence or translocation levels of a DspE-CyaA fusion. Deletion of the putative chaperones of Eop1 and Eop3 caused no effect on virulence, although chaperone gene deletions in the *dspF* mutant background caused a small early spike in population growth on pears, suggesting that other chaperones may slightly antagonize growth on pear. These findings point toward a model of type III secretion in *E. amylovora* in which chaperones each promote secretion of a single cognate effector.

## **MATERIALS and METHODS**

**Genetic techniques and bacterial strains, plasmids, and primers.** Bacterial strains and plasmids are listed in Table 1. Oligonucleotides used for cloning are listed in Table 2.

PCR and gene cloning was performed using standard techniques (Ausubel). All constructs were confirmed by sequencing, which was performed at the Research Technology Support Facility at Michigan State University.

**Mutant construction and complementation.** All chromosomal mutants of *E. amylovora* were constructed using the Red recombinase system using an adapted technique as previously described (Zhao *et al.* 2009, Triplett *et al.* 2009) The resistance cassette for

*esc1* mutagenesis was amplified from pKD3 using primers *esc1mutF* and *esc1mutR*, and the *esc3* mutagenesis cassette was amplified using primers *esc3mutF* and R. Gene knockout was verified by PCR amplification of the insertion cassette from primers inside the resistance cassette and flanking the inserted gene (Datsenko and Wanner, 2000), and PCR products were sequenced to confirm the structure of the insert. To complement the *esc1* mutant, *esc1* was amplified with primers *esc1pH* and *esc1RXh*, digested with *HindIII* and *XhoI*, and ligated into the vector pBBR1-MCS5.

**Pear population counts and virulence assays.** Bacterial population growth and lesion size on immature pears was measured as previously described (Triplett *et al.* 2009, Zhao *et al.* 2004). Briefly, bacterial strains were suspended in 0.5x phosphate buffered saline (PBS) to a concentration of  $1.5 \times 10^8$  cfu/ml, and 2  $\mu$ L was inoculated onto surface-sterilized immature pears. At the noted timepoints, a core of 0.5 cm was collected from the point of inoculation on each pear, macerated in PBS, and serially diluted and plated onto LB medium. Developing lesions on the remaining uncored pears were measured for diameter using digital calipers as previously described (Triplett *et al.*, 2009).

**Yeast two-hybrid assays.** *esc1* and *esc3* were amplified from genomic DNA using the primers *Esc1 F* and *R* and *Esc3 F* and *R*, and PCR products were digested with *BamHI* and *EcoRI* and ligated into the prey vector pB42AD. Bait vector inserts for *eop1*, *eop3*, *eop4*, *hrcU*, *hrcN*, and *hrcQ* were amplified with primers listed in Table 2, digested with *BamHI* and *XhoI*, and ligated into pGilda in frame with the LexA DNA binding domain. Bait and prey vectors were co-transformed into *Saccharomyces cerevisiae* strain EGY48 p80 (pLacZ) using the Zymo yeast transformation kit (Zymo; Orange, CA). Yeast were

plated onto SD-galactose medium amended with X-gal, and color change was visualized after incubation at 30° C for 72h.

**Adenylate cyclase assays.** Selected *E. amylovora* genes were amplified with primers pEop1F and Eop1R, pEop3F and Eop3R, and pEop4F and Eop4R. Primers pEop1F, pEop3F, and pEop4F incorporate a *hrp* box promoter into the forward primer to confer *hrp*-inducible gene expression. Eop3 was also cloned without the *hrp* promoter using forward primer Eop3F. PCR products were digested with *XbaI* and *SspI* and ligated into pMJH20. Bacterial strains were transformed with CyaA fusion constructs, and expression was confirmed by western blot of cells grown in *hrp*-inducing conditions using anti-CyaA antibody. Overnight cultures were resuspended in phosphate-buffered saline to an O.D. 600 of 0.3, and infiltrated into the leaves of 8-week-old tobacco plants. Two leaf disks of 0.5 cm in diameter were collected between 8 and 9 hours post-infiltration, when the first signs of cell collapse were becoming visible. cAMP levels were measured as previously described (Triplett *et al.*, 2009). Statistical analyses were done using a one-way analysis of variance and mean separation was accomplished using Fisher's protected least significant difference test.

## RESULTS

**The requirement of DspF in virulence can be partially overcome by ectopic expression of DspE.** It was previously reported that the T3SS chaperone DspF is required for stable accumulation of the pathogenicity factor DspE in *E. amylovora* cells, and for secretion into the medium (Gaudriault *et al.*, 2002). However, we observed that a fusion of the N-terminus of DspE with an adenylate cyclase reporter was stably expressed and translocated into host cells from a *dspF* deletion mutant (Triplett *et al.*, 2009). We

proposed that the requirement for *dspF* may either be conferred by the C-terminus of DspE, or overcome by ectopic expression of DspE from a plasmid. To test whether the requirement for DspF is overcome by plasmid expression, a full-length clone of *dspE* with a C-terminal 6x-histidine tag was constructed in a high-copy cloning vector. This clone (pLRT43) was introduced into 1189 $\Delta$ *dspE* and Ea1189 $\Delta$ *dspF*. Degradation or repression of some effector proteins is mediated by the Lon protease (25). To determine whether this is true of DspE, a deletion mutant of the *lon* protease gene of *E. amylovora* was generated in the Ea1189 $\Delta$ *dspF* mutant background and transformed with pLRT43 (*dspE*-6xHis).

Western blot analysis of lysates from cells grown eight hours in *hrp*-inducing media revealed that DspE-6xHis accumulates to detectable levels in 1189 $\Delta$ *dspE* and Ea1189 $\Delta$ *dspF*, with no difference in band intensity between the two strains. (Figure 4-1A). DspE-6xHis was present in much greater levels in Ea1189 $\Delta$ *dspF* $\Delta$ *lon*. These results demonstrate a negative role for the Lon protease in DspE accumulation, and indicate that DspE accumulates to equivalent levels in Ea1189 $\Delta$ *dspE* and Ea1189 $\Delta$ *dspF*.

Complemented strains were tested for virulence on immature pear fruit. Ea1189 $\Delta$ *dspF* carrying *dspE*-6xHis caused lesions significantly larger than Ea1189 $\Delta$ *dspF* alone, but significantly smaller than Ea1189 or Ea1189 $\Delta$ *dspE*/*dspE*-6xHis (Figure 4-1B). These results indicate that the *dspF* virulence phenotype is partially, but not fully, compensated by ectopic expression of *dspE*.

Our previous work showed no difference between secretion levels of an N-terminal DspE-CyaA fusion from Ea1189 $\Delta$ *dspE* or Ea1189 $\Delta$ *dspF*. This study was expanded to include secretion from wild-type Ea1189 and from Ea1189 $\Delta$ *dspF*

complemented with *dspF*. To determine whether an N-terminal fragment of DspE is secreted from the DspF mutant at levels lower than the wild-type, a CyaA assay was performed as described in Materials and Methods. DspE(1-737)-CyaA was translocated into host cells at lower levels from Ea1189 $\Delta$ *dspF* and Ea1189 $\Delta$ *dspE* than from Ea1189 or Ea1189 $\Delta$ *dspF/dspF* (Figure 4-1C). There was no clear difference in protein accumulation between Ea1189, Ea1189 $\Delta$ *dspE*, and Ea1189 $\Delta$ *dspF* (data not shown). Together, these results confirm that that full-length DspE can be secreted in the absence of DspF, and indicate that the N-terminus of DspE is translocated at lower levels from Ea1189 $\Delta$ *dspF* and Ea1189 $\Delta$ *dspE* than from wild-type Ea1189.

**Figure 4-1.** DspE-6xHis accumulates to reduced levels in Ea1189  $\Delta dspF$  and partially complements the *dspF* pathogenicity phenotype. **A.** Western blots of lysates of Ea1189 $\Delta dspE$ , Ea1189 $\Delta dspF$ , and Ea1189  $\Delta dspF\Delta lon$  carrying pLRT43 (DspE-6xHis) after 8 hr incubation *hrp*-inducing minimal medium. Ea1189 $\Delta dspE$  and Ea1189 $\Delta dspF$  samples are from the same blot, whereas Ea1189 $\Delta dspF\Delta lon$  samples were visualized on a separate blot and exposed for a shorter amount of time. **B.** Average lesion diameters on immature pear fruits 5 days after inoculation with Ea1189, Ea1189 $\Delta dspE$ , Ea1189 $\Delta dspF$ , Ea1189 $\Delta dspE$  (pLRT43) and Ea1189 $\Delta dspF$  (pLRT43). Error bars denote standard error. Letters above bars indicate statistically separate groups ( $p < 0.01$ ). **C.** cAMP accumulation in tobacco leaves infiltrated with Ea1189, Ea1189 $\Delta dspE$ , Ea1189 $\Delta dspF$ , and Ea1189 $\Delta dspF/dspF$  expressing DspE(1-737)-CyaA. Letters denote statistical groups ( $p < 0.05$ ). **D.** Western blot of DspE(1-737)-CyaA expression in Ea1189, Ea1189 $\Delta dspE$ , and Ea1189 $\Delta dspF$ .

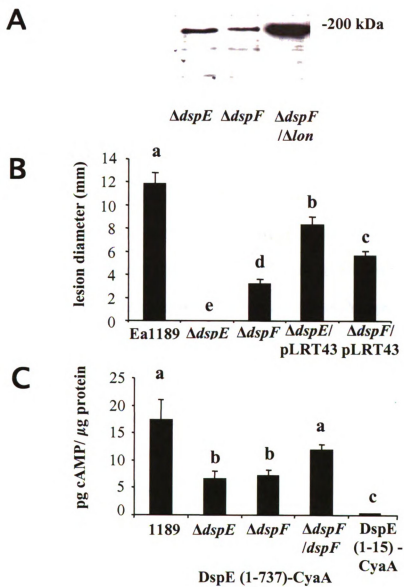


Figure 4-1.

**A directed yeast two-hybrid screen identifies secreted proteins and T3SS apparatus components as new putative interactors of DspF.** Chaperone function is often mediated by the formation of complexes between the chaperone, effector, and other chaperone-interacting proteins. T3SS chaperone interactors may include components of the secretion apparatus, multiple effectors, or regulatory proteins. DspF interacts with at least one protein other than DspE (17), and a recent report indicated that DspF interacted with Eop1 in a yeast two-hybrid assay (2). We used a yeast two-hybrid assay approach to test whether DspF interacted with *E. amylovora* effector proteins or T3SS apparatus components in yeast. In a study of *hrp*-dependent secreted proteins of *E. amylovora*, Nissinen *et al.* identified three *hrp*-dependent secreted effector-like proteins in addition to DspE, named Eop1, Eop3, and AvrRpt2Ea (28). LexA fusions of these three effectors were constructed and tested for interaction with DspF as described in Materials and Methods. In a yeast two-hybrid assay, Eop1 and Eop3 interacted with DspF, but AvrRpt2Ea did not (Table 3). In addition to effector proteins, highly conserved components of the secretion apparatus have been demonstrated to interact with various T3SS chaperones: The EscN/HrcN ATPase (1, 19, 24), the predicted C-ring (HrcQ/YscQ/Spa33) (30), and a putative substrate specificity switch (HrcU/YscU/Spa40) (24). NCBI searches of previously annotated *E. amylovora* genes and Blast analysis of the finished, unpublished *E. amylovora* genome ([www.sanger.ac.uk](http://www.sanger.ac.uk)) were used to identify the homologous genes in *E. amylovora* to assay for interaction with DspF. LexA fusions of *E. amylovora* HrcN and C-terminal derivatives did not interact with B42-HA-DspF in yeast (Table 3). Attempts to co-purify HrcN and DspF *in vitro* were unsuccessful due to difficulty solubilizing HrcN. B42-HA-DspF interacted strongly in yeast with a C-

terminal fragment of HrcU corresponding to a predicted cleaved cytoplasmic tail. In addition, a weaker interaction was detected between DspF and the C-terminal 194 amino acids of the putative C-ring HrcQ (Table 3). Neither HrcU nor HrcQ demonstrated transactivation activity when co-transformed into yeast with the empty pB42AD plasmid (data not shown). Examination of a putative interaction between the full-length HrcQ and DspF is still underway.

**Annotation and yeast two-hybrid analysis of other putative chaperone genes in *E. amylovora*.** T3SS chaperone-encoding genes have often been identified as short open reading frames immediately adjacent to genes encoding the cognate effector. There are two putative T3SS chaperone genes adjacent to *eop1*; these were designated *orfA* and *orfC* (2). *orfC* was annotated as a putative gene encoding a chaperone to HrpW, the product of the other gene adjacent to *orfC*. To determine whether there are other T3SS chaperones in *E. amylovora*, I searched the *E. amylovora* unpublished, finished genome ([www.sanger.ac.uk](http://www.sanger.ac.uk)) for short, chaperone-like open reading frames encoded adjacent to previously reported T3SS effector proteins. The secreted protein Eop3 is encoded downstream of an open reading frame encoding a putative 137-aa protein predicted to have the acidic pI and three  $\alpha$ -helical structure characteristic of T3SS chaperones (Figure 4-2A). However, annotation of the sequence surrounding the gene encoding the secreted protein AvrRpt2Ea, as well as that surrounding the putative effector gene HopPtoC, did not yield any open reading frames with the characteristics of a type III chaperone. Secondary structure prediction by 3D-Jury and Phyre Blast indicated that the product of *orfC* would not share the secondary structural characteristics of a Class I T3SS chaperone. A search of the preliminary genome annotation of *E. amylovora* for genes

annotated as “secretion chaperone” yielded additional orfs predicted to be type III secretion chaperones, but these were located in genomic islands associated with type III secretion systems SSP-1 and SSP-2, which are not expressed under the same conditions as the *hrp* secretion system (Y. Zhao, pers. comm.). Blast searches of the *E. amylovora* genome against the sequences of several characterized chaperones did not reveal any other strong candidates for additional T3SS chaperones. In summary, three of the five putative or confirmed effector-encoding genes previously reported in *E. amylovora* are encoded adjacent to predicted chaperone sequences, and no additional putative chaperones of the *hrp* system were found. Because the effectors predicted to have chaperones are called Eop1 and Eop3, I propose that the putative chaperone genes adjacent to these be called *esc1* and *esc3* for *Erwinia* secretion chaperones 1 and 3, respectively.

**Yeast two-hybrid assay for Esc1 and Esc3 interaction with *E. amylovora* effectors and DspF.** A previous study demonstrated Esc1 and Eop1 interact directly in a yeast two-hybrid assay (2). To determine whether Esc1 and Esc3 are capable of interaction with multiple effector proteins in yeast, we examined the interaction of Esc1 and Esc3 with the three known *E. amylovora* secreted proteins. Both chaperones interacted with Eop1, Eop3, and the N-terminal 600 residues of DspE, but did not interact with Eop4/AvrRpt2Ea or a RecA control fusion (Fig 2B). We previously reported that DspF interacts strongly with residues 51-100 of DspE in yeast and *in vitro* (32). Esc1 and Esc3 fusions did not interact with the N-terminal DspF-binding domain of DspE (Figure 4-2B). The chaperone binding region of Eop1 was mapped using further yeast studies. While Esc1 and DspF both interacted with an N-terminal fragment of Eop1, the interaction

appeared much weaker for DspF than Esc1. A putative C-terminal binding domain for Esc1, Esc3, and DspF was also identified, although this interaction was masked in longer fragments. Color development was stronger in the Esc3 and DspF interaction of the C-terminus of Eop1 than in the Esc1 interaction. To rule out the possibility of heterodimerization, DspF was also tested for interaction with Esc1 or Esc3, and no interaction was found (data not shown).

**Figure 4-2.** Gene organization and interactions of putative chaperone effector pairs in *E. amylovora*. A. *eop1* and *eop3*, but not *eop4*, are encoded next to putative chaperone genes. Depiction of *eop1* region adapted from Vannesste *et al.*, 2000; *eop4* region adapted from Zhao *et al.*, 2006, and *eop3* region based on analysis of finished *E. amylovora* genome sequence ([www.sanger.ac.uk](http://www.sanger.ac.uk)). *esc1* and *esc3* are predicted to encode effector-binding secretion chaperones, and *orfC* is predicted to encode a putative HrpW-specific chaperone. Accessions for Eop1, Eop3, Eop4, Esc1(OrfA) and OrfC are AAA98413.1, ABM65604.1, ABC70473, AAF63396.1, and AAC62316. The predicted product of *esc3* is 94% identical to accession YP\_002648387 from the genome of *Erwinia pyrifoliae*, a close relative of *E. amylovora*. *yegS*, *efp*, and *blc* are predicted to encode proteins homologous to a diacylglycerol kinase (nearly identical to *Erwinia pyrifoliae* accession YP\_002648385), elongation factor P (YP\_002647518), and an outer membrane lipoprotein (YP\_002647520), respectively. B. Yeast two-hybrid interaction between prey fusions of predicted chaperones Esc1, Esc3, and DspF and bait fusions of effectors Eop1, Eop3, DspF, and Eop4. C. Color development in Eop1-chaperone interactions in yeast. Esc1, Esc3, and DspF showed no color change when co-transformed with the empty prey vector pGilda (not shown).

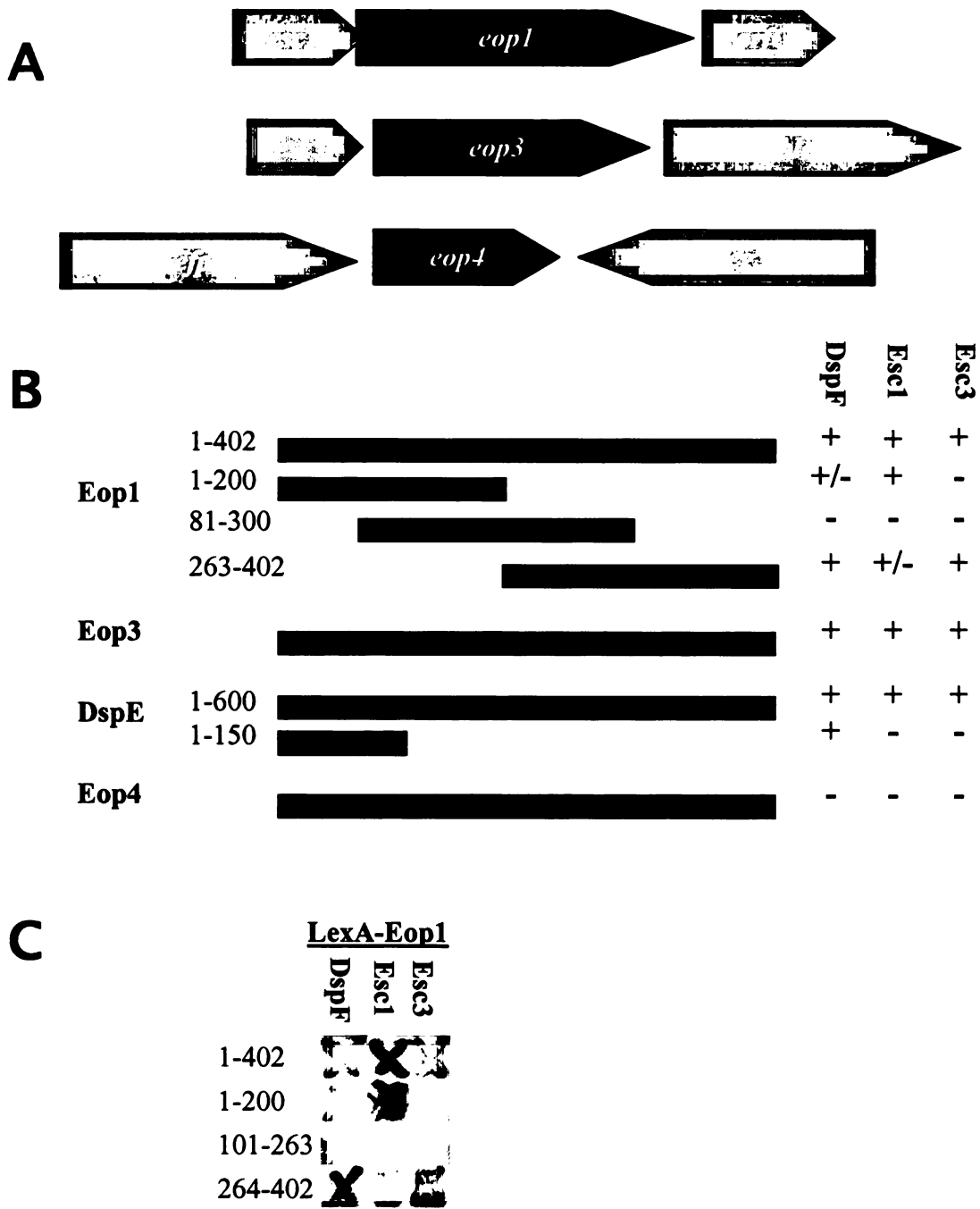


**Figure 4-2.**

**DspF does not facilitate translocation of Eop1, Eop3, or Eop4 in an adenylate cyclase assay.** Because Eop1 and Eop3 were identified as putative interactors of DspF in yeast, we wanted to determine whether DspF influences translocation levels of fusions of Eop1, Eop3, or Eop4 in a CyaA translocation assay. To determine the effect of DspF on translocation of heterologous effectors, plasmids expressing Eop1-CyaA, Eop3-CyaA, and Eop4-CyaA from a *hrp* box promoter were constructed. These clones were introduced into Ea1189, Ea1189 $\Delta$ *dspF*, and Ea1189 $\Delta$ *dspF/dspF*. CyaA fusion expression was confirmed by western blot of *hrp*-induced cultures; levels of protein accumulation in cultured cells appeared similar between strains (data not shown). cAMP levels in infiltrated tobacco leaves was measured at between 8 and 9 hr post-inoculation, when the wild-type and *dspF* complemented treatments were showing early signs of water-soaking. Although *E. amylovora* expressing DspE(1-737)-CyaA accumulated cAMP to greater levels when translocated from the wild-type Ea1189 than from Ea1189 $\Delta$ *dspE* or  $\Delta$ *dspF* (Figure 4-1C), CyaA fusions of Eop1 and Eop3 elicited a greater accumulation of cAMP levels from an Ea1189 $\Delta$ *dspF* mutant than from the wild-type (Figure 3A and 3B). However, deletion of *dspF* did not have a significant influence on cAMP accumulation mediated by Eop4-CyaA (Figure 3C). Preliminary results indicate that Eop1-CyaA and Eop3-CyaA, but not Eop4-CyaA, also elicited increased cAMP levels when expressed from Ea1189 $\Delta$ *dspE*, indicating that the effect is not *dspE*-independent (data not shown). DspE(1-15)-CyaA, a non-translocated fragment of DspE, was used as a negative control to measure background levels of cAMP. These results demonstrate that DspF does not promote the translocation of effectors other than DspE, and that DspF affects Eop1 and Eop3 translocation levels differently than Eop4.

**Deletion of *Esc1* causes a decrease in translocation levels of an Eop1-CyaA fusion, but does not affect translocation levels of a DspE-CyaA fusion.** Because *Esc1* and *Esc3* both interacted with Eop1 and Eop3 in yeast, I wanted to determine whether these chaperones affect translocation of the effectors with which they interact. I focused these studies on *Esc1* due to time constraints. cAMP accumulation was measured in tobacco leaves 8 to 9 hours after infiltration with *Ea1189ΔdspF* or *Ea1189Δesc1ΔdspF* expressing Eop1-CyaA or DspE(1-737)-CyaA. cAMP accumulation elicited by Eop1-CyaA was significantly lower in *Ea1189Δesc1ΔdspF* than in *Ea1189ΔdspF*, and this phenotype was partially complemented by expression of *esc1* from the plasmid pLRT224. (Figure 4-4A). However, cAMP accumulation elicited by DspE(1-737)-CyaA was not significantly affected by deletion of *esc1* (Figure 4-4B). These results demonstrate that *esc1* is required for full levels of Eop1-CyaA translocation, but not for translocation of a DspE-CyaA fusion.

**Figure 4-3.** cAMP accumulation in tobacco leaves mediated by *E. amylovora* expressing CyaA fusion proteins. A-C. cAMP levels in tobacco after infiltration with Ea1189, Ea1189 $\Delta$ *dspF*, and Ea1189 $\Delta$ *dspF/dspF* expressing Eop1-CyaA (A), Eop3-CyaA (B), and Eop4-CyaA (C). DspE (1-15)-CyaA was expressed in Ea1189 as a negative control. D. cAMP levels after infiltration with Ea1189 $\Delta$ *dspE* or Ea1189 $\Delta$ *dspF* expressing a low-expression clone of Eop3-CyaA. Bars represent the means of three samples collected from separate plants. Error bars denote standard error. Letters above bars denote different statistical groups ( $p < 0.05$ ). Each experiment was performed at least twice in different months with similar results

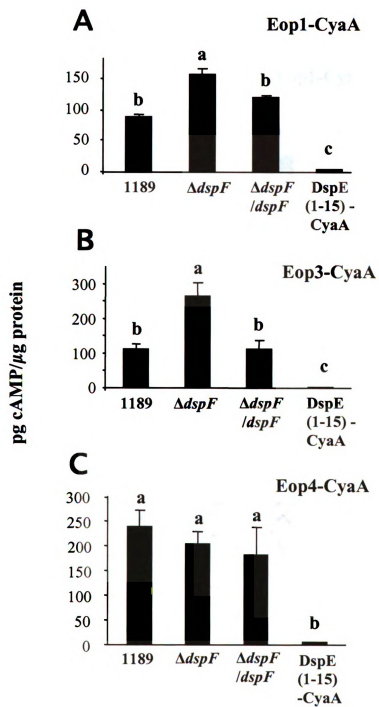
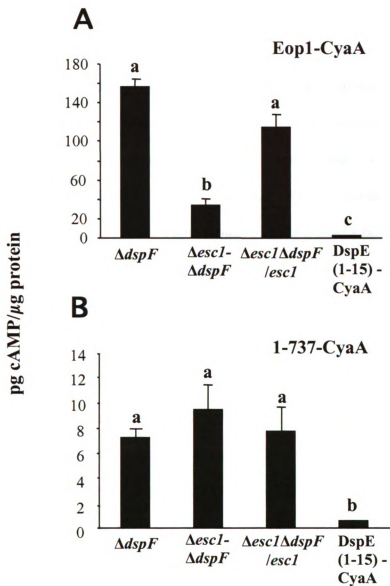
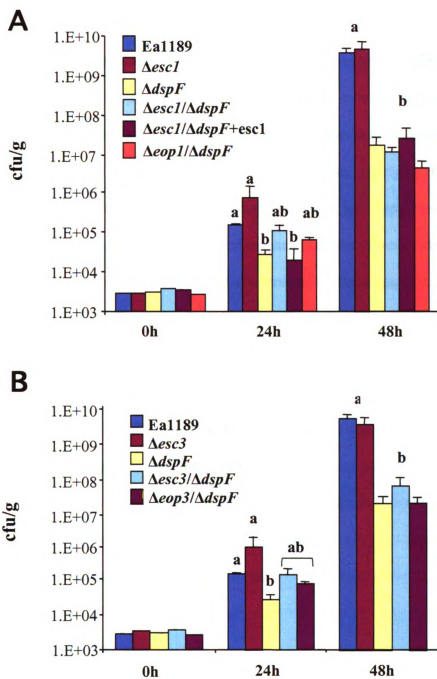


Figure 4-3.



**Figure 4-4.** cAMP accumulation in tobacco leaves mediated by *E. amylovora* strains expressing effector-CyaA fusion proteins. A. cAMP levels in tobacco after infiltration with Ea1189 $\Delta dspF$ ,  $\Delta esc1\Delta dspF$ , and  $\Delta esc1\Delta dspF/esc1$  expressing Eop1-CyaA. B. cAMP levels in tobacco after infiltration with the same parent strains expressing DspE (1-737)-CyaA. Bars represent the means of three samples from separate plants  $\pm$  standard error. Letters above bars denote different statistical groups ( $p < 0.05$ ). Each experiment was performed twice with similar results.

**Deletion of *esc1* from a *dspF* mutant background does not affect virulence, but causes a slight increase in early population growth on pear.** To further examine the effects of the chaperone genes *esc1*, *esc3*, and *dspF*, I measured population growth and virulence of chaperone and effector mutant strains in immature pears. Pears were surveyed for population growth 0, 24, and 48 hr after inoculation with Ea1189, single or double chaperone mutants, or effector mutant *E. amylovora*. After 24 hours, pears inoculated with Ea1189 $\Delta$ *dspF* accumulated roughly 10-fold fewer bacterial cells than did the wild-type Ea1189-treated pears. Populations of Ea1189 $\Delta$ *esc1* $\Delta$ *dspF* consistently accumulated to higher levels than Ea1189 $\Delta$ *dspF*, accumulating to near wild-type levels after 24 hours. However, there was no difference between Ea1189 $\Delta$ *dspF* and Ea1189 $\Delta$ *esc1* $\Delta$ *dspF* after 48 hr, and no significant difference in the lesion diameters elicited by the two strains. Early population growth of Ea1189 $\Delta$ *esc1* $\Delta$ *dspF* was reduced by complementation with *esc1* on pLRT224. Although the differences in early population growth between Ea1189 $\Delta$ *dspF* and Ea1189 $\Delta$ *esc1* $\Delta$ *dspF* are only five to seven-fold, they are consistently repeatable and were statistically significant in two of four experiments. We also noticed a consistent trend that Ea1189 $\Delta$ *esc3* $\Delta$ *dspF* accumulated higher population growth than Ea1189 $\Delta$ *dspF* after 24 hours (Figure 4-5B). Simultaneous deletion of *esc1* and *esc3* caused a phenotype similar to that of deleting *esc1* or *esc3* alone, with a slight but not significant increase in population growth on day one, and no effect on virulence (data not shown). Deletion of *eop1*, *eop3*, *esc1*, or *esc3* from Ea1189 or the *dspF* mutant background had no significant effect on lesion development in immature pear fruits. Together, these results indicate that the *esc1*, *esc3*, *eop1*, and *eop3* genes do not contribute substantially to virulence *in planta*.



**Figure 4-5.** Bacterial population counts on immature pear fruit inoculated with Ea1189 and mutant derivatives. Pears were inoculated with  $1.5 \times 10^3$  cfu of Ea1189, Ea1189 $\Delta$ *dspF*, and *orfA* and *eop1* (A) or *escB* and *eop3* (B) deletion derivatives. Bars represent the mean of four replicate pears  $\pm$  S.D. Letters represent groups of statistical significance ( $p < 0.05$ ). Experiments were performed twice (B) or three times (A) on separate days with similar results.

## DISCUSSION

The events leading to type III secretion are complex and tightly regulated. While pre- and post-transcriptional modulation of expression controls the timely abundance of secretion apparatus components and substrates, mechanisms also exist to control secretion levels of pre-formed proteins. The mechanism underlying this effect is still under investigation. T3SS chaperones may function in both capacities, although the role of these chaperones has not been tested in many plant pathogens. This study examined the roles of DspF and two other T3SS chaperones in interaction with potential chaperone interactors and in effector translocation efficiency. We also tested the effect of these effectors and chaperones on virulence and population growth *in planta*.

We also identified putative DspF interactors among known secreted proteins of *E. amylovora*. Interestingly, two effectors encoded next to predicted chaperones interacted with B42-HA-DspF, while an effector with no predicted chaperone did not. The capacity of DspE for DspF-independent translocation and the putative interaction of DspF with other secreted proteins led us to hypothesize that DspF might contribute to the translocation of other effectors. Translocation studies demonstrated that deletion of *escI* had a negative effect on translocation levels of the predicted cognate effector Eop1 but not the non-cognate effector DspE. So, contrary to our initial hypothesis, DspF does not facilitate translocation of multiple effectors.

Interestingly, deletion of *dspF* had a moderate positive effect on cAMP accumulation mediated by Eop1 and Eop3-CyaA fusions, a negative effect on translocation of a DspE-CyaA fusion. One possibility is that while effectors that interact with chaperones compete for T3SS access, effectors binding no chaperone are not

affected by chaperone levels. Alternatively, it is possible that DspF could have some direct antagonistic effect, or that lowered DspE translocation levels could otherwise increase translocation efficiency.

It should be noted that plant material was collected as the first visible signs of hypersensitive cell death were beginning to appear, and we did not rule out the possibility that early-stage cell death or other effects of DspE translocation might have caused artificial reduction in cAMP levels in Ea1189 and Ea1189 $\Delta$ *dspF/dspF*. Another limitation of the cAMP assay strategy is that effector expression from a multicopy plasmid may reduce the true effect of chaperones or competition between effectors; studies with chromosomal reporter genes would be ideal to assess the role of DspF in its true scope. Despite these limitations, patterns of cAMP accumulation induced by DspE and Eop4 suggest that these effectors are affected by *dspF* in a different manner than the chaperone-binding effectors Eop1 or Eop3. Preliminary studies with a Eop3-CyaA fusion expressed at low levels have been conducted, and indicate that Eop3 is translocated at threefold greater levels from Ea1189 $\Delta$ *dspF* than from Ea1189 $\Delta$ *dspE*, suggesting that DspF reduces Eop3 translocation in a manner that is neither DspE-dependent nor an artefact of cell death. These results led us to hypothesize that some chaperones in *E. amylovora* may negatively affect translocation mediated by other chaperone-effector complexes. Further studies will be conducted to confirm a potential antagonistic effect of DspF on Eop1 and Eop3 translocation and determine its scope and mechanism.

Deletion of effector and chaperone genes in this study yielded no virulence phenotype. In population growth studies, the only phenotype observed among the *esc1* and *esc3* chaperone deletions was a slight increase in early growth. This difference was

less than tenfold, and was only statistically significant in the *esc1/dspF* double mutant, but was consistently repeatable and complemented by addition of *esc1* on a plasmid. Interestingly, Ea1189 strains expressing Eop1-CyaA or Eop3-CyaA displayed reduced virulence in preliminary pear pathogenicity assays, and a slight negative effect was also observed in strains overexpressing *esc1* or *esc3*. Clearly, the role of these chaperones, if any, in bacterial growth is minor. Further population studies, complementations, and bacterial fitness assays will be performed to help confirm whether certain effectors and chaperones confer a disadvantage in early growth on pear.

This study identifies two components of the T3SS base as interactors of DspF in yeast. Although the interaction between T3SS chaperones and the T3SS ATPase have been the focus of much study since 2003 (1, 19, 31), T3SS chaperones are now thought to interact with other secretion system components (24, 30). The putative interactions between DspF and secretion apparatus components have not been tested *in vitro*, but because interactions between the orthologous secretion proteins and structurally homologous chaperones have been identified in *Xanthomonas campestris* and *Chlamydia reinhardtii* (24, 30), we consider them strong candidate DspF interactors. Given the high degree of conservation among structural components of the T3SS, it was proposed that the conserved shape of T3SS chaperones might act as a signal for recognition by the secretion apparatus (5). The identification of interactions between diverse chaperones and components of the T3SS base is very consistent with this theory. If the DspF- T3SS interactions can be confirmed *in vitro*, compatibility with the yeast two-hybrid strategy could be helpful in determining the scope of these interactions and identifying the requisite chaperone features. No functional role for interaction between T3SS chaperones

and HrcU or HrcQ homologs has been identified, and characterization of these interactions would greatly expand our understanding of chaperone function.

This work includes an examination of the potential role of DspF and the Lon protease on DspE accumulation. DspE-6xHis was detected at roughly equivalent levels in Ea1189 $\Delta$ *dspE* and Ea1189 $\Delta$ *dspF*, although protein accumulation was greatly increased by inactivation of the Lon protease in the *dspF* mutant background. This finding is consistent with a previous report implicating T3SS chaperones in protection from Lon-mediated degradation in *P. syringae* (25). In addition, DspE-6xHis partially complemented the virulence phenotype of Ea1189 $\Delta$ *dspF*, confirming our previous findings that *dspF* is not inherently required for DspE secretion. These results suggest that the requirement for DspF in DspE translocation can be overcome in a concentration-dependent manner. Although stabilization is a common function of chaperones, ectopic expression is often not sufficient to overcome this function (26).

It is still unclear why DspE fusions accumulate in and are translocated from Ea1189 $\Delta$ *dspE* at reduced levels equivalent to Ea1189 $\Delta$ *dspF*, rather than wild-type levels. We considered the possibility that the mutation in Ea1189 $\Delta$ *dspE* might be polar, but the sequenced structure of the mutation is the same as the dozens of insertional mutants confirmed to be non-polar by Datsenko and Wanner (13). Alternatively, DspE could positively regulate its own secretion. Transcriptional and protein blot analysis will be needed to confirm the putative self-regulation of DspE and determine whether it occurs at the transcriptional, translational, or secretion level.

The aim of this study was to determine whether DspF functions in a variety of roles common to other secretion chaperones. We determined that DspF interacts with

multiple chaperoned effectors and secretion system components in yeast, and affects translocation of some effectors differently than others. In the process of characterizing these roles, we also demonstrated that Eop1, Eop3, and Eop4 are translocated into tobacco cells and that *eop1* and *eop3* and the putative chaperones *esc1* and *esc3* are not required for virulence. Further studies are being planned to determine whether the protein-protein interactions identified here in yeast are replicated *in vitro*, and to determine their functional significance. Many questions remain regarding the mechanism of these chaperone roles and their significance to real-world pathogenesis, but these findings contribute significantly to the understanding of *Erwinia amylovora* chaperone function.

**Table 4-1.** Bacterial strains and plasmids used in Chapter 4.

| strain                               | relevant characteristics   | source                        |
|--------------------------------------|--|-------------------------------|
| <i>Escherichia coli</i> DH5 $\alpha$ | F- 80 <i>dlacZ</i> $\Delta$ <i>M15</i> $\Delta$ ( <i>lacZYA-argF</i> ) <i>U169</i><br><i>endA1 recA1 hsdR17</i> (rK-mK+) <i>deoR</i><br><i>thi-1 supE44 gyrA96 relA1</i> $\lambda$ - | Invitrogen                    |
| <i>Erwinia amylovora</i>             |  |                               |
| Eal189                               | Wild type  | Burse <i>et al.</i> 2004      |
| Eal189 $\Delta$ <i>dspE</i>          | <i>dspE</i> deletion mutant, KmR   | Triplett <i>et al.</i> , 2009 |
| Eal189 $\Delta$ <i>dspF</i>          | <i>dspF</i> deletion mutant, KmR   | Triplett <i>et al.</i> , 2009 |
| Eal189 $\Delta$ <i>esc1</i>          | <i>esc1</i> deletion mutant, CmR   | This study                    |
| Eal189 $\Delta$ <i>esc3</i>          | <i>esc3</i> deletion mutant, CmR   | This study                    |
| Eal189 $\Delta$ <i>dspF/esc1</i>     | <i>dspF/esc1</i> deletion mutant, CmR  | This study                    |
| Eal189 $\Delta$ <i>dspF/esc3</i>     | <i>dspF/esc3</i> deletion mutant, CmR  | This study                    |
| Eal189 $\Delta$ <i>esc1/esc3</i>     | <i>esc1/esc3</i> deletion mutant, CmR  | This study                    |
| plasmids                             | relevant characteristics   | source                        |
| pLRT43                               | DspE-6xHis   | This study                    |
| pLRT224                              | pBRR1-MCS5 expressing <i>esc1</i>  | This study                    |
| pLRT225                              | pBRR1-MCS5 expressing <i>esc3</i>  | This study                    |
| pLRT226                              | B42-AD-Esc1  | This study                    |
| pLRT227                              | B42-AD-Esc3  | This study                    |
| pLRT215                              | B42-AD-DspF  | Triplett <i>et al.</i> , 2009 |
| pLRT93                               | LexA-DspF  | This study                    |
| pLRT219                              | LexA-DspE (1-600)  | Triplett <i>et al.</i> , 2009 |
| pLRT131                              | LexA-DspE (1-150)  | Triplett <i>et al.</i> , 2009 |
| pLRT83                               | LexA-HrcN  | This study                    |
| pLRT131                              | LexA-HrcN(c200)  | This study                    |
| pLRT228                              | LexA-HrcQ(c105)  | This study                    |
| pLRT229                              | LexA-HrcU  | This study                    |
| pLRT230                              | LexA-HrcU (c128)   | This study                    |
| pLRT111                              | LexA-Eop1  | This study                    |
| pLRT169                              | LexA-Eop1 (1-200)  | This study                    |
| pLRT231                              | LexA-Eop1 (135-263)  | This study                    |
| pLRT232                              | LexA-Eop1 (264-402)  | This study                    |
| pLRT167                              | LexA-Eop3  | This study                    |
| pLRT168                              | LexA-Eop4  | This study                    |
| pLRT177                              | Eop1-CyaA  | This study                    |
| pLRT178                              | Eop3-CyaA  | This study                    |
| pLRT209                              | Eop3-CyaA  | This study                    |
| pLRT210                              | Eop4-CyaA  | This study                    |
| pLRT201                              | DspE (1-737)-CyaA  | Triplett <i>et al.</i> , 2009 |
| pBRR1-MCS5                           | broad host-range cloning vector, GmR   | Kovach <i>et al.</i> 1995     |
| pGilda                               | HIS3 LexA BD bait vector, AmpR   | Clontech                      |
| pB42-AD                              | TRP1 B42 AD bait vector, AmpR  | Clontech                      |

**Table 4-2. Primers for cloning and mutagenesis used in Chapter 4.**

| Primer Name  | Primer sequence 5'→ 3'   |
|--------------|--|
| Eop1FBam     | gatcggatccgcatgaaattatctggactgagtagc                                     |
| Eop1RXh      | gatcctcgagctactttctttgtttcttgcggccag                                     |
| Eop3FB       | gatcggatcctcatgagtaaaatgccttcaaggcat                                     |
| Eop3RXh      | gatcctcgagttagaggtgatcctcgccaactctct                                     |
| Eop4Fb       | gatcggatcctctgtaaagtcagtcacatcc  |
| Eop4RXh      | gatcctcgagctaattttcactgtataacatggcg                                      |
| HrcNFB       | gctggatcctcatggtgatgagcgcgctacagcag                                      |
| HrcNRXh      | gatcctcgagtcaatcaggggcatggcgctgac  |
| HrcN 200FB   | gatggatcctcgccatcgtctttggcctgatcgg                                       |
| HrcUFB       | acagaattcatgcaaagcttcagggcgtgat  |
| HrcU(c128)FB | agaggatcctaataaaggccaccgctcatgcg   |
| HrcURXh      | atactcgagttattcggcttccagttcgatcacc                                       |
| HrcQ(c105)FB | gatcggatcctcgcgcagctggcgcactggctg  |
| HrcQRXh      | gatcctcgagctatcatccaacctcctggcagg  |
| pEop1F       | gatccttagagggaaccgggtgcagagaattgcaacataaaaaatctacaacgtttccagctgccatcag   |
| Eop1R        | gcgaatatttcttgcggccagaaattcacctg   |
| Eop3F        | gcgtctagactgttccagaaagttttcatctg   |
| pEop3F       | gcgtctagagggaaccgggtgcagagaattgcaacataaaaaatctactgttccagaaagttttcatctg   |
| Eop3R        | gatcaatattgtgatggctgtgaaaagataatca                                       |
| pEop4F       | gatccttagagggaaccgggtgcagagaattgcaacataaaaaatctactgttccagaaagttttcatctg  |
| Eop4R        | gataatattattttcactgtataacatggcgtgtgg                                     |
| EscIFH       | gactctagagatctctagagggaaccgggtgcagagaattgcaacataaaaaatctagctttagcatggc   |
| EscIRxh      | ggg<br>catcctcgagtcacatgtgattttcccgg                                     |
| Eop1mutF     | atggcactatctcgtcagttcggtaaccgtgagagcccagcgttggccggggtgtaggctggagctgcttc  |
| Eop1mutR     | ctactttctttgtttcttgcggccagaaattcacctgcccgtgtatttcatatgaatatcctcctta      |
| Eop3mutF     | atgagtaaaatgccttcaaggcataatctgattttgatacataagactgagggtgtaggctggagctgcttc |
| Eop3mutR     | tcagtgatggctgttgaagataatcaaaactctgccataaactggccatatgaatatcctcctta        |
| Esc1mutF     | atgatcatacaagatttactgggtggattagccagacggctggaagccgggtgtaggctggagctgcttc   |
| Esc1mutR     | tcatgtgattttcccggcgagattcaacgttaacccctgctgcgccagcacatatgaatatcctcctta    |
| Esc3mutF     | atgcgcaataaagagtttactctctttgtggagccatcacaaggtatagttaggctggagctgcttc      |
| Esc3mutR     | ctcagttaccgggttgcgtgactccccacggatcatcccgtgcgccacatatgaatatcctcctta       |
| LonmutF      | atgaatcctgagcgttctgaacgcattgaaatccctgtgttccggtgagctgtaggctggagctgcttc    |
| LonmutR      | ctattttaccgaggcaacctgcatgccataaggtgcattttgcagcggccagcatatgaatatcctcctta  |

**Table 4-3.** Yeast two-hybrid identification of putative DspF-interacting proteins.

| Prey        | Interaction with DspF |
|-------------|-----------------------|
| Eop1        | +                     |
| Eop3        | +                     |
| Eop4        | -                     |
| HrcN        | -                     |
| HrcN (c200) | -                     |
| HrcU        | -                     |
| HrcU (c128) | +                     |
| HrcQ (c105) | +                     |

## WORKS CITED

1. **Akeda, Y. and J.E. Galan.** 2005. Chaperone release and unfolding of substrates in type III secretion. *Nature* **437**: 911-915.
2. **Asselin, K.E., C. Oh, RM Nissinen, and S.V. Beer.** 2006. The secretion of EopB from *Erwinia amylovora*. Proceedings of the X International Workshop on Fire Blight. Ed. C. Bazzi and U. Mazzucchi. *Acta Hort* **704**: 409-415.
3. **Asselin, J.E., K.N. Yip, and S.V. Beer.** 2008. Eop1 differs in strains of *Erwinia amylovora* that differ in host specificity. Proceedings of the XI International Workshop on Fire Blight. Ed. K.B. Johnston and V.O. Stockwell. *Acta Hort* **793**: 213-214.
4. **Ausubel, F. M., R. Brent, R.E. Kingston, D.D. Moore, J.G. Seidman, J.A. Smith, and K. Struhl,** eds. 1997. Current Protocols in Molecular Biology. Wiley, New York.
5. **Birtalan, S.C., R.M. Phillips, and P. Ghosh.** 2002. Three-dimensional secretion signals in chaperone-effector complexes of bacterial pathogens. *Mol. Cell* **9**: 971-980.
6. **Boureau, T., H. El Maarouf-Boteau, A. Garnier, M.-N. Brisset, C. Perino, I. Pucheu, and M.-A. Barny.** 2005. DspA/E, a type III effector essential for *Erwinia amylovora* pathogenicity and growth in planta, induces cell death in host apple and nonhost tobacco plants. *Mol. Plant Pathogen Interactions* **19**: 16-24.
7. **Boyd, A.P., Lambermont, I. and Cornelis, G.R.** 2000. Competition between the Yops of *Yersinia enterocolitica* for delivery into eukaryotic cells : role of the SycE chaperone binding domain of YopE. *J. Bacteriol.* **182**: 4811-4821.
8. **Burse, A., H. Weingart, and M.S. Ullrich.** 2004. The phytoalexin-inducible multidrug efflux pump AcrB contributes to virulence in the fire blight pathogen, *Erwinia amylovora*. *Mol. Plant-Microbe Interact.* **17**: 43-54.
9. **Buttner, D., and Bonas,** 2006. Who comes first? How plant pathogenic bacteria orchestrate type III secretion. *Curr. Opin. Microbiol.* **9**: 193-200.
10. **Cornelis, G.** 2006. The Type III secretion injectosome. *Nature Rev. Microbiol.* **4**: 811-825.
11. **Darwin, K.H. and V.L. Miller.** 2001. Type III secretion chaperone-dependent regulation: activation of virulence genes by SicA and InvF in *Salmonella typhimurium*. *EMBO J.* **20**: 1850-1862.

12. **Dasgupta, N., G.L. Lykken, M.C. Wolfgang, and T.L. Yahr.** 2004. A novel anti-anti-activator mechanism regulates expression of the *Pseudomonas aeruginosa* type III secretion system. *Mol. Microbiol.* **53**: 297-308.
13. **Datsenko, K.A. and Wanner, B.L.** 2000. One-step inactivation of chromosomal genes in *Escherichia coli* using PCR products. *Proc. Natl. Acad. Sci. USA* **97**: 6640-6645.
14. **Debroy, S., R. Thilmony, Y.-B. Kwack, K. Nomura, and S.-Y. He.** 2004. A family of conserved bacterial effectors inhibits salicylic acid-mediated basal immunity and promotes disease necrosis in plants. *Proc. Natl. Acad. Sci. USA* **101**: 9927-9932.
15. **Ehrbar, K., B. Winnen and W. Hardt.** 2005. The chaperone binding domain of SopE inhibits transport via flagellar and SPI-1 TTSS in the absence of InvB. *Mol. Microbiol.* **59**: 248-264.
16. **Galan, J., and H. Wolf-Watz.** 2001. Protein delivery into eukaryotic cells by Type III secretion machines. *Nature* **444**: 567-573.
17. **Gaudriault, S., L. Malandrin, J.-P. Paulin and M.-A. Barny.** 1997. DspA, an essential pathogenicity factor of *Erwinia amylovora* showing homology with AvrE of *Pseudomonas syringae*, is secreted via the Hrp secretion pathway in a DspB-dependent way. *Mol. Microbiol.* **26**: 1057-1069.
18. **Gaudriault, S., J.-P. Paulin and M.A. Barny.** 2002. The DspB/F protein of *Erwinia amylovora* is a type III secretion chaperone ensuring efficient intrabacterial production of the Hrp-secreted DspA/E pathogenicity factor. *Mol. Plant Pathology* **3**: 313-320.
19. **Gauthier, A. and B.B. Finlay.** 2003. Translocated intimin receptor and its chaperone interact with ATPase of the type III secretion apparatus of enteropathogenic *Escherichia coli*. *J. Bacteriol.* **185**: 6747-6755.
20. **Kovach, M.E., P.H. Elzer, D.S. Hill, G.T. Robertson, M.A. Farris, R.M. Roop, and K.M. Peterson.** 1995. Four new derivatives of the broad host-range cloning vector pBBR1MCS, carrying different antibiotic-resistance cassettes. *Gene* **166**: 175-176.
21. **Letzelter, M. I. Sorg, L. J. Mota, S. Meyer, J. Stalder, M. Feldman, M. Kuhn, I. Callebaut and G.R. Cornelis.** 2006. The discovery of SycO highlights a new function for type III secretion effector chaperones. *EMBO J.* **25**: 3223-3233.
22. **Lloyd, S.A., M. Norman, R. Rosqvist and H. Wolf-Watz.** 2001. Yersinia YopE is targeted for type III secretion by N-terminal, not mRNA, signals. *Mol. Microbiol.* **39**: 520-532.

23. **Lorenz, C., O. Kirchner, M. Egler, J. Stuttmann, U. Bonas, and D. Buttner.** 2008. HpaA from *Xanthomonas* is a regulator of type III secretion. *Mol. Microbiol.* **69**: 344-360.
24. **Lorenz, C. and D. Buttner.** 2009. Functional characterization of the type III secretion ATPase HrcN from the plant pathogen *Xanthomonas campestris* pv. *vesicatoria*. *J. Bacteriol.* **191**: 1414-1428.
25. **Losada, L.C. and S.W. Hutcheson.** 2005. Type III secretion chaperones of *Pseudomonas syringae* protect effectors from Lon-associated degradation. *Mol. Microbiol.* **55**: 941-953.
26. **Matsumoto, H, and G.M. Young.** 2009. Essential role of the SycP chaperone in type III secretion of the YspP effector. *J. Bacteriol.* **191**: 1703-1715.
27. **Mills, E., K. Baruch, X. Charpentier, S. Kobi, and I. Rosenshine.** 2008. Real-time analysis of effector translocation by the type III secretion system of enteropathogenic *Escherichia coli*. *Cell Host and Microbe* **3**: 104-113.
28. **Nissinen, R.M., A.J. Ytterburg, A.J. Bogdanove, K.J. Van Wijk and S.V. Beer.** 2006. Analyses of the secretomes of *Erwinia amylovora* and selected hrp mutants reveal novel type III secreted proteins and an effect of HrpJ on extracellular harpin levels. *Mol. Plant Pathol.* **8**: 55-67.
29. **Parsot, C., Hamiaux, C., and Page, A.L.** 2003. The various and varying roles of specific chaperones in type III secretion systems. *Curr. Opin. Microbiol.* **6**: 7-14.
30. **Spaeth, K.E., Y.-S. Chen, and R.H. Valdivia.** 2009. The *Chlamydia* type III secretion C-ring engages a chaperone-effector protein complex. *PloS Pathog.*: e1000579.
31. **Thomas, N., W. Deng, J. Puente, E.A. Frey, C.K. Yip, N.C.J. Strynadka and B.B. Finlay.** 2005. CesT is a multi-effector chaperone and recruitment factor required for the efficient type III secretion of both LEE and non-LEE-encoded effectors of enteropathogenic *Escherichia coli*. *Mol. Microbiol.* **57**: 1762-1779.
32. **Triplett, L.R., M. Melotto, and G.W. Sundin.** 2009. Analysis of the N-terminus of the *Erwinia amylovora* secreted effector DspA/E reveals features required for secretion, translocation, and interaction with the chaperone DspB/F. *Mol. Plant Microbe Interact.* **22**: 1282-1292.
33. **Wulff-Strobel, C.R., A.W. Williams and S.C. Straley.** 2002. LcrQ and SycH function together at the Ysc type III secretion system in *Yersinia pestis* to impose a hierarchy of secretion. *Mol. Microbiol.* **43**: 411-423.

34. **Winnen, B., M.C. Schlumberger, A. Sturm, K. Schupbach, S. Siebenmann, P. Jenny and W. Hardt.** 2008. Hierarchical effector protein transport by the *Salmonella typhimurium* SPI-1 type III secretion system. *PLOS One* **3**: e2178 1-8.
35. **Zhao, Y., S.E. Blumer, and G.W. Sundin.** 2005. Identification of *Erwinia amylovora* genes upregulated during infection of immature pear tissue. *J. Bacteriol.* **187**: 8088-8103.
36. **Zhao, Y., S.-Y. He and G. Sundin.** 2006. The *Erwinia amylovora* avrRpt2EA gene contributes to virulence on pear and AvrRpt2EA is recognized by Arabidopsis RPS2 when expressed in *P. syringae*. *Mol. Plant Microbe Interact.* **19**: 644-654.

## Chapter 5: Conclusions and Future Directions

### Summary of Work

The type III secretion system of gram-negative bacteria is an elegant, ancient, and powerful piece of equipment, enabling bacterial manipulation of eukaryotic cellular pathways and establishment of countless pathogenic and symbiotic relationships that shape our world. The research accomplishments of the last two decades in this area have revealed the complexity and variety of these systems; they have also shown that an understanding of the processes leading to secretion and the selective forces shaping it will require contributions from a variety of fields and from diverse organisms. Efforts to elucidate the nature of the type III secretion signal and the role of secretion chaperones have been rewarding, but much of this work so far has been limited to a few families of T3SS in human pathogens.

My dissertation research has focused on the molecular signals required for the type III translocation of effector proteins from *Erwinia amylovora* into plant cells. *E. amylovora* is both a devastating pathogen and a system well-suited to translocation research: it shares many genetic characteristics with other Enterobacterial species, it has few chaperones and effectors in the genome, and it harbors a conserved chaperone-effector pair required for pathogenesis. I began this research with the goal of determining to what extent T3SS signaling and chaperone roles in *Erwinia* reflect the patterns elucidated by research in mammalian pathogens. Based on work in these other systems, I hypothesized that DspF and a DspF-binding domain would be critical for translocation of DspE. Instead, my work demonstrates that the DspE secretion/ translocation signal is distinct from the chaperone binding domain and that DspF facilitates but is not required

for DspE translocation. In addition, I provide an initial characterization of class I type III secretion chaperones in the *E. amylovora hrp* system, candidate interactors, and putative function.

Chapter 2 describes the N-terminal signals required for secretion of the pathogenicity factor DspE. The most commonly proposed model of the type III secretion signal is a bipartite signal, in which an N-terminal secretion signal is followed by a domain necessary for translocation into host cells. In many ways, the N-terminal characteristics targeting DspE for secretion are similar to those targeting proteins for secretion from the well-studied T3S systems in *Yersinia* and *Salmonella*. DspE has an N-terminal translocation signal and chaperone binding signal with common size and predicted secondary structural characteristics. However, the secretion and translocation signals coincided. If the N-terminal secretion signal is actually an ancient secretion signal for the flagellar T3SS, it is possible that secretion of N-terminal DspE truncations is suppressed by *hrp*-inducing, flagellar secretion system-repressing media conditions used here. An experiment testing whether the N-terminal fragments of DspE are secreted under flagellar-permissive conditions could lend support to the flagellar signal theory.

The secretion/translocation signal of DspE did not coincide with the chaperone-binding domain, and neither this domain nor the chaperone itself were required for translocation. Longer DspE fragments were translocated at greater levels, indicating the presence of a minimal and optimal secretion signal, but the optimal secretion signal also did not correspond with the chaperone binding domain. This finding demonstrates that the DspF does not cover a secretion-blocking domain on DspE, nor is it an inherent requirement for translocation. Although no single mutation completely abolished the

DspE translocation signal, I discovered that mutation of a segment including serine-stretch reduced translocation levels significantly without reducing fusion expression. Phylogenetic and functional studies would help determine whether the serine stretch is a valuable part of a translocation signal in *E. amylovora*.

To determine the significance of *dspF* on translocation of the N-terminus of DspE, DspE translocation was initially measured from *dspE* and *dspF* deletion mutants to allow avoidance of DspE-induced cell death and resulting effects on translocation levels and cAMP accumulation. Unexpectedly, DspE (1-737)-CyaA was translocated at similar levels from Ea1189 $\Delta$ *dspE* and  $\Delta$ *dspF*. Translocation studies later adapted to include translocation from Ea1189 revealed that translocation levels from *dspE* and *dspF* mutant strains were significantly lower than from the wild-type, and that the deletion of Ea1189 $\Delta$ *dspE* had an unforeseen negative effect on DspE fusion protein translocation levels. Translocation levels, as indicated by cAMP levels, were only reduced by about 50% in Ea1189 $\Delta$ *dspF* compared with Ea1189. This finding contrasts with wild-type DspE, secretion of which is barely detectable from Ea1189 $\Delta$ *dspF*.

The mild phenotype of Ea1189 $\Delta$ *dspF* in translocation assays and the complementation of Ea1189 $\Delta$ *dspF* by DspE-6xHis suggest that the phenotype of DspF is partially overcome by ectopic expression of DspE. I did not rule out the possibility that the C-terminal histidine tag may affect DspE secretion or accumulation levels, but my findings suggest that the functional significance of *dspF*, whether in stabilization or secretion system targeting or both, may be partially compensated for in a concentration-dependent manner. As Eop1 is also translocation-competent in the absence of its chaperone, it appears that the functional role of *E. amylovora* chaperones is to make a

quantitative improvement in secretion, rather than impose a qualitative requirement. In wild-type cells, effector levels may be maintained at low enough levels during infection that chaperones are effectively required. However, given that previous observations regarding chaperone function rely heavily on findings from plasmid-expressed fusion proteins, my work underscores the importance of achieving wild-type effector expression levels in future studies of chaperone function. Chaperones are thought to play a critical role in controlling the temporal or concentration dynamics of effector secretion, and to understand the scale and significance of these phenomena, future work should aim to assess translocation levels from chromosomally tagged bacterial lines.

T3SS chaperones have a nearly universally conserved folded shape, confirmed by numerous solved structures. Surface features proposed to mediate effector-binding specificity include two conserved hydrophobic pockets, an general overall pattern of hydrophobic surface sites, or hydrogen bonding mediated by electronegative surface residues. Functional studies of these features are few; although a conserved  $\beta$ -sheet groove is often discussed as a probable site critical to the chaperone-effector interaction, this site has never previously been functionally analyzed by systematic mutagenesis. I reasoned that the structural conservation between chaperones could be used to identify features required for function of diverse chaperones. Using a homology-based model of DspF, eleven residues with probable placement in the helix-binding groove were identified. Four highly-conserved residues were identified to be required for DspF virulence function, three of which are required for interaction with the N-terminus of DspE, and two of which significantly reduced translocation of a DspE-CyaA fusion in a dominant-negative manner. The DspF residues required for virulence were predicted to

cluster near the same point in the helix-binding groove, suggestive of an effector-binding hotspot. My research provides evidence that polar residues in the effector-binding groove are important contributors to the chaperone-effector interaction. Although it is likely that this groove could interact with residues of the putative helices in residues 51-60 and 73-82 of DspE, attempts to model such an interaction would be extremely speculative.

Chaperones serve diverse functions in secretion, and these functions are mediated through interaction with diverse cellular proteins. The third goal of this research was to identify interactors of DspF in yeast and to determine whether selected interactions have functional significance. DspF interacted with *E. amylovora* secreted proteins Eop1 and Eop3 in yeast. Because DspF interacts with the same sites of Eop1 and Eop3 as the predicted cognate chaperones of these effectors, I predicted that DspF would influence translocation levels of several secreted effector proteins, and that deletion of other secreted effectors might influence virulence in a *dspF* mutant. In fact, chaperones had no positive impact on translocation levels of non-cognate effectors, suggesting that chaperone function is highly specific in *E. amylovora*. Interestingly, deletion of *dspF* had a positive effect cAMP accumulation mediated by Eop1-CyaA and Eop3-CyaA, although it is unknown whether this effect is indirect or related to the interaction with DspF. Although deletion of *eop1* and *eop3* and the presumed cognate chaperone genes *esc1* and *esc3*, respectively, had no effect on symptom development in pear, *esc1* or *esc3* deletion led to a slight early increase in population growth. Based on the findings in this study, I hypothesized that the three *hrp* chaperones in *E. amylovora* may compete with or antagonize translocation of other chaperoned effectors. This hypothesis will continue to be tested in the Sundin lab.

DspF and other *E. amylovora* chaperones were also shown to interact with putative components of the type III secretion system in yeast. These interactions have not been confirmed *in vitro* in *E. amylovora*, although similar interactions have been confirmed in other species. The increasingly apparent universality of chaperone-T3SS base interactions supports the theory that the three-dimensional chaperone structure serves as a signal in this interaction.

### Questions for the Future

Deletion of *dspF* could result in a reduction of accumulation of wild-type *dspE* and this reduction may be dependent on Lon and other proteases. However, this reduced accumulation phenotype was not observed in N-terminal DspE fragments or cloned full-length DspE-6xHis. This suggests that, in contrast to previously characterized effectors such as SycO and SopE, the chaperone binding domain of DspE is not inherently destabilizing or secretion-inhibitory. Determining the mechanism by which *dspF* might protect *dspE* from the effects of proteases will be an important step toward connecting the significance of the chaperone-binding domain, protease targeting sites, and the translocation signal.

Some of the most intriguing recent work on T3SS targeting in plant pathogens has been the first characterization of proteins with predicted involvement in secretion substrate recognition, including a homolog of the *Yersinia* substrate-specificity switch YscU. T3SS chaperones were shown to interact *in-vitro* with YscU or several other putative cytosol-exposed components of the T3SS, demonstrating that T3S chaperones could interact with the secretion apparatus in a manner much more complex than previously suspected. Exploring these interactions in diverse T3SS and assessing their

functional significance will contribute substantially to our understanding of chaperone function and type III secretion. The materials developed through this work would provide a good start for investigating these questions in *Erwinia amylovora*. *E. amylovora* secretes a limited number of *hrp*- associated chaperones, for which a series of deletion mutants have been constructed in this work. Interactions between the three *hrp* chaperones identified here and predicted T3SS apparatus components would be assessed *in-vitro*, helping to address the question of whether all the chaperones of a T3SS bind to the same secretion apparatus components with the same affinity. Because the *E. amylovora* genome harbors five T3SS, these studies could be expanded to examine the specificity of the chaperone-T3SS apparatus interaction. The structural model of DspF could inform mutagenesis studies aimed at identifying surface features required for interaction with the T3SS, and translocation and secretion assays could help assess the functional significance of these interactions. This line of research will add to the quest to understand the murkiest areas of type III secretion- the substrate recognition machinery, the translocation apparatus, and the uncharacterized peripheral proteins- and connect the dots among them.

## **Appendix 1: Genetic Differences Among Blight-Causing *Erwinia* Species with Differing Host Specificities Identified by Suppression Subtractive Hybridization**

This appendix was published as an article with the above title, co-authored by Y. Zhao and G.W. Sundin, in *Applied and Environmental Biology* (2006) vol. 72: 7359-7364.

### **ABSTRACT**

The factors determining host specificity in *Erwinia amylovora*, the causal agent of fire blight of apple and pear, are unknown. PCR-based subtractive hybridization was used to isolate sequences from *E. amylovora* strain Ea110, pathogenic on apples and pears, that were not present in three closely-related strains with differing host specificities: *E. amylovora* MR1, pathogenic only on *Rubus* spp.; *E. pyrifoliae* Ep1/96, the causal agent of shoot blight of Asian pears; and *Erwinia* sp. Ejp556, the causal agent of bacterial shoot blight of pear in Japan. Six subtractive libraries were constructed and analyzed. Recovered sequences included type III secretion components, hypothetical membrane proteins, and ATP-binding proteins. In addition, we identified an Ea110-specific sequence with homology to a type III secretion apparatus component of the insect endosymbiont *Sodalis glossinidius*, as well as an Ep1/96-specific sequence with homology to the *Yersinia pestis* effector protein tyrosine phosphatase YopH.

## INTRODUCTION

*Erwinia amylovora* is the causal agent of fire blight disease of apple, pear, and many other rosaceous species. Interestingly, strains of *E. amylovora* that infect raspberry and other brambles (*Rubus* spp.) are unable to infect apple and pear (5, 15). The *Rubus*-infecting strains of *E. amylovora* are closely related to the apple and pear-infecting strains, as evidenced by similar amplified fragment length polymorphism (AFLP) and PCR fingerprints, species-level total DNA-DNA homology, and nearly identical sequences in pathogenicity and virulence genes (13, 17, 24-26). Recently, other blight-causing *Erwinia* spp. strains with restricted host ranges have been described; *E. pyrifoliae* was identified as the cause of Asian pear blight (18), and *Erwinia* sp. strains isolated in Japan cause bacterial shoot blight of pears (19). The Asian strains produced no symptoms when inoculated on apple seedlings (19, 20). Comparisons of chromosomal and plasmid sequences and AFLP profiles have indicated that *E. pyrifoliae* is genetically distinct from but closely related to *E. amylovora*, and that the *Erwinia* sp. strains from Japan are more closely related to *E. pyrifoliae* than to *E. amylovora* (18-20, 24, 25). Despite their phenotypic and genetic similarities, the basis for differences in host specificity between these *Erwinia* strains remains unknown. An understanding of the factors restricting host range in these bacteria could provide important new insights into plant-pathogen interactions and provide new targets for disease control.

Much of our understanding about the host specificity of bacterial phytopathogens comes from the study of avirulence (*avr*) genes, the products of which elicit a hypersensitive response and disease resistance in plants encoding corresponding resistance (*R*) genes (22). However, gene-for-gene interactions have not been identified

among any of the blight-causing *Erwinia* species and their respective hosts. As more bacterial genome sequences become available, genomic comparison of closely related strains with different host ranges can provide clues regarding the nature of host specificity. This approach has led to the identification of several strain-specific genes with possible host-limiting functions in pathogenic strains of *Pseudomonas*, *Xanthomonas*, and *Xylella*, respectively (3, 12, 33).

Hybridization-based methods such as suppression subtractive hybridization (SSH) are useful in the genetic comparison of organisms for which a genome sequence is unavailable (1). SSH is a PCR-based method that has been used to identify differences between prokaryotic genomes with differing phenotypes, including pathogenic and non-pathogenic strains of the same species (27) and between different, closely-related species (6, 38). SSH has also been used to analyze genetic differences between plant pathogenic strains varying in host specificity (14, 40).

Our objective in this study was to identify genomic differences among plant pathogenic *Erwinia* strains. We used SSH to generate six subtracted libraries to compare the genomes of fruit tree-infecting *E. amylovora* strains with *E. pyrifoliae*, a Japanese *Erwinia* sp. strain, and a *Rubus*-infecting strain of *E. amylovora*. We hypothesized that this analysis could reveal novel virulence determinants required for disease on distinct hosts. These experiments resulted in the identification of strain-specific sequences including genes encoding a putative type III secretion system (T3SS) effector, a T3SS apparatus component, and several putative membrane proteins.

**Pathogenicity of *Erwinia* strains on immature pears.** The bacterial strains used in this study are listed in Table 1. Immature pears were inoculated with *E. amylovora*

strains Ea110, Ea273, and MR1, *Erwinia* sp. Ejp556, and *E. pyrifoliae* Ep 1/96 as previously described (41). After incubation for three days, pears infected with strains Ea110, Ea273, and Ep1/96 displayed symptoms typical of fire blight infection including extensive water-soaking and necrosis accompanied by the production of bacterial ooze (Figure 1). Pears infected with Ejp556 displayed these same symptoms to a reduced extent, and pears inoculated with MR1 showed no signs of infection (Figure A-1). Cell counts from inoculated pears revealed that populations of MR1 neither increased nor decreased in number in immature pears over the four day period following inoculation (data not shown).

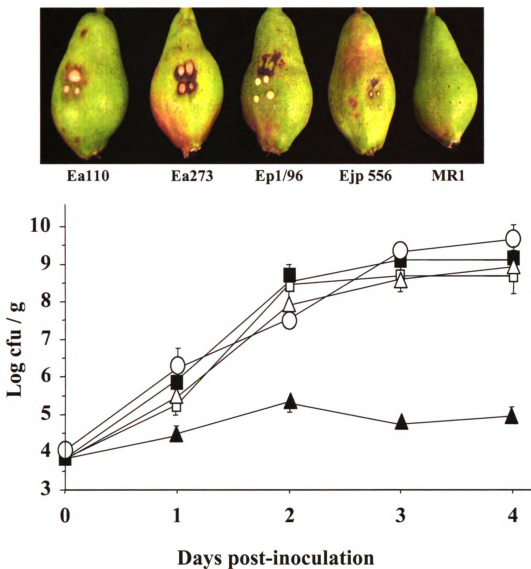


**Figure A-1.** (A) Symptom expression in immature pear fruit following inoculation with *Erwinia amylovora* strains. Each fruit was inoculated in four places. (B) Growth of *E. amylovora* Ea110 (■), Ea273 (□), and MR1 (▲); *E. pyrifoliae* Ep1/96 (△); and *Erwinia* sp. strain EJP556 (○) during infection of immature pears. The growth of bacterial strains was monitored at 0, 1, 2, 3, and 4 days after inoculation. Data points represent the means of three replicates  $\pm$  standard errors. Similar results were obtained in two additional independent experiments.

**SSH and isolation of *E. amylovora*-specific sequences.** SSH is used to enrich for PCR products unique to a tester strain, with amplification of sequences from a driver strain suppressed. Six subtracted libraries were made: three were enriched for sequences specific to *E. amylovora* Ea110- but not hybridizing to restricted host-range strains *E. pyrifoliae* Ep1/96, *Erwinia* sp. Ejp556, or *E. amylovora* MR1, and three were enriched for sequences specific to the restricted host-range strains (Table 2). *E. amylovora* Ea273 was a strain of choice because a genome sequencing project of this strain is underway, ([http://www.sanger.ac.uk/Projects/E\\_amylovora/](http://www.sanger.ac.uk/Projects/E_amylovora/)) and so this strain was used as a driver in subtractions enriching for restricted host-range strains. However, Ea273 also contains a 71.5 kb indigenous plasmid previously thought to be similar to a plasmid in *E. amylovora* Ea322 (35). The plasmid from *E. amylovora* Ea322 has no known involvement in virulence and no known counterpart in Ea110, Ep1/96, Ejp556, or MR1 (25). To avoid the creation of subtractive libraries enriched with sequences from this plasmid or the ubiquitous plasmid pEA29, a plasmid-cured strain of *E. amylovora* Ea110 designated Ea110- was used as the tester in SSH experiments.

SSH was performed using the PCR-Select Bacterial Genome Subtraction Kit (Clontech) following the manufacturer's instructions except that the primary PCR reaction was increased to 28 cycles. PCR products were ligated into the pGEM T-Easy vector (Promega; Madison, WI) and transformed into chemically competent cells of *Escherichia coli* DH5 $\alpha$ . For the three subtractions that used *E. amylovora* Ea110- as the tester, inserts from 96 randomly selected clones were amplified by PCR using primers specific to the oligonucleotide adapters, denatured for 10 minutes at 95° C, and spotted onto duplicate Immobilon-P nylon membranes (Millipore; Bedford, MA). Tester and

driver genomic DNA was labeled with digoxigenin by random priming using the DIG DNA labeling kit (Roche Applied Science; Indianapolis, IN) according to the manufacturer's instructions. Duplicate membranes were hybridized overnight to tester and driver probes at 63° C as described in the DIG application manual (Roche). PCR products hybridizing more strongly to tester DNA were purified, spotted onto new membranes, and re-probed. Products hybridizing only to tester DNA were sequenced at the Michigan State University Genomics Technology Support Facility, and sequences were analyzed using BLASTx and BLASTn (<http://www.ncbi.nlm.nih.gov/BLAST/>).

The subtraction [Ea110- - MR1] yielded 10 unique Ea110- -specific sequences, including three with no significant BlastX match. Four sequences matched hypothetical genes of unknown function, and two of these were similar to sets of predicted genes from the insect pathogen and nematode endosymbiont *Photorhabdus luminescens* (Table 3). EM4 shared greater than 30% amino acid identity with several exopolysaccharide acetyltransferases in *Burkholderia*, *Xanthomonas*, and *Pseudomonas*, including an ExoZ homolog from *Pseudomonas syringae* pv. tomato. Although the functional role of EPS acetylation has not been studied in plant pathogens, ExoZ is thought to reduce EPS susceptibility to cleavage in *Rhizobium meliloti* (39).

The subtraction [Ea110- - Ep1/96] yielded nine non-redundant clones with significant BlastX hits, including two with no predicted function (Table 3). A sequence from clone EP1 was similar to that of *amsF* from *E. amylovora*, a gene involved in synthesis of the exopolysaccharide (EPS) amylovoran (7). EPS, which comprises the capsule, is an essential pathogenicity factor in *E. amylovora*. A sequence matching EP1

was obtained from the *E. amylovora* sequence database website ([http://www.sanger.ac.uk/Projects/E\\_amylovora/](http://www.sanger.ac.uk/Projects/E_amylovora/)), revealing a 1.8 kb Orf with 37% amino acid similarity to AmsF. However, the Orf does not appear to be flanked by other *ams* gene homologs and thus is most likely in a different genomic location than the *ams* operon. Another sequence, EP2, shared 31% amino acid identity with the type III secretion T3SS gene *ysaQ* from the insect endosymbiont *Sodalis glossinidius* (Table 2). This T3SS is required for host cell invasion and host transfer of the endosymbiont (10). EP6 was 91% identical to 268 amino acids of the 506-aa protein MglA, a highly conserved ABC transporter involved in galactose uptake in *Salmonella typhimurium* (34). Although a role for sugar uptake in host specificity has not been determined, the ability to utilize certain simple carbohydrates is critical for *Erwinia* virulence (2, 4). In addition, a number of carbon source utilization and transporter genes were identified in a recent analysis of genes expressed during *E. amylovora* pathogenesis (41).

The subtraction [Ea110- - Ejp556] lead to the identification of seven unique sequences with matches to known genes (Table 3). EJ1 shared 24% amino acid similarity to RfaK from *E. coli*, a protein thought to be involved in modification of the lipopolysaccharide (LPS) core to facilitate O-antigen attachment (21). LPS O-antigen biosynthetic genes have been found to differ significantly between closely related *Xanthomonas*, *Xylella*, and *Serratia marcescens* genomes (33, 36, 40). LPS and EPS form the interface at which *Erwinia* interacts with its host, so some basis for specificity may lie in these molecules. More study is needed to determine whether EPS or LPS structure has a role in *Erwinia* host range selection.

Sequence EJ3 isolated in this library was identical to sequence EM5 from the library [Ea110- - MR1], matching an *E. coli* ATPase; sequence EJ6 was also similar to a predicted ATPase. Other sequences isolated from this library matched OrfL and Orfs 106 and 81, predicted genes of unknown function previously identified in the *E. amylovora* genome (11, 29).

**Isolation of sequences specific to Asian *Erwinia* strains.** For subtractions enriching for sequences specific to Asian *Erwinia* strains, clone inserts were sequenced at random prior to hybridization screening. Sequences were screened against the genome of the driver, Ea273, to screen for tester-specificity. Results were then confirmed by dot-blot hybridization as described above. Sequences with matches of greater than 80% in the Sanger database always hybridized to DIG-labeled Ea273 total genomic DNA (data not shown).

Of 48 clones sequenced from the subtraction [Ejp556 - Ea273], 14 clones were tester-specific, with nine of these sharing significant homology with known sequences (Table 4). JE1 contained *ejp19*, a putative membrane ABC transporter previously identified in Ejp556 (24), and JE2, JE3, and JE4 also contained gene sequences with similarity to hypothetical transmembrane proteins. Transporters and other membrane proteins could influence the host range and lifestyle of a pathogen by determining the range of substrates and niches available to it. Previous work has reported differences in outer membrane proteins and an ABC transporter between PAGE profiles of *Rubus* strains and other isolates of *E. amylovora* (5). Ejp556-specific clones JE6 and JE5 shared 69% identity with residues 40-75 of the 75 amino acid precursor to the bacteriocin

divergicin A, and to the serine protease-like domain of a hypothetical *Burkholderia* chitin-binding protein, respectively.

In the subtraction [Ep1/96 – Ea273], Ep1/96 plasmid DNA (300 ng) was added to the primary and secondary hybridization of Ea273 genomic DNA and Ep1/96 genomic DNA to reduce preferential amplification of the small plasmids specific to this strain (25). Nevertheless, over half of the tester-specific sequences resulting from this subtraction matched known sequences from these small plasmids (data not shown). Of the remaining eight tester-specific sequences, five unique sequences were identified with significant BlastX matches (Table 3). Sequence analysis of clone PE3 showed a predicted 48% amino acid similarity with the *Yersinia pestis* type III effector YopH. YopH is a protein tyrosine phosphatase that targets the actin cytoskeleton and a variety of host signaling pathways involved in both adaptive and innate immunity (37). Comparison of this sequence with the *E. amylovora* genomic database revealed a 1,587-nucleotide orf with 57% nucleotide sequence similarity to the Ep1/96 putative YopH homolog, and 33% similarity to YopH itself. The putative *Erwinia* YopH homologs, if functional, could play a role in disrupting signaling pathways in host plants. Mutagenesis of these sequences in *E. amylovora* and *E. pyrifoliae* is underway to determine whether the YopH homologs have a role in virulence or host specificity.

Analysis of clone PE1 revealed it to be nearly identical to clone JE2 from the subtraction [Ejp556 - Ea273]. These sequences are predicted to share 44% amino acid identity with predicted *Thiomicrospira crunogena* protein Tcr\_0083, and over 30% identity with several proteins with putative transmembrane domains. Sequence analysis of Ep1/96-specific clone PE5 yielded a 479-nt Orf with homologs present in many gram-

negative pathogens of plants and animals. Downstream of this Orf is a sequence containing a putative Duf796 domain, usually found in family 19 chitin-binding genes. Family 19 chitin-binding proteins are common in plants, although they have been recently found in several plant pathogenic bacteria, including *Xanthomonas* strains (33) and a chitinolytic strain of *Burkholderia gladioli* (31).

**Assay for sequences specific to MR1 but not Ea273.** SSH libraries were also constructed using *Rubus*-specific strain MR1 as the tester, but no MR1-specific sequences were found after screening 36 sequences from two independent subtractions. A previous SSH study of *Xylella fastidiosa* genomes failed to find tester-specific clones when the tester genome was slightly smaller than that of the driver (14). Similarly, the MR1 genome could be smaller than that of Ea273. Comparison of *Bordetella* genomes found evidence of substantial gene loss during speciation, and it was hypothesized that genomic decay could have occurred subsequent to host range restriction (9, 28). It is possible that, once restricted to bramble hosts, the MR1 genome may have lost genes selected for in pathogens of apple and pear.

**Distribution of isolated sequences among *Erwinia* strains.** Ea110-specific sequence EP2, which was similar to YsaQ from *S. glossinidius*, was blasted against the *E. amylovora* Ea273 genomic sequence ([http://www..sanger.ac.uk/Projects/E\\_amylovora/](http://www..sanger.ac.uk/Projects/E_amylovora/)). Further analysis of the shotgun database revealed two copies of a putative T3SS with high similarity to *S. glossinidius* symbiosis island SSR-1, required for *Sodalis* invasion of insect host cells (10). The first copy is approximately 23.5 kb in length and contains 20 predicted orfs. This is preceded by a putative phage integrase gene and has an overall base composition (38.4% mol G+C) significantly lower than that predicted for the *E.*

*amylovora* genome (53.5% mol G+C). The second putative T3SS is approximately 33.4 kb and contains 26 predicted orfs with an overall base composition of 43.4% mol G+C.

To determine the distribution of the new T3SS sequences among *Erwinia* strains, DNA probes were generated from PCR products from four predicted Orfs including *ysaQ* and *yspB*, a predicted apparatus protein and effector in the first putative T3SS, respectively; and *ysaC2* and *ysaH2*, both predicted apparatus components in the second putative T3SS. A fifth probe was created from *ycgZ*, a hypothetical protein flanking the first putative T3SS. All of these probes hybridized to genomic DNA from strains of *E. amylovora*, but not to DNA from other *Erwinia* strains (Table 5). Thus, if a *Sodalis*-like T3SS does exist in the Asian pear pathogens, it is divergent from that of *E. amylovora*. The Type III (Hrp) secretion systems of *E. pyrifoliae* and *E. amylovora* associated with plant infection, in contrast, are highly conserved, sharing 84-96% nucleotide sequence similarity (32). *E. amylovora* is insect-disseminated and has been isolated from orchard populations of several orders of insects with diverse habitats (16), although the exact interaction between the pathogen and its insect hosts remains poorly understood. The presence of sequences highly similar to insect endosymbionts could indicate a common ancestry and close phylogenetic relationship between *Erwinia* spp. and insect-related enterics, raising the possibility that an insect host might be serving as a mixing vessel for the exchange of genes between *Erwinia* strains and other enteric bacteria, facilitating genetic variation and divergence. Another possibility is that *E. amylovora* could use these type III secretion genes in its own symbiotic relationship with an insect host. Studies are currently underway to determine whether these genomic islands have a role in the virulence and spread of *Erwinia* spp.

DIG-labeled DNA probes were created from PCR products of several other sequences isolated in this study to determine their distribution among *Erwinia* strains. Results of dot-blot hybridizations are summarized in Table 5. Generally, Ea110-specific sequences hybridized to all four strains of *E. amylovora* tested. However, the predicted AmsF homolog sequence EP1 hybridized to DNA from strains Ejp556 and Ejp557 as well as to *E. amylovora*, indicating that this sequence is not specific to apple pathogens. Sequence JE5, a putative chitin-binding protein sequence specific to Ejp556, hybridized to all four of the Asian *Erwinia* strains tested. However, both probes derived from Ep1/96-specific sequences, including the putative YopH homolog PE5, hybridized only to *E. pyrifoliae* strains (Table 5). A probe derived from the YopH homolog found in Ea273 hybridized to all four *E. amylovora* strains.

**Summary.** In this study, we used SSH and dot-blot hybridization screening to identify a number of genomic differences between *Erwinia* strains with differing host ranges, including components of two novel type III secretion systems in *E. amylovora*, a putative tyrosine phosphatase effector, and several sequences related to membrane transport or polysaccharide biosynthesis. These putative genes could distinguish the molecular arsenals of *Erwinia* strains from one another, and under further investigation could help explain their differing abilities for invasion, survival, and virulence in their respective hosts. Our findings also provide some clues about the nature and possible origin of genetic variation between these *Erwinia* strains. Alternatively, host range differences between *Erwinia* strains could stem from a number of complex factors not detectable by SSH, including minute sequence differences in pathogenicity genes, post-transcriptional protein modifications, or a combination of these.

## WORKS CITED

1. **Akopyants, N. S., A. Fradkov, L. Diatchenko, J. E. Hill, P. D. Siebert, S. A. Lukyanov, E. D. Sverdlov, and D. E. Berg.** 1998. PCR-based subtractive hybridization and differences in gene content among strains of *Helicobacter pylori*. *Proc. Natl. Acad. Sci. USA* **95**:13108-13113.
2. **Aldridge, P., M. Metzger, and K. Geider.** 1997. Genetics of sorbitol metabolism in *Erwinia amylovora* and its influence on bacterial virulence. *Mol. Gen. Genet.* **256**: 611-619.
3. **Bhattacharyya, A., S. Stilwagen, N. Ivanova, M. D'Souza, A. Bernal, A. Lykidis, V. Kapatral, I. Anderson, N. Larsen, T. Los, G. Reznik, E. Selkov, Jr., T. L. Walunas, H. Feil, W. S. Feil, A. Purcell, J.-L. Lassez, T. L. Hawkins, R. Haselkorn, R. Overbeek, P. F. Predki, and N. C. Kyrpides.** 2002. Whole-genome comparative analysis of three phytopathogenic *Xylella fastidiosa* strains. *Proc. Natl. Acad. Sci. USA* **99**:12403-12408.
4. **Bogs, J., and K. Geider.** 2000. Molecular analysis of sucrose metabolism of *Erwinia amylovora* and influence on bacterial virulence. *J. Bacteriol.* **182**:5351-5358.
5. **Braun, P. G., and P. D. Hildebrand.** 2005. Infection, carbohydrate utilization, and protein profiles of apple, pear, and raspberry isolates of *Erwinia amylovora*. *Can. J. Plant Pathol.* **27**:338-346.
6. **Brown, N. F., and I. R. Beacham.** 2000. Cloning and analysis of genomic differences unique to *Burkholderia pseudomallei* by comparison with *B. thailandensis*. *J. Med. Microbiol.* **49**:993-1001.
7. **Bugert, P., and K. Geider.** 1995. Molecular analysis of the *ams* operon required for exopolysaccharide synthesis of *Erwinia amylovora*. *Mol. Microbiol.* **15**:917-933.
8. **Cheng, H.-P., and G. C. Walker.** 1998. Succinoglycan is required for initiation and elongation of infection threads during nodulation of alfalfa by *Rhizobium meliloti*. *J. Bacteriol.* **180**:5183-5191.
9. **Cummings, C. A., M. M. Brinig, P. W. Lepp, S. v. d. Pas, and D. A. Relman.** 2004. *Bordetella* species are distinguished by patterns of substantial gene loss and host adaptation. *J. Bacteriol.* **186**:1484-1492.
10. **Dale, C., S. A. Young, D. T. Haydon, and S. C. Welburn.** 2001. The insect endosymbiont *Sodalis glossinidius* utilizes a type III secretion system for cell invasion. *Proc. Natl. Acad. Sci. USA* **98**:1883-1888.

11. **Du, Z., V. Jakovljevic, H. Salm, and K. Geider.** 2004. Creation and genetic restoration of *Erwinia amylovora* strains with low levan synthesis. *Physiol. Mol. Plant Pathol.* **65**:115-122.
12. **Feil, H., W. S. Feil, P. Chain, F. Larimer, G. DiBartolo, A. Copeland, A. Lykidis, S. Trong, M. Nolan, E. Goltsman, J. Theil, S. Malfatti, J. E. Loper, A. Lapidus, J. C. Detter, M. Land, P. M. Richardson, N. C. Kyrpides, N. Ivanova, and S. E. Lindow.** 2005. Comparison of the complete genome sequences of *Pseudomonas syringae* pv. *syringae* B728a and pv. *tomato* DC3000. *Proc. Natl. Acad. Sci. USA* **102**: 11064-11069.
13. **Giorgi, S., and M. Scortichini.** 2005. Molecular characterization of *Erwinia amylovora* strains from different host plants through RFLP analysis and sequencing of *hrpN* and *dspA/E* genes. *Plant Pathol.* **54**:789-798.
14. **Harakava, R., and D. W. Gabriel.** 2003. Genetic differences between two strains of *Xylella fastidiosa* revealed by suppression subtractive hybridization. *Appl. Environ. Microbiol.* **69**:1315-1319.
15. **Heimann, M. F., and G. L. Worf.** 1985. Fire blight of raspberry caused by *Erwinia amylovora* in Wisconsin. *Plant Dis.* **69**:360.
16. **Hildebrand, M., E. Dickler, and K. Geider.** 2000. Occurrence of *Erwinia amylovora* on insects in a fire blight orchard. *J. Phytopathol.* **148**:251-256.
17. **Jock, S., and K. Geider.** 2004. Molecular differentiation of *Erwinia amylovora* strains from North America and of two Asian pear pathogens by analyses of PFGE patterns and *hrpN* genes. *Environ. Microbiol.* **6**:480-490.
18. **Kim, W. S., L. Gardan, S.-L. Rhim, and K. Geider.** 1999. *Erwinia pyrifoliae* sp. nov., a novel pathogen that affects Asian pear trees (*Pyrus pyrifolia* Nakai). *Int. J. Syst. Bacteriol.* **49**:899-906.
19. **Kim, W. S., M. Hildebrand, S. Jock, and K. Geider.** 2001. Molecular comparison of pathogenic bacteria from pear trees in Japan and the fire blight pathogen *Erwinia amylovora*. *Microbiology* **147**:2951-9.
20. **Kim, W. S., S. Jock, J.-P. Paulin, S.-L. Rhim, and K. Geider.** 2001. Molecular detection and differentiation of *Erwinia pyrifoliae* and host range analysis of the Asian pear pathogen. *Plant Dis.* **85**:1183-1188.
21. **Klena, J. D., R. S. d. Ashford, and C. A. Schnaitman.** 1992. Role of *Escherichia coli* K-12 *rfa* genes and the *rfp* gene of *Shigella dysenteriae* 1 in generation of lipopolysaccharide core heterogeneity and attachment of O antigen. *J. Bacteriol.* **174**:7297-7307.

22. **Leach, J.E., and F.F. White.** 1996. Bacterial avirulence genes. *Annu. Rev. Phytopathol.* **34**: 153-179.
23. **Mavrodi, D. V., O. V. Mavrodi, B. B. McSpadden-Gardener, B. B. Landa, D. M. Weller, and L. S. Tomashow.** 2002. Identification of differences in genome content among phlD-Positive *Pseudomonas fluorescens* strains by using PCR-based subtractive hybridization. *Appl. Environ. Microbiol.* **68**:5170-5176.
24. **Maxson-Stein, K., G. C. McGhee, J. J. Smith, A. L. Jones, and G. W. Sundin.** 2003. Genetic analysis of a pathogenic *Erwinia* sp. isolated from pear in Japan. *Phytopathology* **93**: 1393-1399.
25. **McGhee, G.C., E.L. Schnabel, K. Maxson-Stein, B. Jones, V.K. Stromberg, G.H. Lacy, and A.L. Jones.** 2002. Relatedness of chromosomal and plasmid DNAs of *Erwinia pyrifoliae* and *Erwinia amylovora*. *Appl. Environ. Microbiol.* **68**: 6182-6192.
26. **McManus, P. S., and A. L. Jones.** 1995. Genetic fingerprinting of *Erwinia amylovora* strains isolated from tree-fruit crops and *Rubus*. spp. *Phytopathology* **85**: 1547-1553.
27. **Miyazaki, J., W. Ba-Thein, T. Kumao, H. Azaka, and H. Hayashi.** 2002. Identification of a type III secretion system in uropathogenic *Escherichia coli*. *FEMS Microbiol. Lett.* **212**:221-8.
28. **Moore, R. A., S. Reckseidler-Zenteno, H. Kim, W. Nierman, Y. Yu, A. Tuanyok, J. Warawa, D. DeShazer, and D. E. Woods.** 2004. Contribution of gene loss to the pathogenic evolution of *Burkholderia pseudomallei* and *Burkholderia mallei*. *Infect. Immun.* **72**:4172-4187.
29. **Oh, C.-S., J. F. Kim, and S. V. Beer.** 2005. The Hrp pathogenicity island of *Erwinia amylovora* and identification of three novel genes required for systemic infection. *Molecular Plant Pathology* **6**:125-138.
30. **Ritchie, D. F., and E. J. Klos.** 1977. Isolation of *Erwinia amylovora* bacteriophage from the aerial parts of apple trees. *Phytopathology* **67**:101-104.
31. **Shimosaka, M., Y. Fukumori, T. Narita, X.-Y. Zhang, R. Kodaira, M. Nogawa, and M. Okazaki.** 2001. The bacterium *Burkholderia gladioli* strain CHB101 produces two different kind of chitinases belonging to families 18 and 19 of the glycosyl hydrolases. *J. Biosci. Bioeng.* **91**:103-105.
32. **Shrestha, R., K. Tsuchiya, S. J. Baek, H. N. Bae, I Hwang, J. H. Hur, and C. K. Lim.** 2005. Identification of *dspEF*, *hrpW*, and *hrpN* loci and characterization of the HrpNEp gene in *Erwinia pyrifoliae*. *J. Gen. Plant Pathol.* **71**:211-220.

33. **Silva, A.C.R., J. A. Ferro, F. C. Reinach, C. S. Farah, L. R. Furlan, R. B. Quaggio, C. B. Monteiro-Vitorello, M. A. Van Sluys, N. F. Almeida, L. M. C. Alves, A. M. do Amaral, M. C. Bertolini, L. E. A. Camargo, G. Camarotte, F. Cannavan, J. Cardozo, F. Chambergo, L. P. Ciapina, R. M. B. Cicarelli, L. L. Coutinho, J. R. Cursino-Santos, H. El-Dorry, J. B. Faria, A. J. S. Ferreira, R. C. C. Ferreira, M. I. T. Ferro, E. F. Formighieri, M. C. Franco, C. C. Greggio, A. Gruber, A. M. Katsuyama, L. T. Kishi, R. P. Leite, E. G. M. Lemos, M. V. F. Lemos, E. C. Locali, M. A. Machado, A. M. B. N. Madeira, N. M. Martinez-Rossi, E. C. Martins, J. Meidanis, C. F. M. Menck, C. Y. Miyaki, D. H. Moon, L. M. Moreira, M. T. M. Novo, V. K. Okura, M. C. Oliveira, V. R. Oliveira, H. A. Pereira, A. Rossi, J. A. D. Sena, C. Silva, R. F. de Souza, L. A. F. Spinola, M. A. Takita, R. E. Tamura, E. C. Teixeira, R. I. D. Tezza, M. Trindade dos Santos, D. Truffi, S. M. Tsai, F. F. White, J. C. Setubal, and J. P. Kitajima.** 2002. Comparison of two *Xanthomonas* pathogens with differing host specificities. *Nature* **417**: 459-463.
34. **Stamm, L. V., N. R. Young, and J. G. Frye.** 1996. Sequences of the *Salmonella typhimurium* *mglA* and *mglC* genes. *Gene* **171**:131.
35. **Steinberger, E.M., G.-Y. Cheng, and S.V. Beer.** 1990. Characterization of a 56-kb plasmid of *Erwinia amylovora* Ea322: Its noninvolvement in pathogenicity. *Plasmid* **24**:12-24.
36. **Van Sluys, M. A., M. C. de Oliveira, C. B. Monteiro-Vitorello, C. Y. Miyaki, L. R. Furlan, L. E. A. Camargo, A. C. R. da Silva, D. H. Moon, M. A. Takita, E. G. M. Lemos, M. A. Machado, M. I. T. Ferro, F. R. da Silva, M. H. S. Goldman, G. H. Goldman, M. V. F. Lemos, H. El-Dorry, S. M. Tsai, H. Carrer, D. M. Carraro, R. C. de Oliveira, L. R. Nunes, W. J. Siqueira, L. L. Coutinho, E. T. Kimura, E. S. Ferro, R. Harakava, E. E. Kuramae, C. L. Marino, E. Giglioti, I. L. Abreu, L. M. C. Alves, A. M. do Amaral, G. S. Baia, S. R. Blanco, M. S. Brito, F. S. Cannavan, A. V. Celestino, A. F. da Cunha, R. C. Fenille, J. A. Ferro, E. F. Formighieri, L. T. Kishi, S. G. Leoni, A. R. Oliveira, V. E. Rosa, Jr., F. T. Sasaki, J. A. D. Sena, A. A. de Souza, D. Truffi, F. Tsukumo, G. M. Yanai, L. G. Zarus, E. L. Civerolo, A. J. G. Simpson, N. F. Almeida, Jr., J. C. Setubal, and J. P. Kitajima.** 2003. Comparative analyses of the complete genome sequences of Pierce's disease and citrus variegated chlorosis strains of *Xylella fastidiosa*. *J. Bacteriol.* **185**: 1018-1026.
37. **Viboud, G. I., and J. B. Bliska.** 2005. *Yersinia* outer proteins: role in modulation of host cell signaling responses and pathogenesis. *Annu. Rev. Microbiol.* **59**:69-89.
38. **Walker, J. C., and N. K. Verma.** 2002. Identification of a putative pathogenicity island in *Shigella flexneri* using subtractive hybridisation of the *S. flexneri* and *Escherichia coli* genomes. *FEMS Microbiol. Lett.* **213**: 257-264.

39. **York, G. M., and G. C. Walker.** 1998. The succinyl and acetyl modifications of succinoglycan influence susceptibility of succinoglycan to cleavage by the *Rhizobium meliloti* glycanases ExoK and ExsH. *J. Bacteriol.* **180**:4184-4191.
40. **Zhang, Q., U. Melcher, L. Zhou, F. Z. Najjar, B. A. Roe, and J. Fletcher.** 2005. Genomic comparison of plant pathogenic and nonpathogenic *Serratia marcescens* strains by suppressive subtractive hybridization. *Appl. Environ. Microbiol.* **71**:7716-7723.
41. **Zhao, Y., S. E. Blumer, and G. W. Sundin.** 2005. Identification of *Erwinia amylovora* genes induced during infection of immature pear tissue. *J. Bacteriol.* **187**:8088-8103.

**Table A-1.** *Erwinia* spp. strains and their indigenous plasmid content.

| Species and strain(s)     | Plasmids and Relevant Characteristics | Host             | Reference     |
|---------------------------|---------------------------------------|------------------|---------------|
| <i>Erwinia amylovora</i>  |                                       |                  |               |
| Ea110                     | pEA29                                 | Apple, Pear      | (30)          |
| Ea110-                    | cured of pEA29                        | Apple, Pear      | (41)          |
| Ea273                     | pEA29, 71.5 Kb plasmid                | Apple, Pear      | CUCPB02<br>73 |
| Ea321                     | pEA29                                 | Crataegus        | CFBP1367      |
| MR1                       | pEA29                                 | <i>Rubus</i> sp. | (26)          |
| <i>Erwinia pyrifoliae</i> |                                       |                  |               |
| Ep1/96                    | pEP36 and 3 small plasmids            | Asian Pear       | (18, 25)      |
| Ep4/97                    | pEP36                                 | Asian Pear       | (18)          |
| <i>Erwinia</i> sp.        |                                       |                  |               |
| Ejp556                    | pEJ30                                 | Asian Pear       | (19)          |
| Ejp557                    | pEJ30                                 | Asian Pear       | (19)          |

**Table A-2.** Libraries generated by suppressive subtractive hybridization.

| Subtraction                               | No. of unique sequences (No. of sequences with significant BlastX match) |
|---|--|
| Ea110- (apple) - MR1 ( <i>Rubus</i> spp.) | 10 (7)   |
| Ea110- (apple) - Ep1/96 (pear)            | 11 (9)   |
| Ea110- (apple) - Ejp556 (pear)            | 10 (7)   |
| Ep1/96 (pear) - Ea273 (apple)             | 8 (5)  |
| Ejp556 (pear) - Ea273 (apple)             | 14 (9)   |
| MR1 ( <i>Rubus</i> spp.) - Ea273 (apple)  | 0  |

**Table A-3.** Sequence analysis of inserts specific to *E. amylovora* Ea110, but not *E. amylovora* MR1, *E. pyrifoliae* Ep1/96, and *Erwinia* sp. Ejp556, respectively.

|                   | SSH clone | Similar protein, organism                 | Predicted function             | BlastX E value | accession no. |
|-------------------|-----------|---|--------------------------------|----------------|---------------|
|                   | EM1       | <i>Photorhabdus luminescens</i> Plu3117   | hypothetical protein           | 2 E-17         | CAE15491      |
|                   | a,b       | <i>Photorhabdus luminescens</i> Plu3116   | hypothetical protein           | 9 E-17         | CAE15490      |
|                   | EM2       | <i>Photorhabdus luminescens</i> Plu4876   | hypothetical protein           | 2 E-41         | CAE17248      |
|                   | a         | <i>Photorhabdus luminescens</i> Plu4875   | hypothetical protein           | 1 E-5          | CAE17247      |
| [Ea110- - MR1]    | EM3       | <i>Photorhabdus luminescens</i> Plu1815   | DNA-damage inducible protein   | 5 E-7          | CAE14108      |
|                   | a         | <i>Shewanella denitrificans</i> Sden_3233 | phage integrase                | 2 E-36         | ZP_00583430   |
|                   | EM4       | <i>Burkholderia xenovorans</i> ExoZ       | exopolysaccharide biosynthesis | 4 E-43         | YP_553663     |
|                   | EM5       | <i>Escherichia coli</i> EcolB7_01003583   | putative ATPase                | 9 E-58         | ZP_00714762   |
|                   | EM6       | <i>Oceanobacter</i> sp. Red65_14712       | hypothetical protein           | 4 E-28         | ZP_0130638    |
|                   | EM7       | <i>Pseudomonas putida</i> Pp2746          | hypothetical protein           | 9 E-61         | ZP_744890     |
|                   | EP1       | <i>E. amylovora</i> Ams F                 | exopolysaccharide biosynthesis | 5 E-3          | CAA54887      |
|                   | EP2b      | <i>Sodalis glossinidius</i> YsaQ          | T3SS invasion protein          | 2 E-23         | AAS66845      |
|                   | EP3b      | <i>Pseudomonas putida</i> Pp5253          | putative arylesterase          | 7 E-28         | NP_747354     |
|                   | EP4       | <i>Salmonella enterica</i> CysQ           | ammonium transport             | 4 E-47         | NP_458840     |
| [Ea110- - Ep1/96] | EP5b      | <i>Pseudomonas syringae</i> Psyr_4778     | hypothetical protein           | 8 E-13         | YP_237843     |
|                   | EP6       | <i>Salmonella typhimurium</i> MglA        | galactoside ABC transporter    | 7 E-127        | AAC44149      |
|                   | EP7       | <i>Klebsiella pneumoniae</i> OrfX         | membrane dipeptidase           | 3 E-46         | CAA41578      |
|                   | EP8       | <i>Salmonella enterica</i> Sc0250         | hypothetical protein           | 9 E-26         | YP_215237     |
|                   | EP9a      | <i>Escherichia coli</i> C3433             | hypothetical protein           | 2 E-6          | ZP_00727249   |
|                   |           | <i>Photorhabdus luminescens</i> FtsI      | ftsI precursor                 | 2 E -5         | CAE16033      |

**Table A-3 (cont'd).**

|                    |      |   |                                 |        |                 |
|--------------------|------|---|---------------------------------|--------|-----------------|
|                    | EJ1  | <i>Escherichia coli</i> RfaK            | lipopolysaccharide biosynthesis | 9 E-6  | AAA24523        |
|                    | EJ2  | <i>Erwinia amylovora</i> OrfL           | unknown, chitin-binding domain  | 1 E-87 | AAX39449        |
|                    | EJ3c | <i>Escherichia coli</i> EcolB7_01003583 | Predicted ATPase                | 9 E-58 | ZP_0071476<br>2 |
| [Ea110-<br>Ejp556] | EJ4  | <i>Escherichia coli</i> EcolB7_01003586 | hypothetical protein            | 1 E-96 | ZP_0071476<br>5 |
|                    | EJ5  | <i>Escherichia coli</i> Orf 5           | hypothetical protein            | 2 E-15 | CAA11511        |
|                    | EJ6  | <i>Salmonella typhimurium</i> YidR      | putative cytoplasmic protein    | 7 E-18 | NP_462711       |
|                    | EJ7a | <i>E. amylovora</i> Orf 106             | hypothetical protein            | 1 E-37 | CAH41996        |
|                    |      | <i>E. amylovora</i> Orf 81              | hypothetical protein            | 7 E-33 | CAH41995        |

a. Clones EM1, EM2, EM3, EP9, and EJ6 contained sequences from two genes.

b. The sequences in clones EM1, EP2, EP3, and EP5 were each found in more than one clone.

c. Clones EM5 and EJ3 contained identical insert sequences

**Table A-4.** Sequence analysis of SSH inserts specific to *Erwinia* sp. Ejp556 and *E. pyrifoliae*, respectively, but not to *E. amylovora* Ea273.

| SSH Clone       | Similar protein, organism                           | Predicted function                  | BlastX E value | accession no. |
|-----------------|---|-------------------------------------|----------------|---------------|
| JE1             | <i>Erwinia</i> sp. Ejp556 Ejp19                     | ATP binding ABC transporter         | 6 E-40         | NP_857628     |
| JE2a            | <i>Thiomicrospira crunogena</i> Tcr_0083            | hypothetical protein                | 7 E-18         | AAB40679      |
| JE3             | <i>Escherichia coli</i> YbiO                        | putative membrane transport protein | 4 E-19         | AAN79366      |
| JE4             | <i>Yersinia mollareti</i> Ymola_01003756            | hypothetical protein                | 7 E-47         | ZP_00823862   |
| [556-273] JE5   | <i>Burkholderia fungorum</i> Bcep02003426           | hypothetical chitin-binding protein | 1 E-15         | ZP_00281547   |
| JE6             | <i>Carnobacterium divergens</i> DvnA                | divergicin A precursor              | 6 E-6          | AAZ29031      |
| JE7             | <i>Escherichia coli</i> C2473                       | transposase                         | 2 E-19         | AAN80932      |
|                 | <i>Erwinia carotovora</i> Eca1054                   | integrase                           | 4 E-11         | YP_215278     |
| JE8             | <i>Caenorhabditis elegans</i> K06A9.1c              | hypothetical protein                | 1 E-5          | AAP82647      |
| JE9             | <i>Photorhabdus luminescens</i> Plu3156             | hypothetical protein                | 4 E-17         | CAE15530      |
| PE1             | <i>Thiomicrospira crunogena</i> Tcr_0083            | hypothetical protein                | 5 E-18         | ABB40679      |
| PE2             | <i>Burkholderia</i> sp. Bcep18194_c7625             | putative conserved lipoprotein      | 3 E-8          | ABB06669      |
| [1/96-273] PE3b | <i>Aeromonas salmonicida</i> AopH                   | type III effector protein           | 6 E-8          | ABD48950      |
| PE4             | <i>Escherichia coli</i> Tsr                         | methyl-accepting chemotaxis protein | 8 E-16         | AAN83850      |
| PE5b,c          | <i>Bordetella parapertussis</i> BPP0716             | hypothetical protein                | 2 E-50         | CAE40125      |
|                 | <i>Novosphingobium aromaticivorans</i> Saro02002220 | family 19 glycoside hydrolase       | 3 E-24         | YP_498016     |

**Table A-5.** Dot-Blot hybridization analysis of the distribution of gene sequence among various blight-causing *Erwinia* strains.

| SSH clone | predicted function                     | Ea110 | Ea273 | Ea321 | MR1 | Ep 1/<br>96 | Ep 4/<br>97 | Ejp 556 | Ejp557 |
|-----------|--|-------|-------|-------|-----|-------------|-------------|---------|--------|
| EP1       | EPS synthesis, similar to AmsF         | +     | +     | +     | +   | -           | -           | +       | +      |
| EJ1       | LPS biosynthesis                       | +     | +     | +     | +   | -           | -           | -       | -      |
| EJ2       | OrfL- unknown                          | +     | +     | +     | +   | -           | -           | -       | -      |
| EM4       | Polysaccharide biosynthesis            | +     | +     | +     | -   | -           | -           | -       | -      |
| JE5       | Chitin-binding protein                 | -     | -     | -     | -   | +           | +           | +       | +      |
| PE3       | YopH-like PTPase (Ep1/96)              | -     | -     | -     | -   | +           | +           | -       | -      |
| -         | YopH-like PTPase (Ea273)               | +     | +     | +     | +   | -           | -           | -       | -      |
| PE5       | <i>Bordetella</i> hypothetical protein | -     | -     | -     | -   | +           | +           | -       | -      |
| EP6       | galactose transporter MglA             | +     | +     | +     | +   | -           | -           | -       | -      |
| EP7       | OrfX- unknown                          | +     | +     | +     | +   | -           | -           | -       | -      |
| EP2       | YsaQ                                   | +     | +     | +     | +   | -           | -           | -       | -      |
| -         | YcgZ                                   | +     | +     | +     | +   | -           | -           | -       | -      |
| -         | YsaC2                                  | +     | +     | +     | +   | -           | -           | -       | -      |
| -         | YsaH2                                  | +     | +     | +     | +   | -           | -           | -       | -      |
| -         | YspB                                   | +     | +     | +     | +   | -           | -           | -       | -      |
| -         | DspE (positive control)                | +     | +     | +     | +   | +           | +           | +       | +      |

MICHIGAN STATE UNIVERSITY LIBRARIES



3 1293 03063 1885